FEL Simulations for the European XFEL

From GW to TW Radiation Power

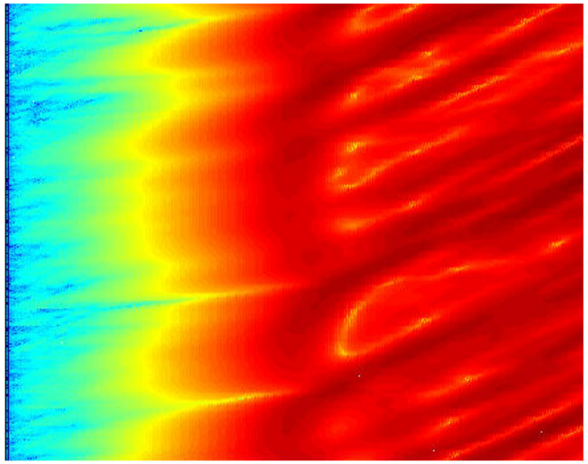

Igor Zagorodnov

Collaboration Meeting at PAL

Pohang, Korea
2-6. September 2013

HELMHOLTZ GEMEINSCHAFT

DESY

Overview

- Numerical Methods for FEL Calculations
  - FEL physics in 1D
  - mathematical model in 3D
  - numerical methods
  - quiet start and shot noise
  - time dependent simulations
  - problems and challenges
- FEL Simulations for the EXFEL
  - SASE for nominal bunch parameters
  - impact of accelerator wakes on SASE
  - self-seeding schemes for TW power
  - strong bunch compresion for TW power
  - undulator tapering in nominal regime
  - harmonic lasing and pSASE

Motivation

Free Electron Laser

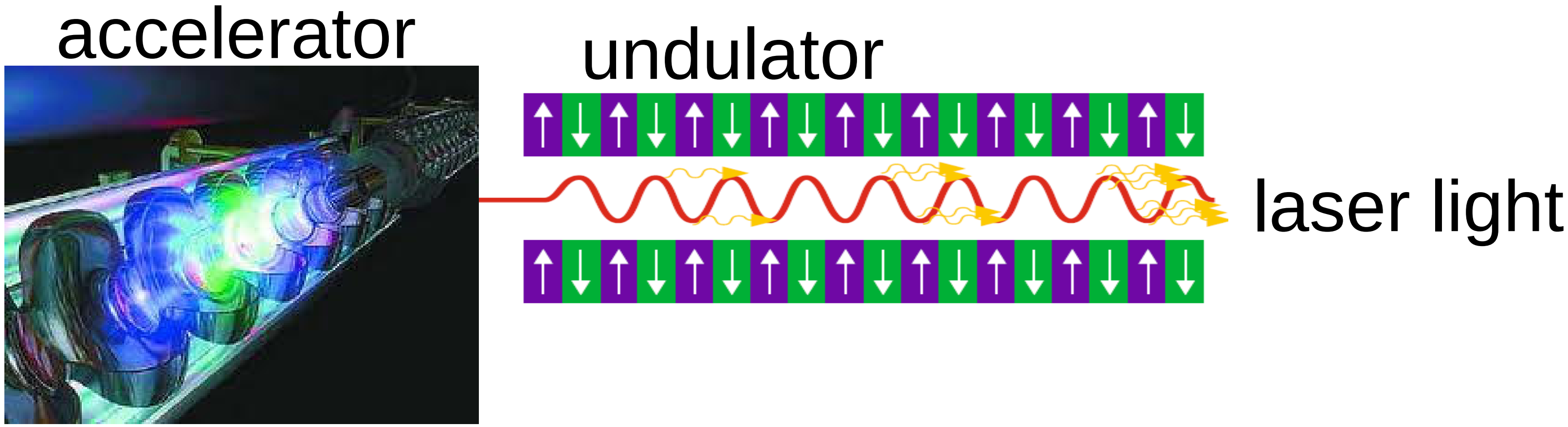

- very short and tunable wavelength
- extreme short pulses with very high energy

John Madey, Appl. Phys. **42**, 1906 (1971)

Motivation

Numerical methods

S. Reiche, *FEL simulations: history, status and outlook*, FEL 2010, Malmö, 2010

- undulator (~ 100 m)

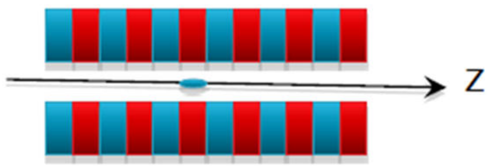

- bunch (~ 10 μm)

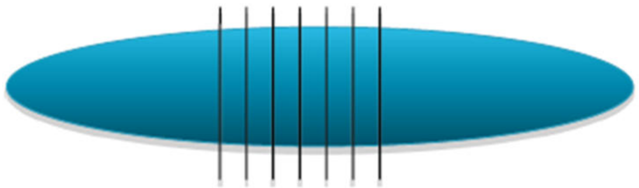

- slice (~ 0.1 nm)

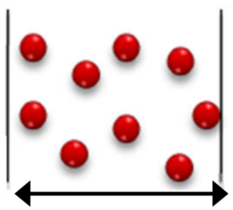

λ – Wellenlänge

12 orders of magnitude

approximations are neccecary

FEL numerical algorithms

FEL Physics in 1D

Motion of one electron in an undulator

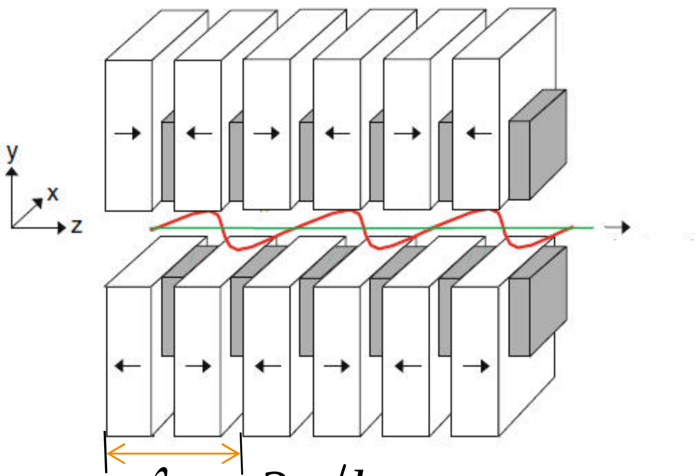

$$\lambda_u = 2\pi/k_u$$

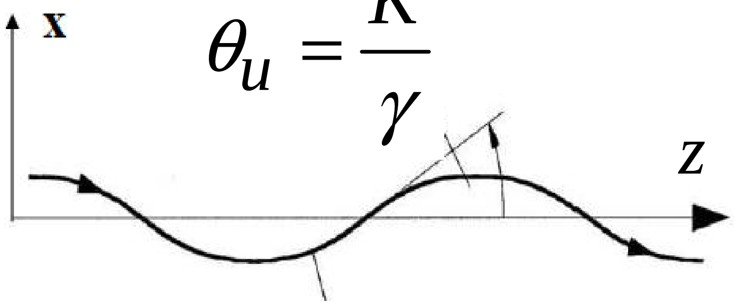

$$\theta_u = \frac{K}{\gamma}$$

electron trajectory

Field on the axis

$$B_y = -B_0 \sin(k_u z)$$

$$K = \frac{eB_0}{m_e c k_u}$$ - undulator parameter

γ - electron energy

FEL Physics in 1D

Energy exchange in FEL

$\overline{v}_z < c$ an electron is slower than the EM field

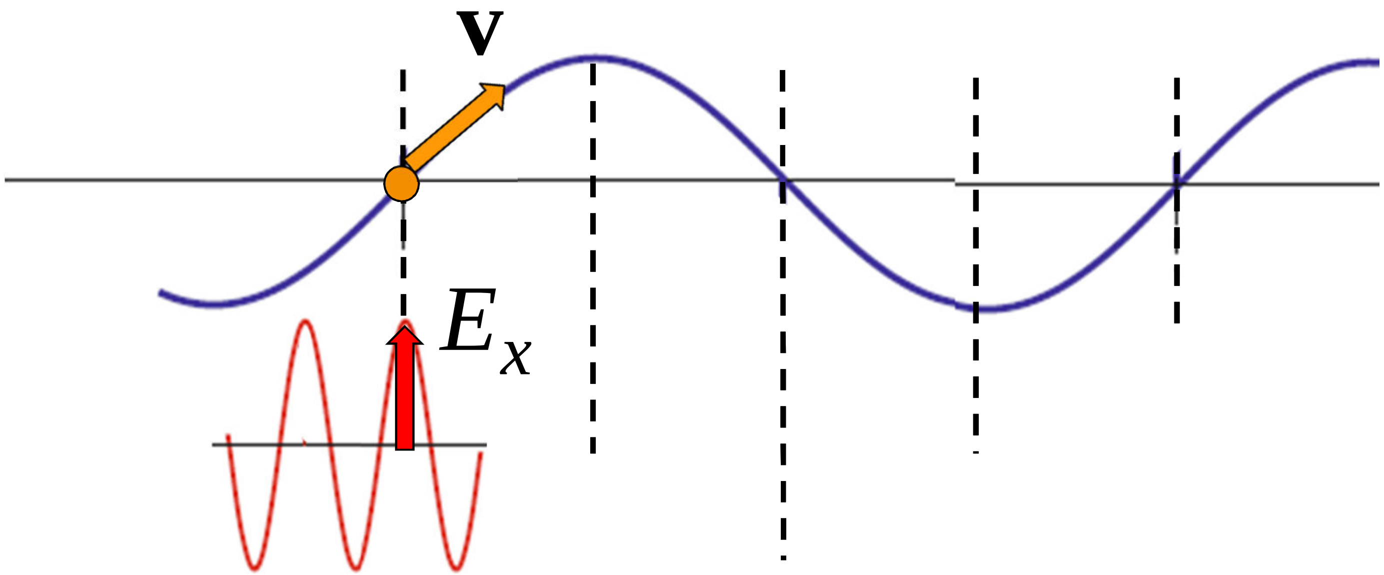

EM field ~ plane wave

$$E_x(z,t) = E_0 \cos(kz - \omega t)$$

FEL Physics in 1D

Energy exchange in FEL

$\bar{v}_z < c$ an electron is slower than the EM field

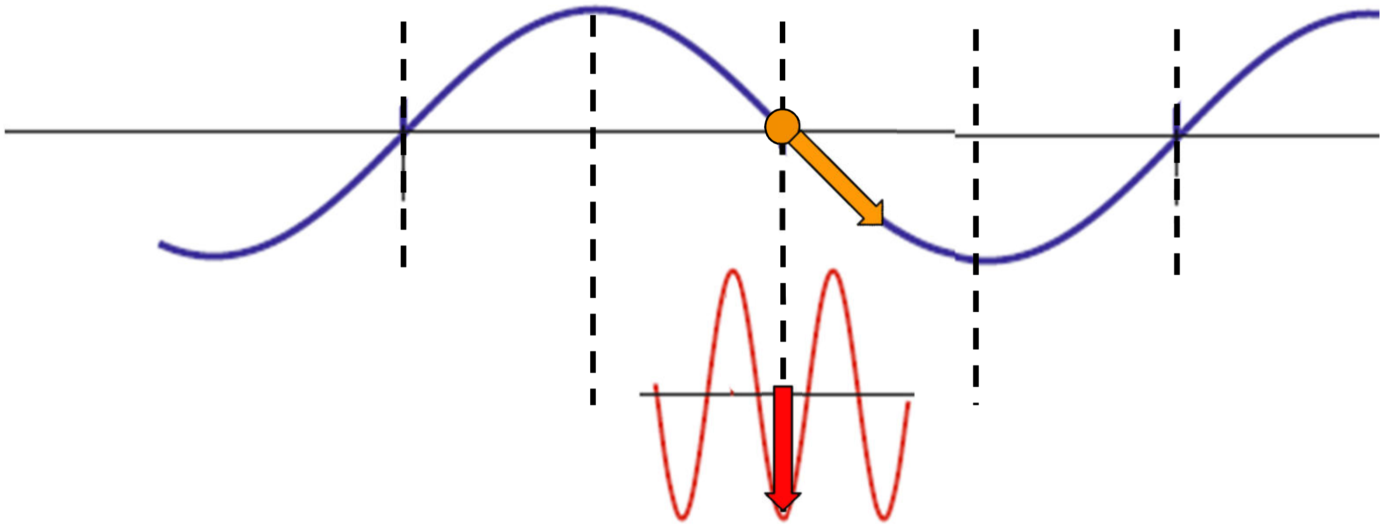

FEL Physics in 1D

Energy exchange in FEL

$\bar{v}_z < c$ an electron is slower than the EM field

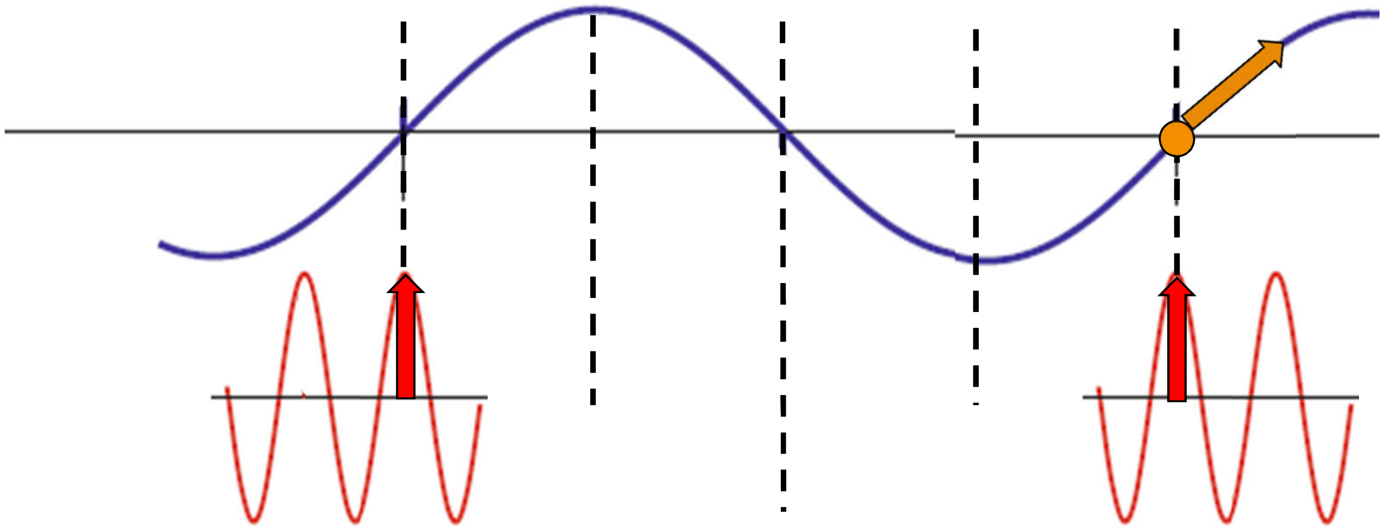

The electron has to be slower exactly by one wave length.

$$\lambda = \frac{\lambda_u}{2\gamma^2}\left(1+\frac{K^2}{2}\right)$$

FEL Physics in 1D

Longitudinal equations of motion (1D model)

$$\frac{d}{dt}\psi = 2k_u c\eta$$

$$\frac{d}{dt}\eta = -\frac{eK[JJ]E_0}{2m_e c\gamma_r^2}\cos\psi$$

$$\psi = (k + k_u)z - \omega t, \; [JJ] \sim 1$$

$$\eta = \frac{\gamma - \gamma_r}{\gamma_r}$$

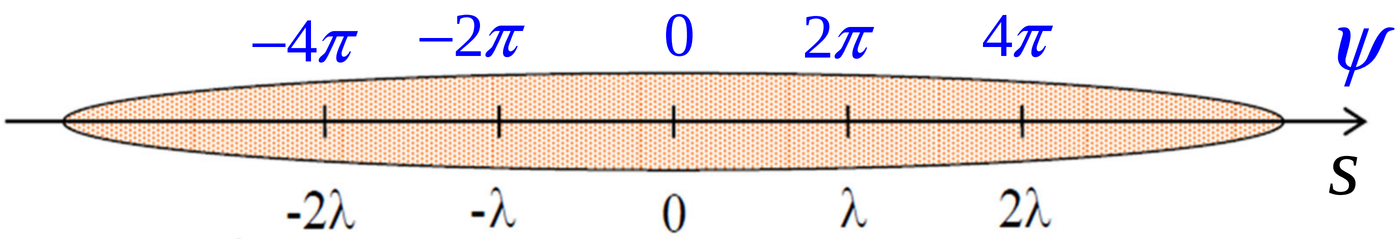

FEL Physics in 1D

„Low gain“ FEL

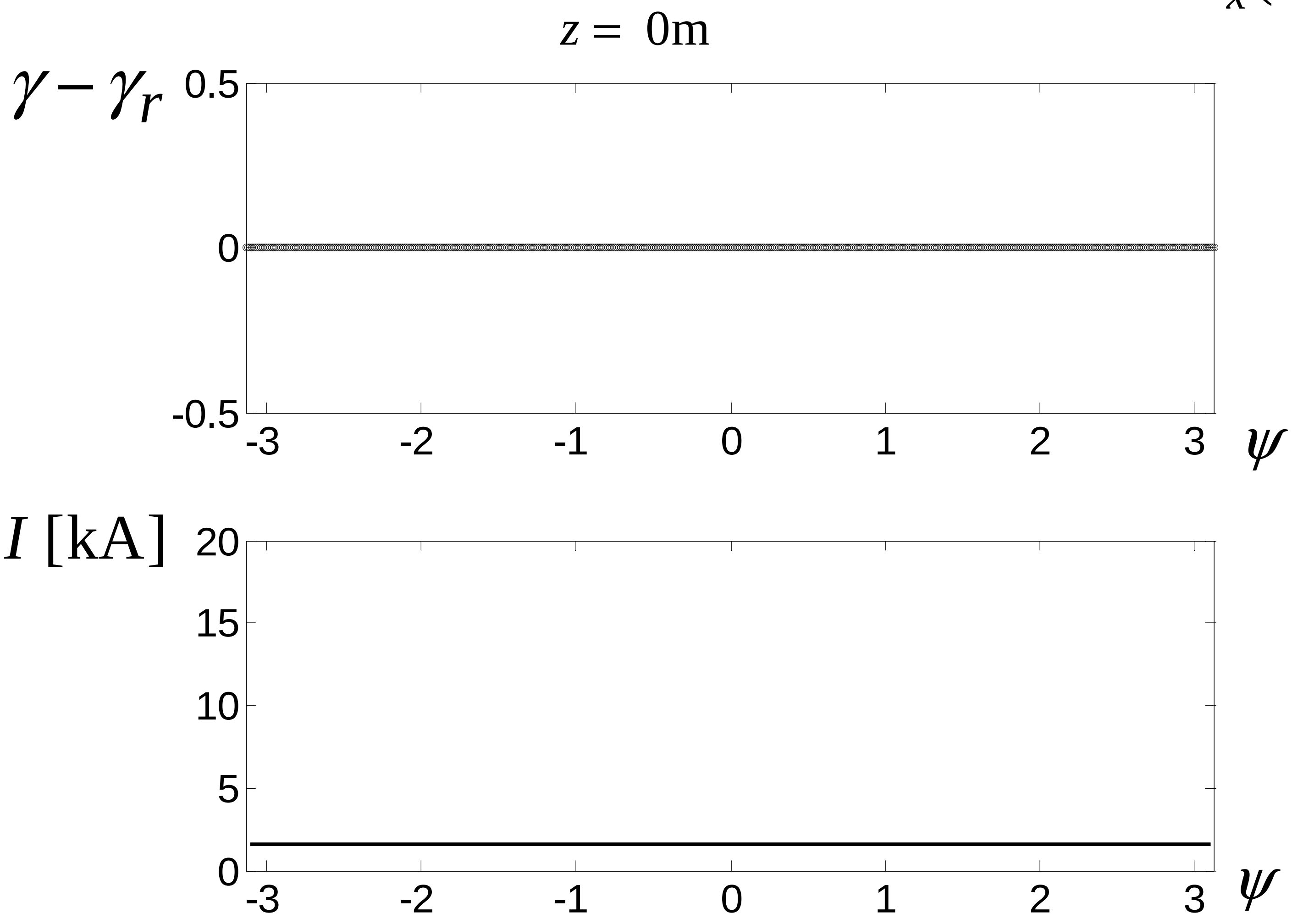

$$E_x(0) = 30\text{MV/m}$$

$$r_{beam} = 0.1\,\text{mm}$$
$$\lambda_u = 27\text{mm}$$
$$K = 1.2$$
$$\lambda = 6\text{ nm}$$
$$I_{peak} = 1.6\text{ kA}$$

FEL Physics in 1D

„Low gain“ FEL

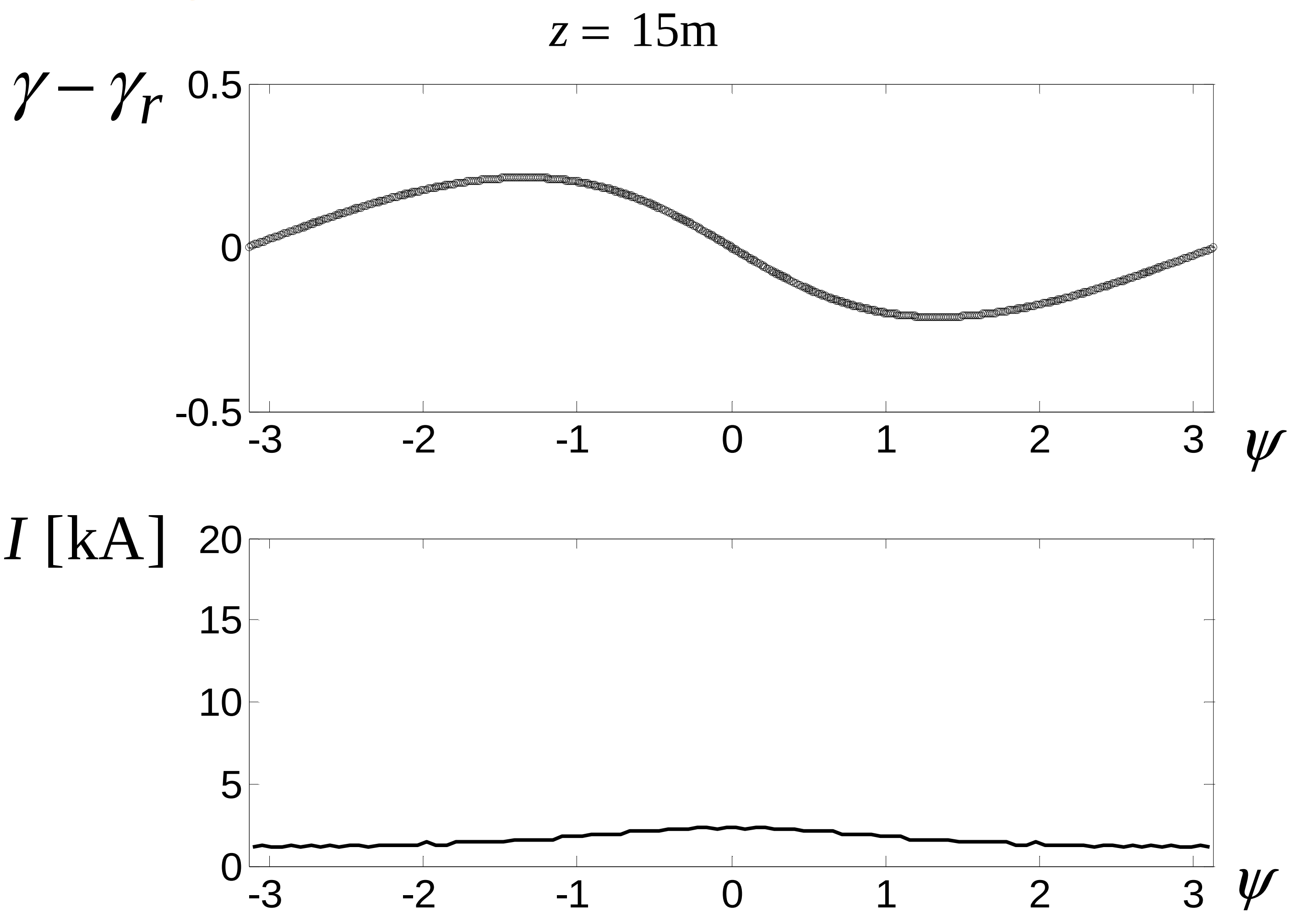

FEL Physics in 1D

„Low gain“ FEL

microbunching

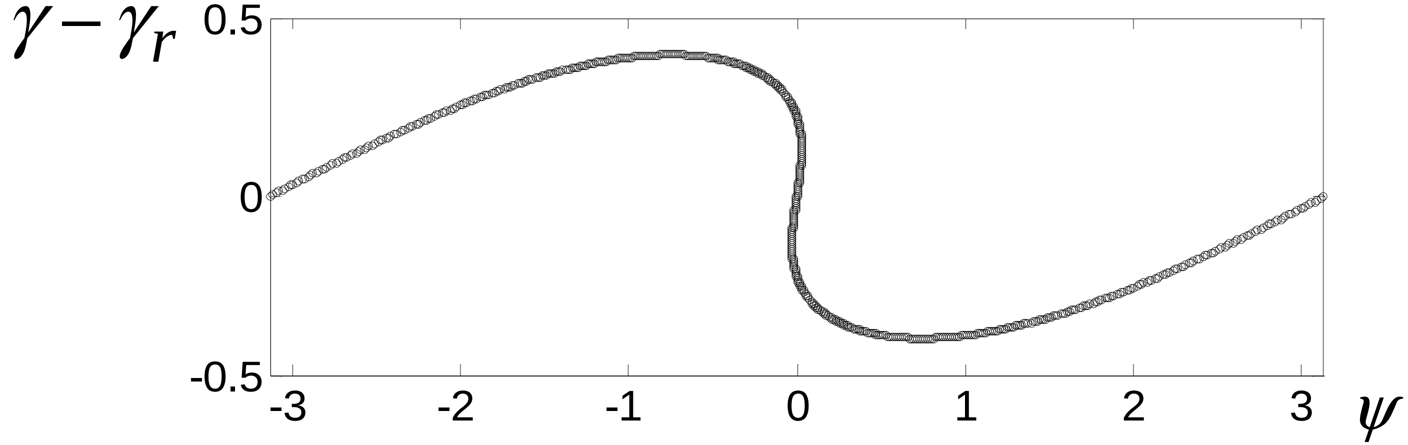

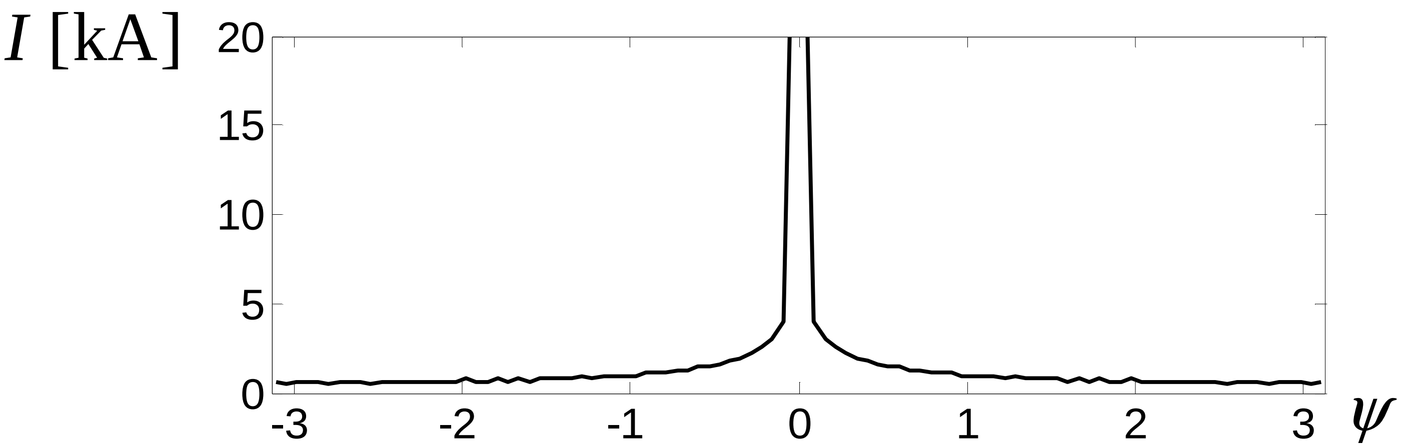

FEL Physics in 1D

Microbunching

$$j_z = \Re(\tilde{j}_z) = j_0 + \Re(\tilde{j}_1(z)e^{i\psi})$$

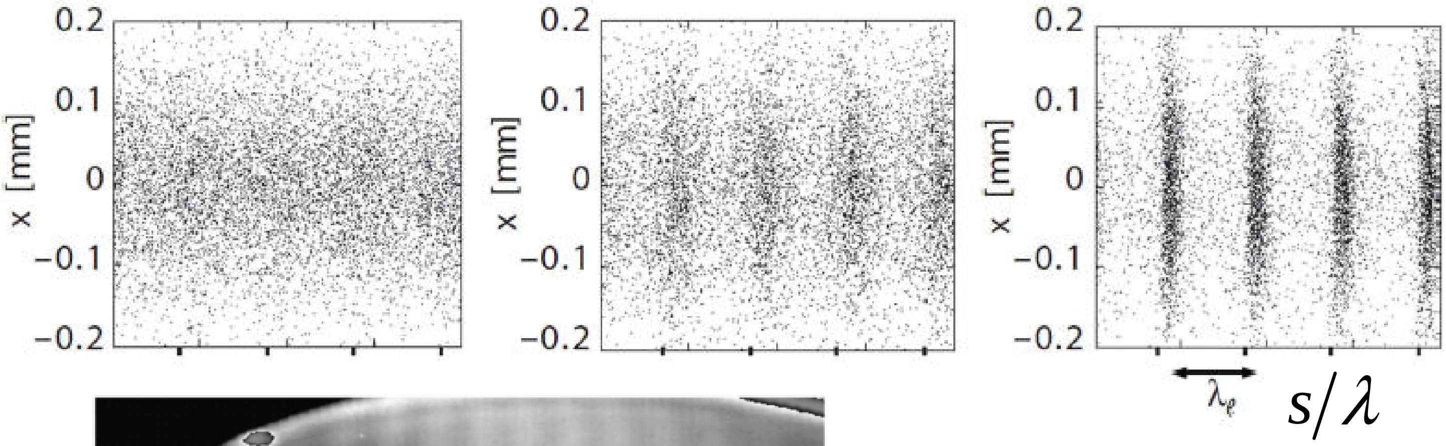

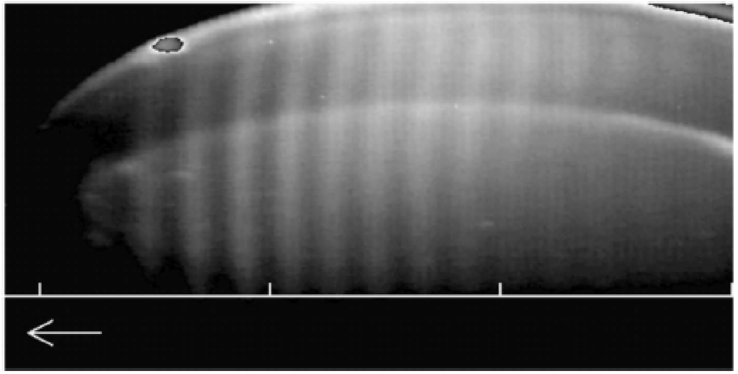

K.N. Ricci ant T.I Smith, PR-STAB **3**, 032801 (2000)

experimental evidence of microbunching in Stanford

FEL Physics in 1D

„High gain“ FEL

$$P_{\text{rad}} \sim N_{el} \Rightarrow P_{\text{rad}} \sim N_{el}^2$$

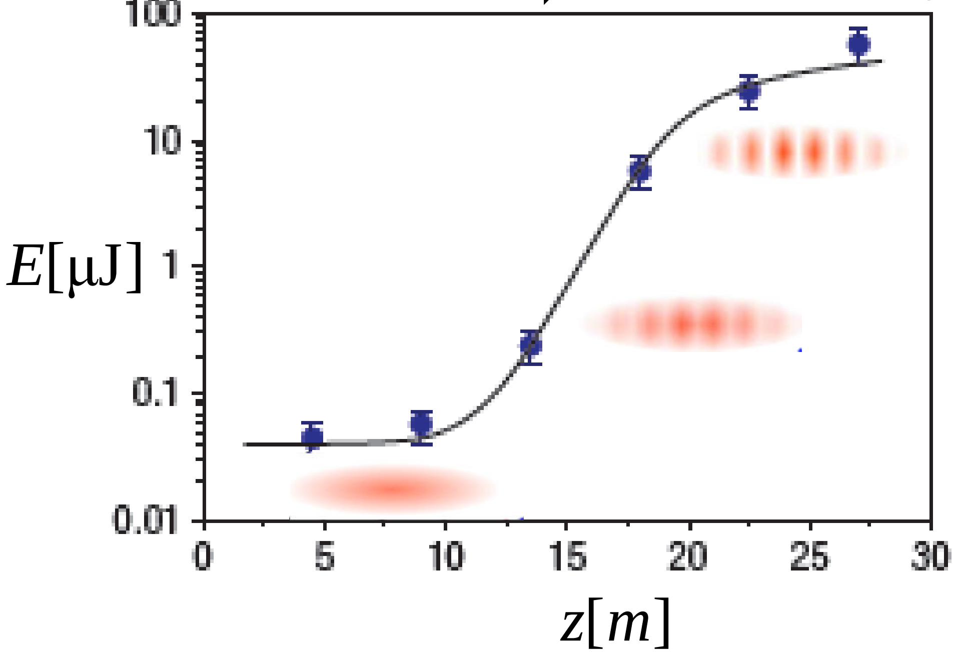

experimental data (FLASH)

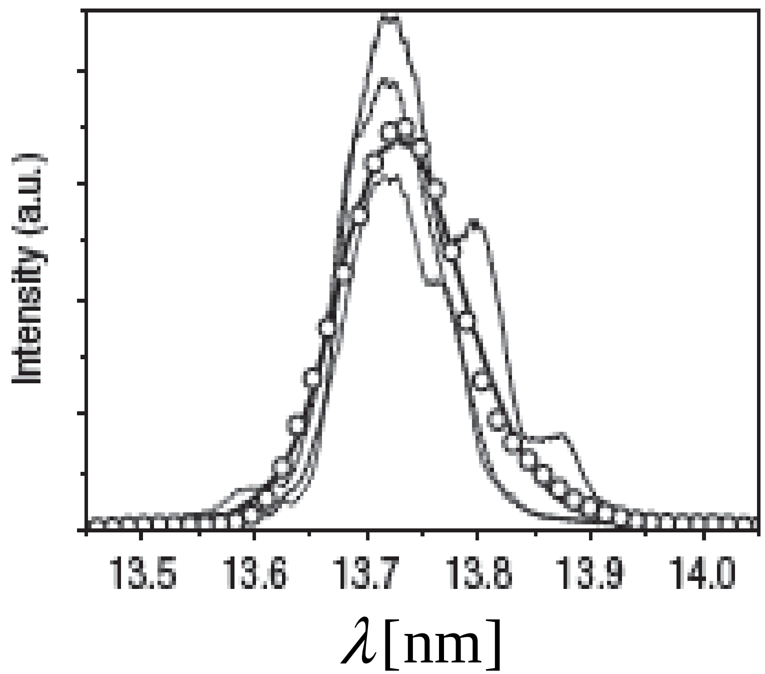

the amplification is very high

W. Ackermann et al, Nature Photonics **1**, 336 (2007)

FEL Physics in 1D

Field equation

The EM field variation has to be taken into account

$$\left(\Delta - \frac{1}{c^2}\frac{\partial^2}{\partial t^2}\right)\mathbf{E} = \mu_0 \frac{\partial \mathbf{j}}{\partial t} + \cancel{\frac{1}{\varepsilon_0}\nabla\rho} \qquad \mathbf{E}(z,t) = \Re\left(\tilde{\mathbf{E}}(z,t)\right)$$

slowly-varying envelope approximation

$$\tilde{E}_x(z,t) = \tilde{E}_x(z)e^{i(kz-\omega t)} \qquad \left|\tilde{E}_x''(z)\right| << k\left|\tilde{E}_x'(z)\right|$$

$$\left[\cancel{\nabla_\perp^2} + 2ik\left(\frac{\partial}{\partial z} + \cancel{\frac{1}{c}\frac{\partial}{\partial t}}\right)\right]\tilde{E} = ik\mu_0 c\frac{K}{\gamma}\tilde{j}_1 \quad \Rightarrow \quad \boxed{\tilde{E}_x'(z) = -\frac{\mu_0 cK}{4\gamma}\tilde{j}_1}$$

DESY

FEL Physics in 1D

Longitudinal equations of motion

$$\frac{d}{dz}\psi_n = 2k_u\eta_n, \qquad n = 1, 2, \ldots N$$

$$\frac{d}{dz}\eta_n = -\frac{eK[JJ]}{2m_e c^2\gamma_r^2}\Re(\tilde{E}_x e^{i\psi_n})$$

Field equation

$$\frac{d}{dz}\tilde{E}_x(z) = -\frac{\mu_0 cK}{4\gamma}\tilde{j}_1$$

FEL Physics in 1D

„High gain“ FEL

$E_x(0) = 0.1\mathrm{MV/m}$

$z = 0\mathrm{m}$

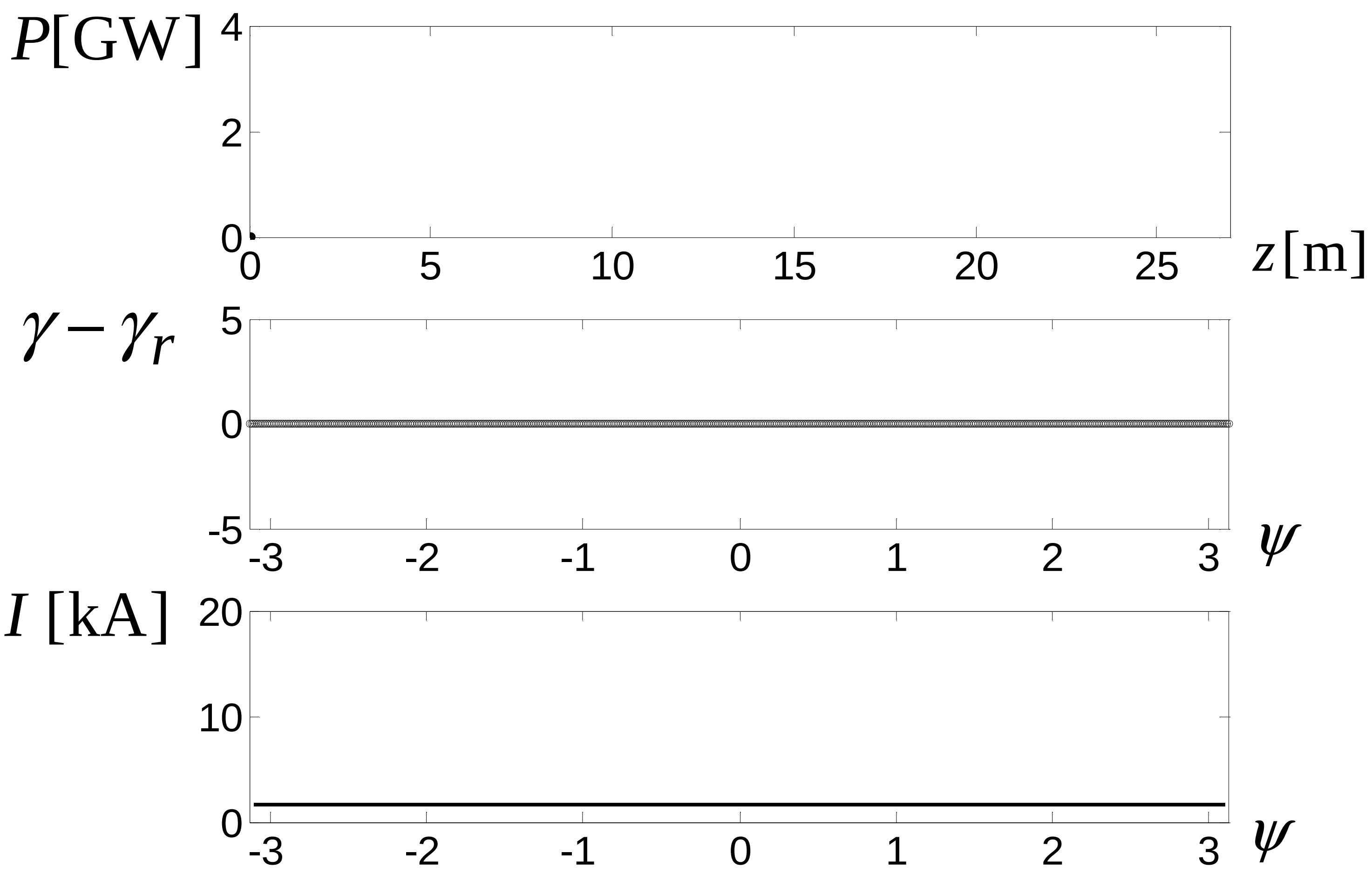

FEL Physics in 1D

„High gain“ FEL

$z = 20\text{m}$

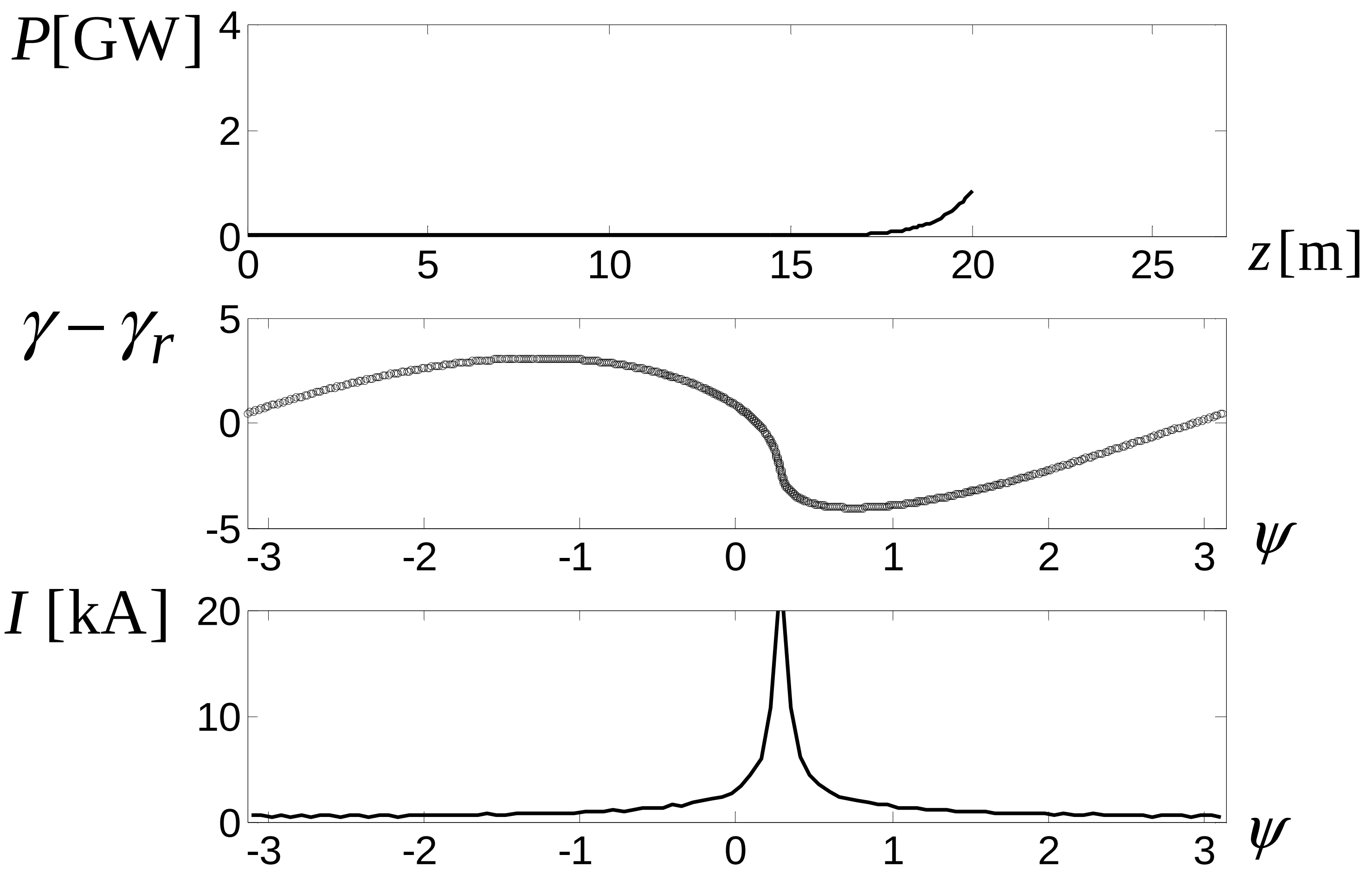

FEL Physics in 1D

„High gain“ FEL

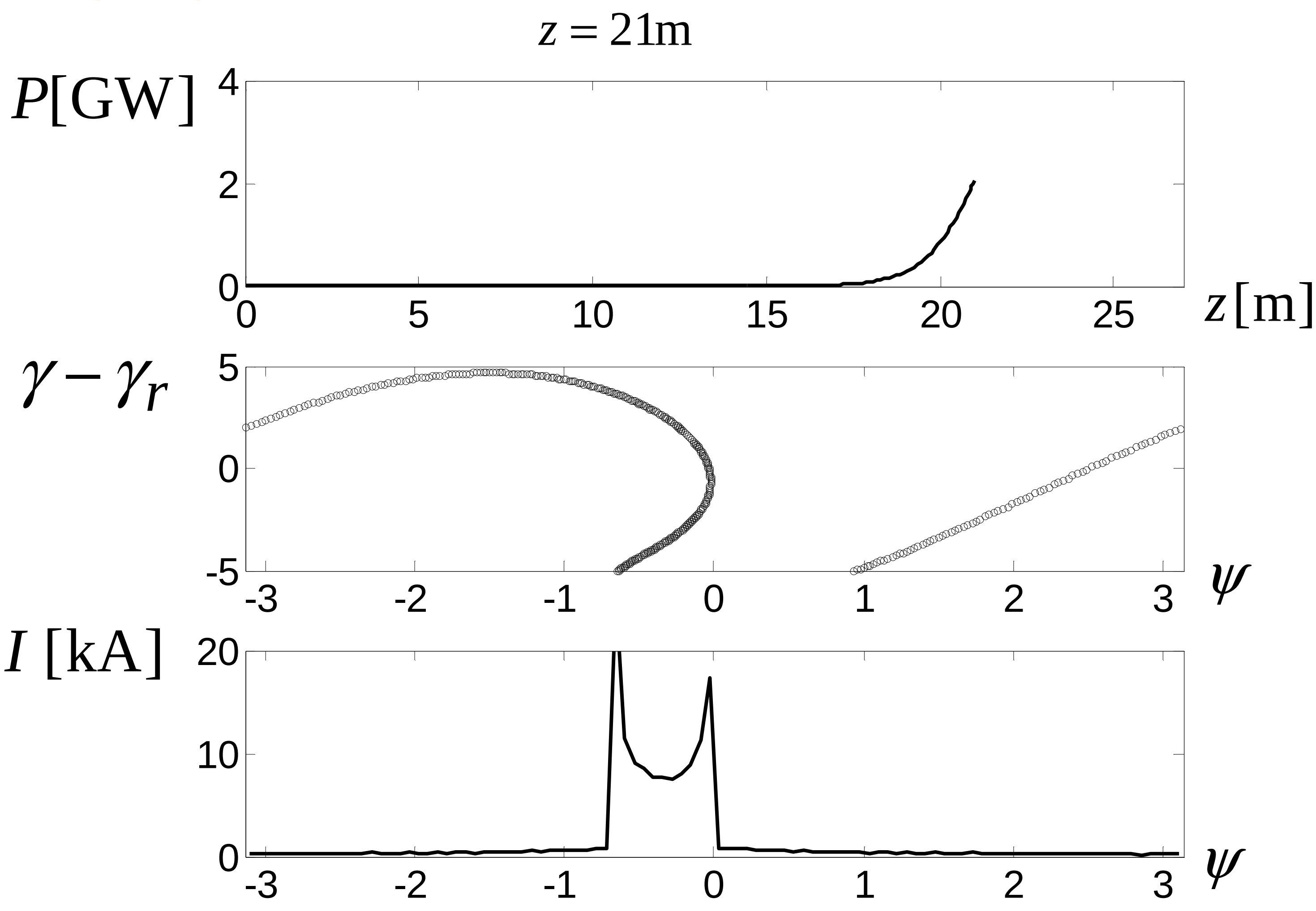

FEL Physics in 1D

„High gain“ FEL

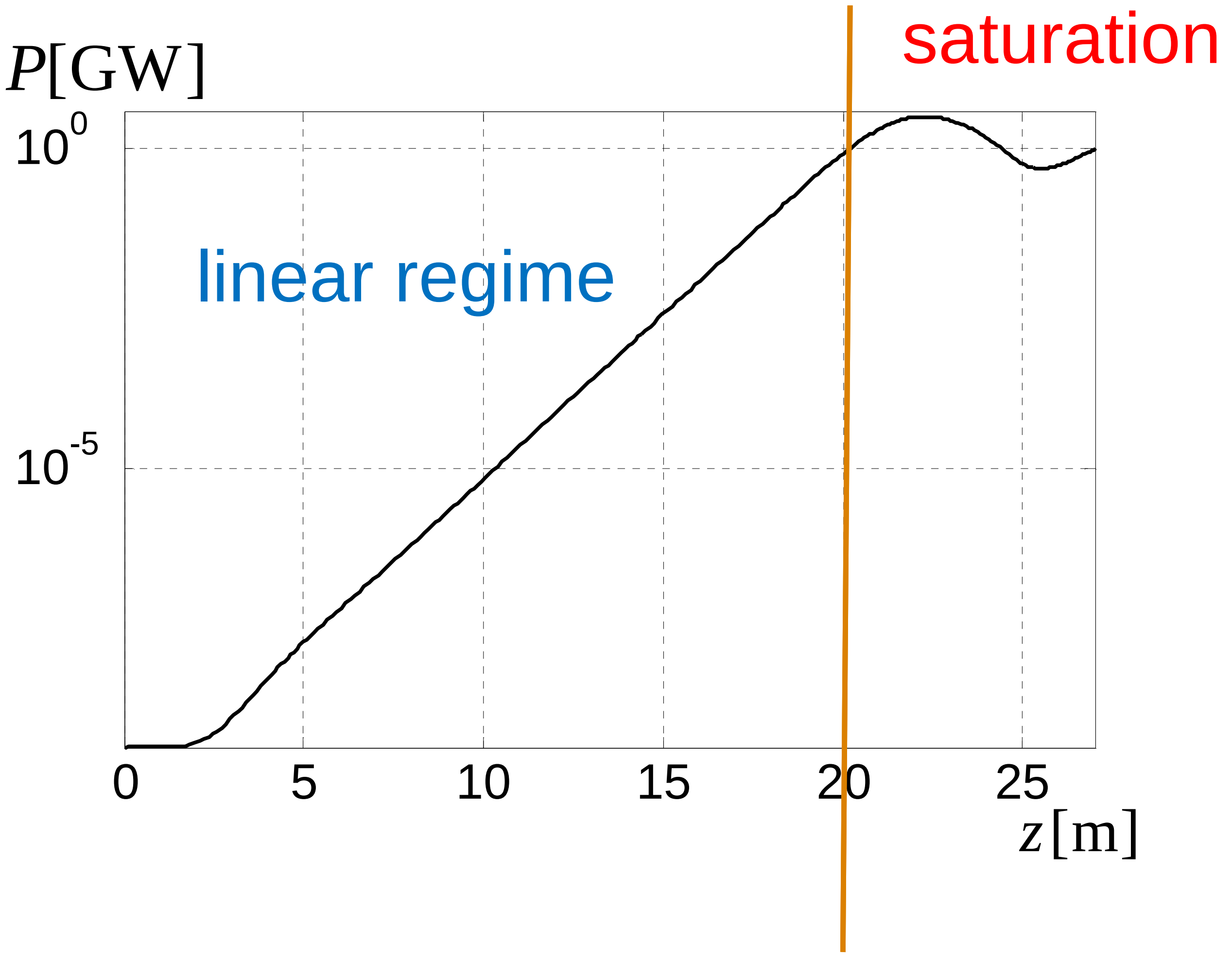

Mathematical Model in 3D

3D Effekte

- transverse beam dynamics
- space charge effects
- beam properties (emittance, energy spread etc.)
- EM field properties
- undulator properties

FEL codes

FAST FELEX FELS FELOS RON FRED3D NUTMEG GENESIS 1.3 GINGER MEDUSA SIMPLEX PERSEO ALICE SARAH TDA3D

Numerical Methods

3D FEL codes used at DESY

	FAST (M.Yurkov)	Genesis 1.3 (S.Reiche)	ALICE (I.Zagorodnov)
Equations of motion	Runge-Kutta		leap-frog
EM field	Integral representation	finite-difference, alternating direction	finite difference, Neumann
Boundary conditions	free space	Dirichlet	free space with PML

- ❑ the codes are parallelized
- ❑ a cluster with 360 processors is used

4:03:39

Mathematical Model in 3D

Equations of motion

T.M. Tran, J.S.Wurtele, *Review of free-electron-laser (FEL) simulation techniques*, Phys. Reports 195 (1990) 1

$$H^0(\mathbf{r},\mathbf{p},t)=c\left(m^2c^2+(\mathbf{p}+e\mathbf{A})^2\right)^{0.5}-e\varphi$$

- change of independent variable

$$\bar{\mathbf{p}}_\perp=\frac{\mathbf{p}_\perp}{mc}$$

$$H(\mathbf{r}_\perp,ct;\bar{\mathbf{p}}_\perp,\bar{p}_t;z)=-\gamma\left(1-\frac{1+|\bar{\mathbf{p}}_\perp|^2+|\mathbf{a}_\perp|^2\cancel{+2(\bar{\mathbf{p}}_\perp,\mathbf{a}_\perp)}}{\gamma^2}\right)^{0.5}+a_z$$

$$\mathbf{a}=\mathbf{A}\frac{e}{mc}$$

- ***wiggler-period-averaging*** (helical undulator)

$$\bar{H}(\mathbf{r}_\perp,ct;\bar{\mathbf{p}}_\perp,\bar{p}_t;z)=-\gamma\left(1-\frac{1+|\bar{\mathbf{p}}_\perp|^2+|\mathbf{a}_\perp|^2}{\gamma^2}\right)^{0.5}+a_z$$

$$a_s\equiv\frac{Ee}{mc\omega}$$

$$|\mathbf{a}_\perp|^2=K^2+2a_sK\sin(\psi+\varphi_s)+a_s{}^2$$

Mathematical Model in 3D

Equations of motion

- longitudinal

$$\frac{d\psi}{dz} = k_w - \frac{1 + \left|\bar{\mathbf{p}}_\perp\right|^2 + K^2}{2\gamma^2}$$

$$\frac{d\gamma}{dz} = -\frac{eK}{m_e c^2 \gamma_r^2} \Re(\tilde{E} e^{i\psi_n}) - \frac{e}{mc^2} E_z$$

transverse EM field

longitudinal space charge

- transverse (slow)

$$\frac{d\,\mathbf{r}_\perp}{d\,z} = \frac{\bar{\mathbf{p}}_\perp}{\gamma\beta_z}$$

$$\frac{d\,\bar{p}_x}{dz} = -\left(\frac{K^2 k_x^2}{\gamma\beta_z} + \frac{eg}{mc}\right)x$$

$$\frac{d\,\bar{p}_y}{dz} = -\left(\frac{K^2 k_y^2}{\gamma\beta_z} - \frac{eg}{mc}\right)y$$

Mathematical Model in 3D

Field equations

- transverse field ***(slowly-varying envelope approximation)***

$$E(\vec{r},t) = \tilde{E}(\vec{r},t)\exp\left(i\left(kz - \omega t\right)\right) + c.c. \qquad E = E_x + iE_y$$

$$\left[\nabla_\perp^2 + 2ik\left(\frac{\partial}{\partial z} + \cancel{\frac{1}{c}\frac{\partial}{\partial t}}\right)\right]\tilde{E} = ik\mu_0 c\frac{K}{\gamma}\tilde{j}_1$$

- longitudinal space charge (on λ scale)

$$\left(\nabla_\perp^2 - \frac{n^2(k+k_w)^2}{\gamma_z^2}\right)E_z^{(n)} = \frac{in(k+k_w)}{\varepsilon_0\gamma_z^2}\rho^{(n)}$$

$$E_z(r,\psi) = \sum E_z^{(n)}(r,z)e^{in\psi}$$

Mathematical Model in 3D

Normalized Equations

- equations of motion

$$\frac{d\psi}{d\hat{z}} = \hat{C} + \hat{\eta} - \frac{B}{2}\left(\hat{x}'^2 + \hat{y}'^2\right)$$

$$\frac{d\hat{\eta}}{d\hat{z}} = |\hat{u}|\cos(\psi + \varphi_s) - \hat{E}_z$$

$$\hat{x}'' = -\left(\hat{k}_x^2 + \hat{g}\right)\hat{x}$$

$$\hat{y}'' = -\left(\hat{k}_y^2 - \hat{g}\right)\hat{y}$$

- field equations

$$\left[\frac{1}{2iB}\hat{\Delta}_\perp + \frac{d}{d\hat{z}}\right]\hat{u}\left(\hat{\mathbf{r}}_\perp, \hat{z}\right) = -2a^{(1)}\left(\hat{\mathbf{r}}_\perp, \hat{z}\right)$$

$$\hat{E}_z = \hat{E}_z^{(0)} - \hat{\Lambda}_p{}^2 \frac{1}{N_{jk}} \sum_{i=1}^{N_{jk}} \left[\pi \operatorname{sgn}(\psi - \psi_i) - (\psi - \psi_i)\right]$$

Zagorodnov I., Dohlus M., *Numerical FEL studies with a new code ALICE*, FEL09, Liverpool, 2009.

Numerical Methods

Equations of motion

- **“leap-frog” scheme** for the longitudinal equations

$$\frac{\psi_{j+0.5}-\psi_{j-0.5}}{\Delta\hat{z}}=\hat{\eta}_j+\hat{C}_j-\frac{B}{2}\left(\hat{x}_j'^{\,2}+\hat{y}_j'^{\,2}\right)\qquad j=1:N_z$$

$$\frac{\hat{\eta}_{j+1}-\hat{\eta}_j}{\Delta z}=\frac{\hat{u}_{j+1}+\hat{u}_j}{2}\cos\left[\psi_{j+0.5}+\frac{\varphi^s_{j+1}+\varphi^s_j}{2}\right]+\hat{E}_{z,j+0.5},$$

- **matrix formalism** for the transverse equations

$$\begin{pmatrix}\hat{x}_{j+1}\\ \hat{x}'_{j+1}\end{pmatrix}=M_x\begin{pmatrix}\hat{x}_j\\ \hat{x}'_j\end{pmatrix}\qquad\qquad \begin{pmatrix}\hat{y}_{j+1}\\ \hat{y}'_{j+1}\end{pmatrix}=M_y\begin{pmatrix}\hat{y}_j\\ \hat{y}'_j\end{pmatrix}$$

Numerical Methods

Field equation

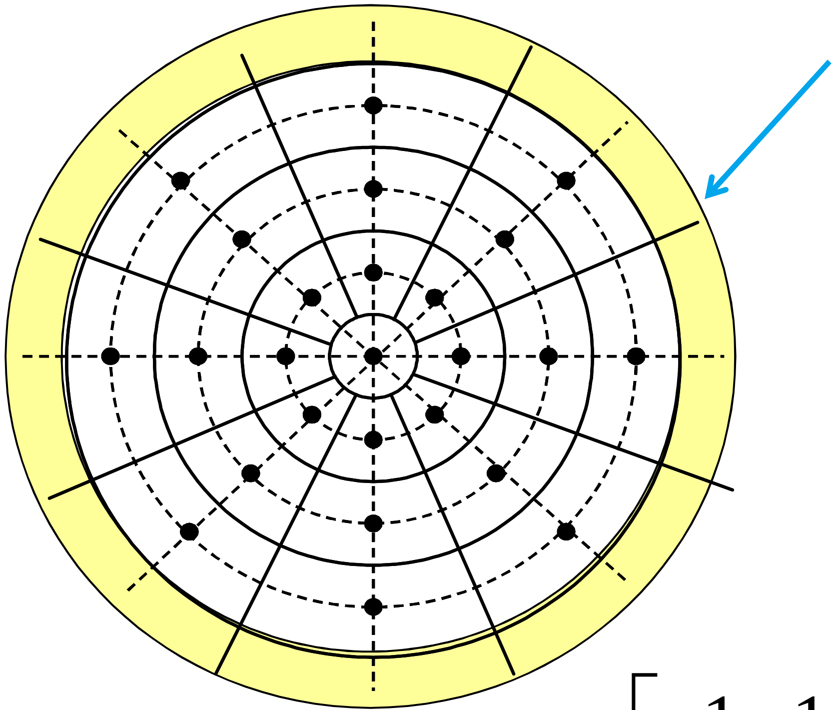

Perfectly Matched Layer

F. Collino, Journal of Computational Physics 131, 164 (1997)

azimuthal expansion

$$\hat{u}(r,z,\varphi)=\sum u^{(m)}(r,z)e^{im\varphi}$$

$$\left[\frac{1}{2iB}\frac{1}{r}\frac{\partial}{\partial r}r\frac{\partial}{\partial r}-\frac{m^2}{r^2}+\frac{d}{dz}\right]u^{(m)}=-2a^{(1)(m)}$$

DESY

Numerical Methods

Perfectly Matched Layer (PML)

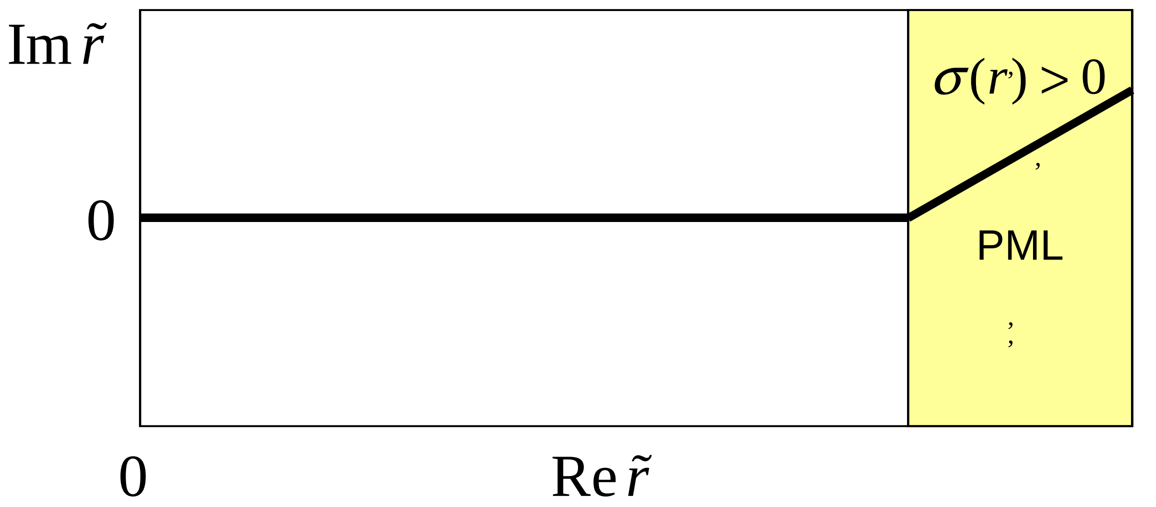

$$\tilde{r} = r + \frac{i}{B}\int_0^r \sigma(\xi)\,d\xi \qquad \sigma(r) = \begin{cases} 0, & r \le r_0 \\ > 0, & r > r_0 \end{cases}$$

- a deformed contour in the complex plane

$$\left[\frac{1}{2iB}\frac{1}{\tilde{r}}\frac{\partial}{\partial \tilde{r}}\tilde{r}\frac{\partial}{\partial \tilde{r}} - \frac{m^2}{\tilde{r}^2} + \frac{d}{dz}\right]u^{(m)} = -2a^{(1)(m)}$$

Numerical Methods

Neumann implicit scheme with PML

$$c_q u_{q+1}^{n+1} + b_q u_q^{n+1} + a_q u_{q-1}^{n+1} = f_q^n$$

The matrix of the system has only three diagonals and we can use the „sweep“ method

$$a_q = \frac{\Delta z}{4iB}\frac{1}{\tilde r_j}\frac{\tilde r_{j-0.5}}{(\tilde r_{j+0.5}-\tilde r_{j-0.5})(\tilde r_j-\tilde r_{j-1})} \qquad b_q = (1-a_q-c_q)-\frac{\Delta z}{iB}\frac{m^2}{\tilde r_j^{\,2}}$$

$$c_q = \frac{\Delta z}{4iB}\frac{1}{\tilde r_j}\frac{\tilde r_{j+0.5}}{(\tilde r_{j+0.5}-\tilde r_{j-0.5})(\tilde r_{j+1}-\tilde r_j)}$$

complex numbers!

Numerical Methods

PML performance

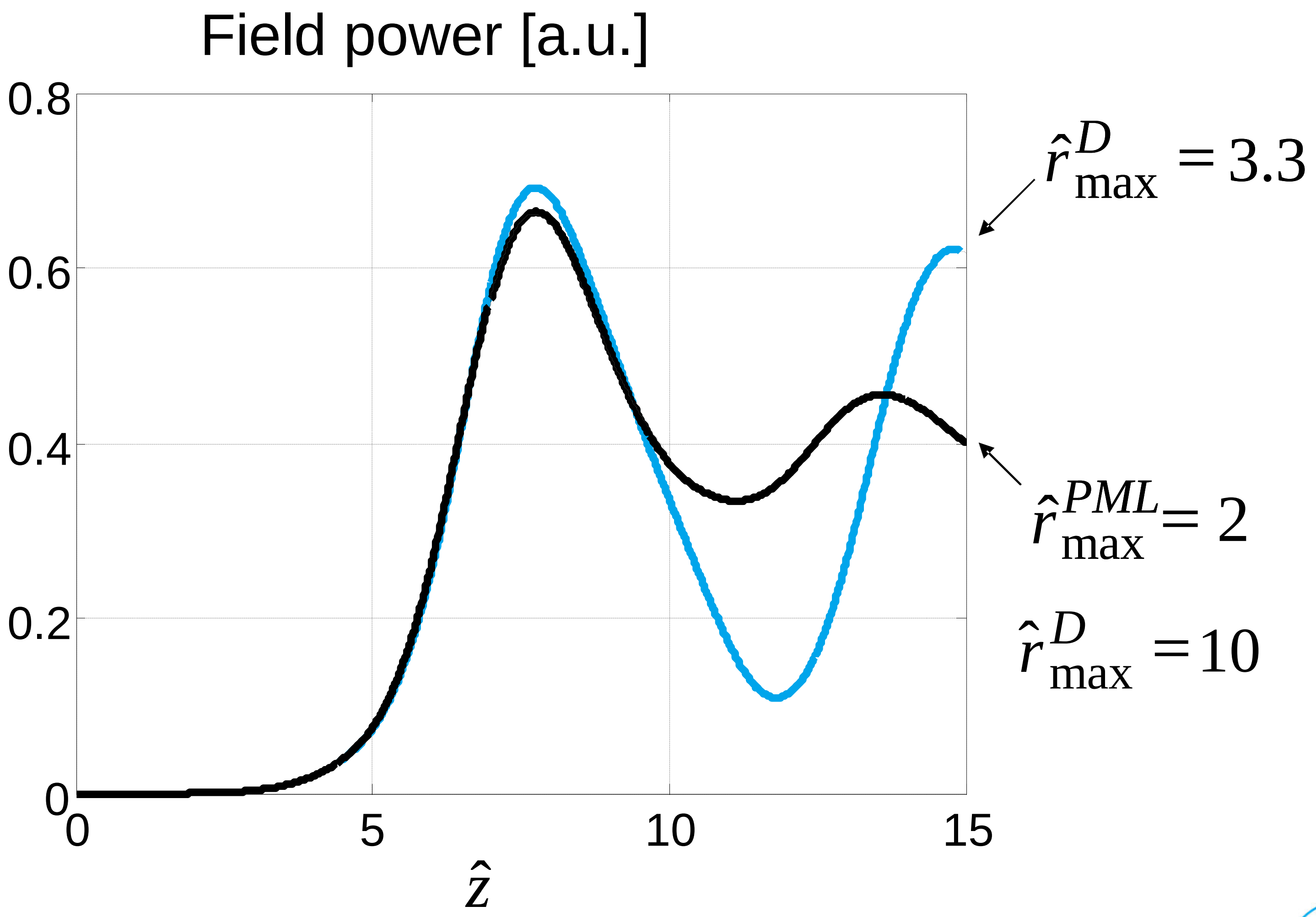

Quiet Start and Shot Noise

Quiet start in FEL amplifier

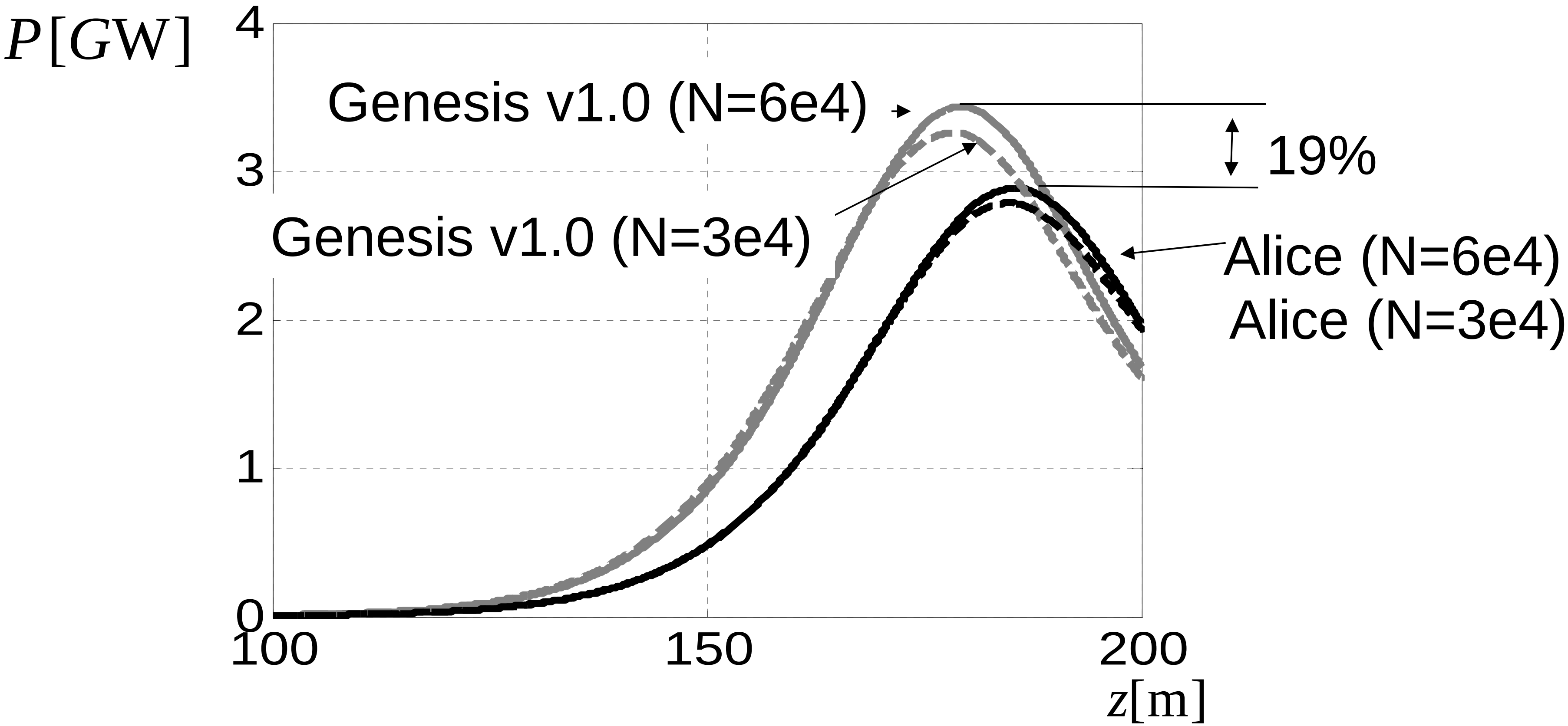

The difference in saturation length is 7 %.

The difference in power gain is 19 %.

Quiet Start and Shot Noise

Quiet Start ?

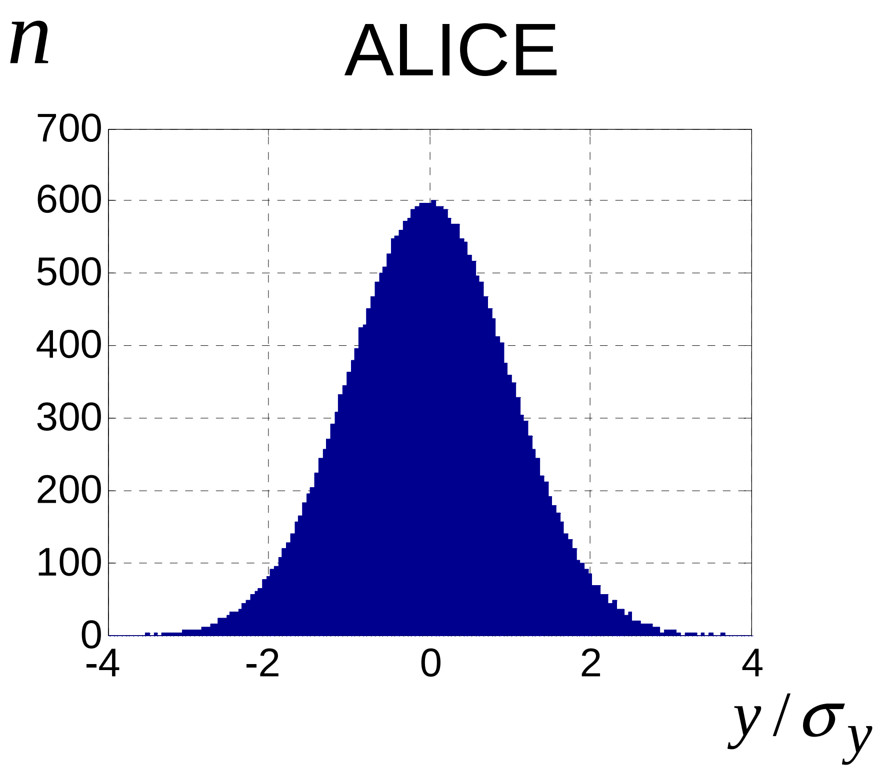

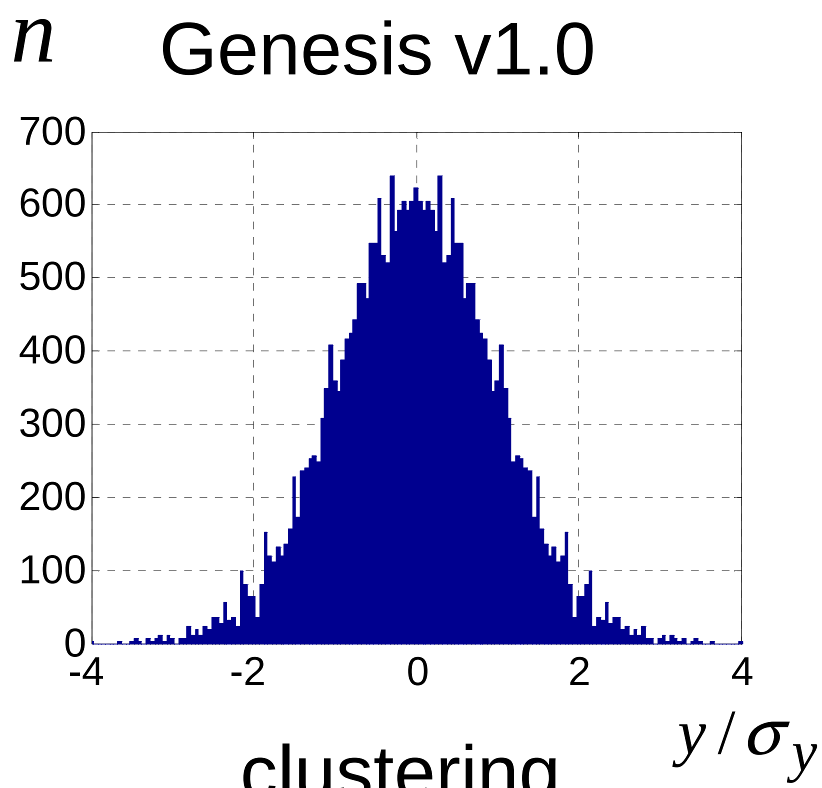

clustering

What is the reason?

Quiet Start and Shot Noise

Quiet Start ?

William H. Press et al, Numerical Recipes in Fortran. The Art of Scientific Computing, 1992

Uniform

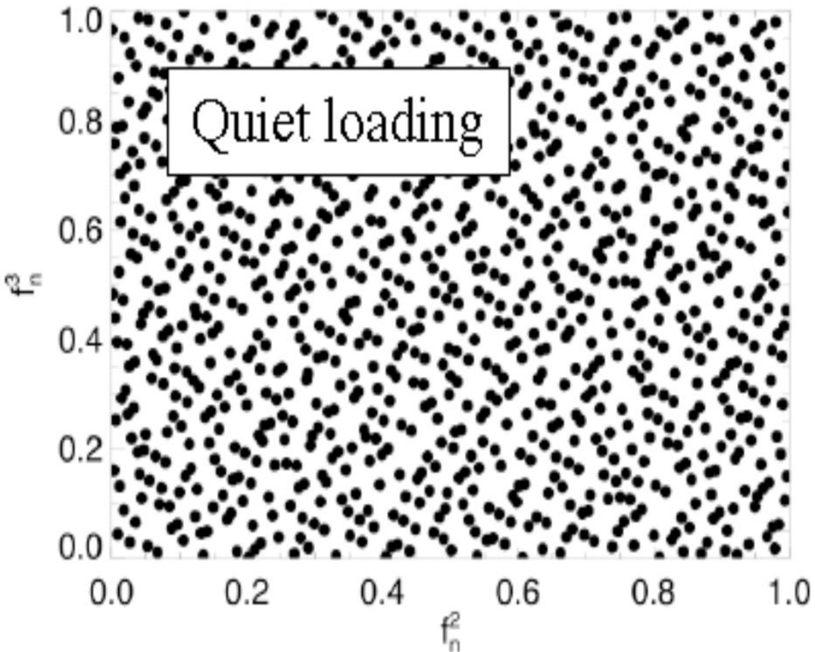

Normal

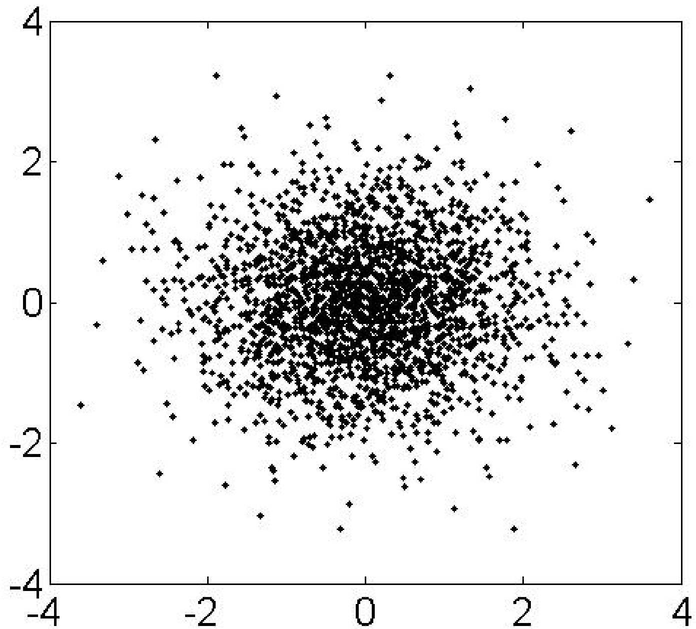

The polar form of Box-Muller algorithm (in Genesis, ASTRA) maps the „quiet" uniform distribution in a clustered normal distribution.

Quiet Start and Shot Noise

Quiet Start ?

ALICE

x'[a.u.]

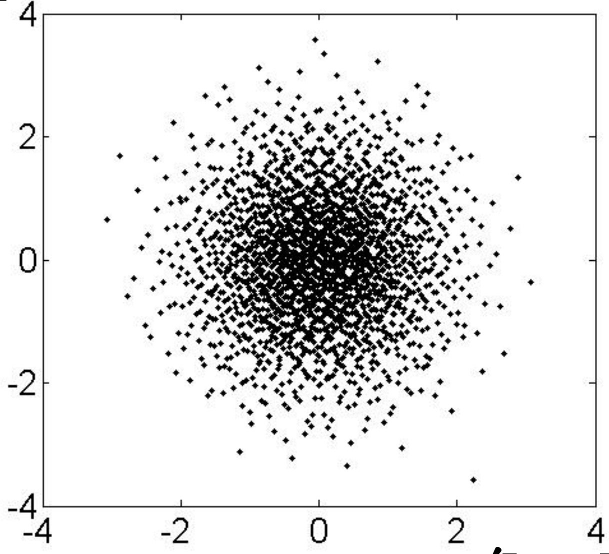

y'[a.u]

inverse error function transformation

$$Y_i = \sigma\sqrt{2}\,\mathrm{erf}^{-1}(2X_i - 1) + \mu$$

Genesis v1.0

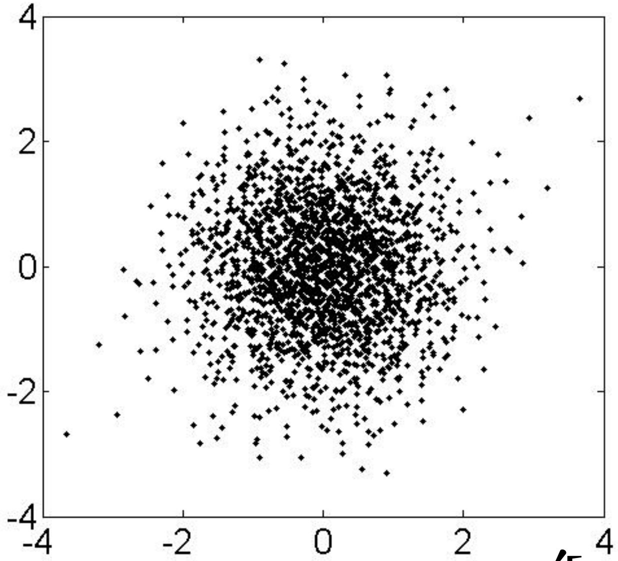

y'[a.u]

Box-Mueller algorithm

Quiet Start and Shot Noise

Properties of the normal distribution

$$\delta = \frac{|\sigma_4 - \tilde{\sigma}_4|}{\sigma_4} 100\%$$

	N	δ_x, %	δ_y, %
Genesis v1.0	7500	**1.5**	**7.5**
	15000	**4.1**	**4.7**
ALICE	7500	**0.8**	**1.0**
	15000	**0.4**	**0.4**

Quiet Start and Shot Noise

New Genesis v2.0 vs. ALICE

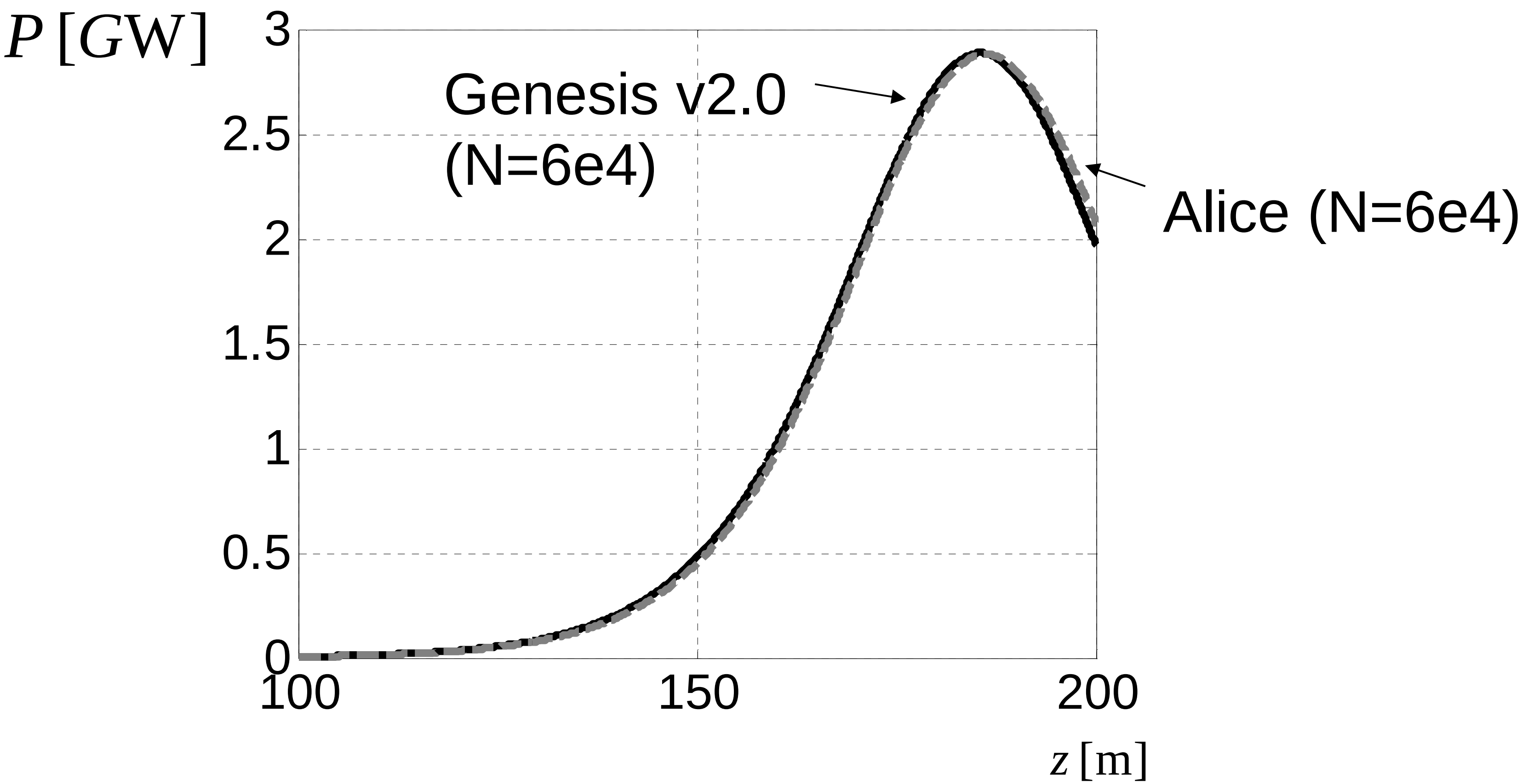

Quiet Start and Shot Noise

Convergence

$$\delta = \frac{|\sigma_4 - \tilde{\sigma}_4|}{\sigma_4} 100\%$$

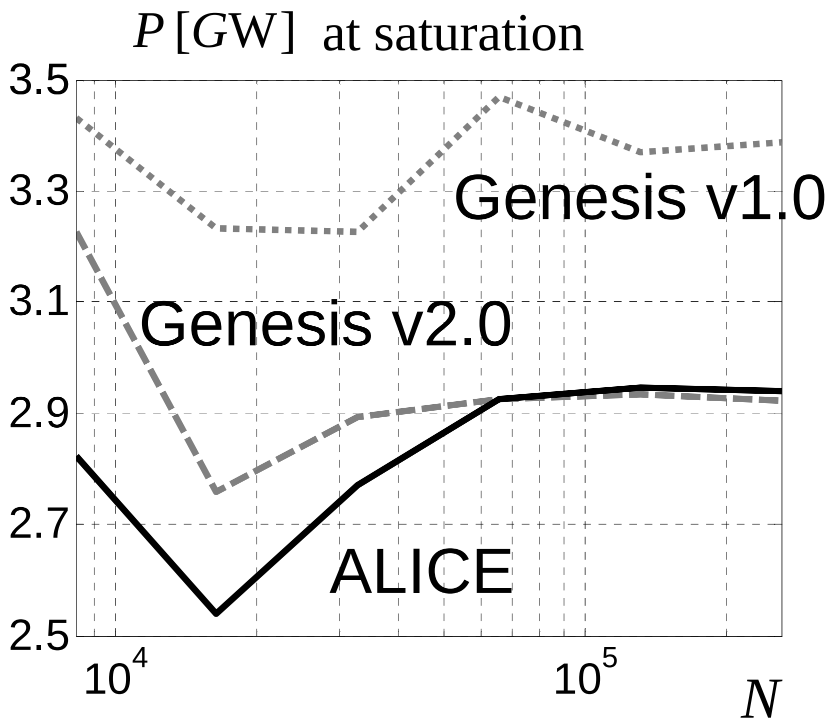

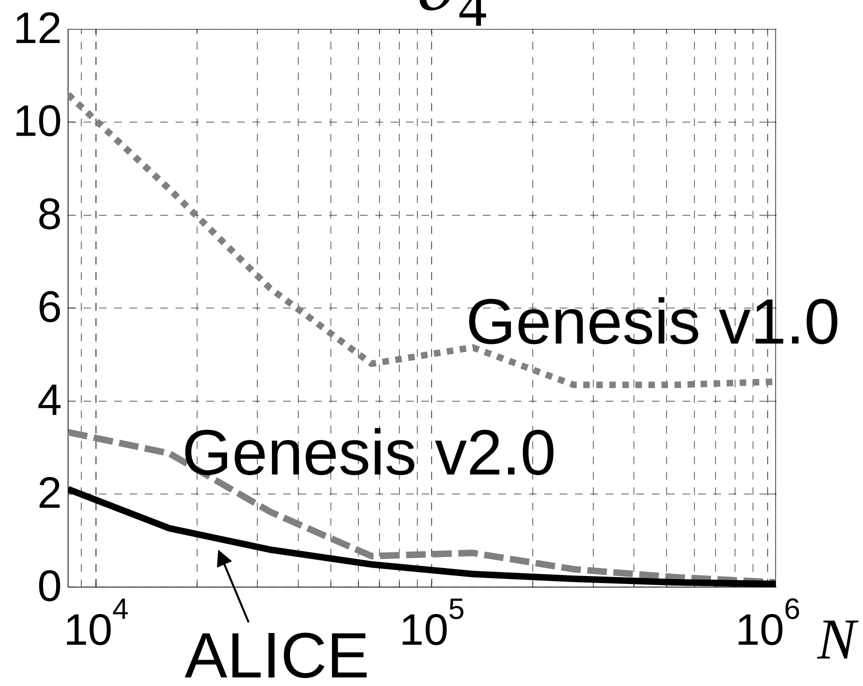

Genesis 1.0: Hammersley and Box-Mueller
Genesis 2.0: Hammersley and the inverse error function
ALICE: Sobol and the inverse error function

Quiet Start and Shot Noise

Shot noise algorithm

$$b^{(n)} = \frac{1}{N_e}\sum_{m=1}^{N_e} e^{in\psi_m}$$

$$\left\langle \left| b^{(n)} \right| \right\rangle = \sqrt{\frac{\pi}{4N_e}}$$

$$\left\langle \left| b^{(n)} \right|^2 \right\rangle = \frac{1}{N_e}$$

- beamlets and variation in position (W.Fawley)
- variations in charges (B.McNeil et al.)

$$\boxed{N \ll N_e}$$

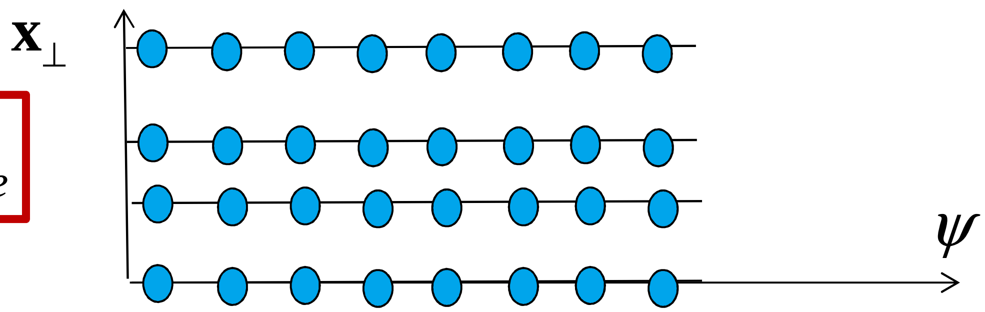

beamlets - a set of 2M particles with the same position $\mathbf{x}_\perp = (x, y, p_x, p_y, \gamma)$

N_b beamlets with 2M particles each.

$$\left\langle \left| b_k^{(j)} \right|^2 \right\rangle = 0; \quad k = 1 : N_b,\ j = 1 : M$$

Quiet Start and Shot Noise

Shot noise algorithm

Small position variations

W.M. Fawley, Phys. Rev. STAB 5 (2002) 070701

$$\delta\theta_j = \sum_{m=1}^{m=M} a_m \cos(m\theta_j) + b_m \sin(m\theta_j) \qquad j = 1:2M$$

$$a_{m,rms} = b_{m,rms} = \sqrt{\frac{2}{N_b m^2}}, \quad m \le M \text{ ?!}$$

A more careful analysis for the highest harmonic m=M yields

$$a_{M,rms} = b_{M,rms} = \sqrt{\frac{1}{N_b M^2}}$$

Time Dependent Simulations

Slice parameters are extracted from "Gun-to-Undulator" simulations

$$\gamma \quad \Delta\gamma \quad \varepsilon_x \quad \varepsilon_y \quad \beta_x \quad \beta_y \quad \langle x \rangle \quad \langle y \rangle \quad \langle x' \rangle \quad \langle y' \rangle \quad \alpha_x \quad \alpha_y \quad I$$

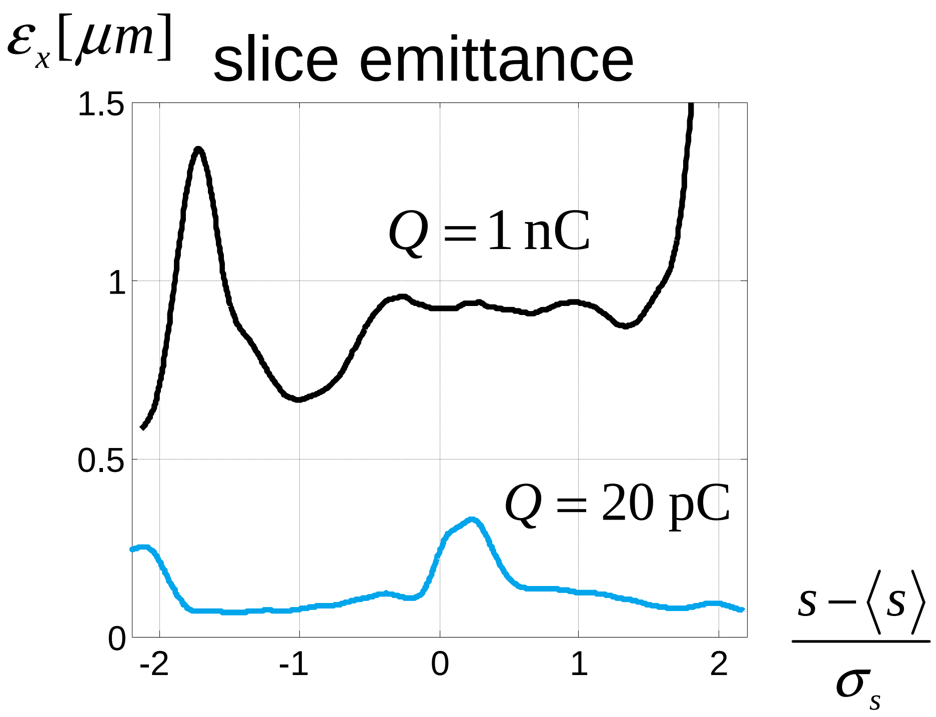

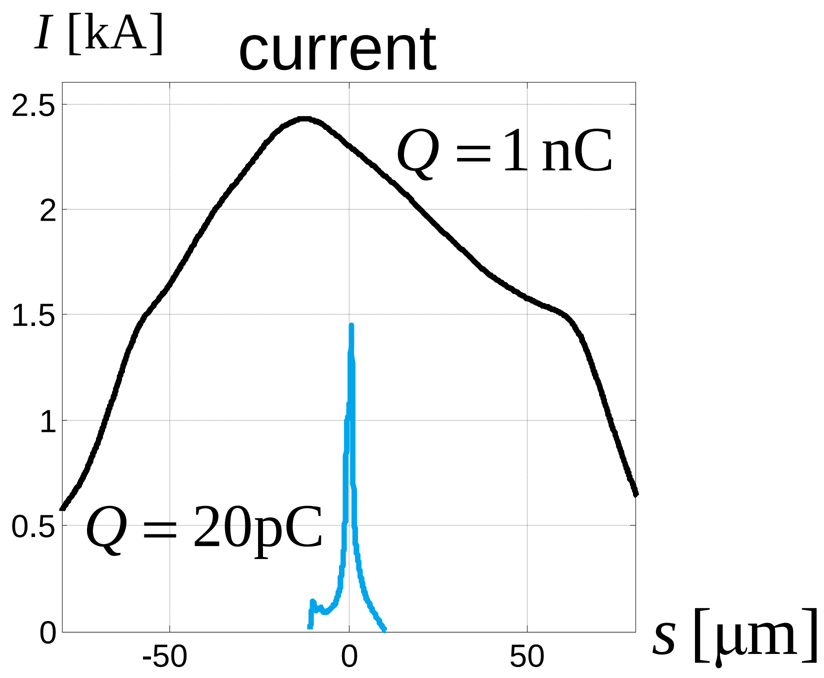

Time Dependent Simulations

Field equation

$$\left[\nabla_\perp^2 + 2ik\left(\frac{\partial}{\partial z} + \frac{1}{c}\frac{\partial}{\partial t}\right)\right]\tilde{E}(z,t) = ik\mu_0 c\frac{K}{\gamma}\tilde{j}_1(z,t)$$

$$t = t_0 + \frac{z}{c} \qquad \Rightarrow \qquad \left[\frac{\nabla_\perp^2}{2ik} + \frac{d}{dz}\right]\tilde{E}\left(z, t_0 + \frac{z}{c}\right) = F\left(z, t_0 + \frac{z}{c}\right)$$

$t_j(z_{n+0.5})$ - the time when slice j reaches position $z_{n+0.5}$

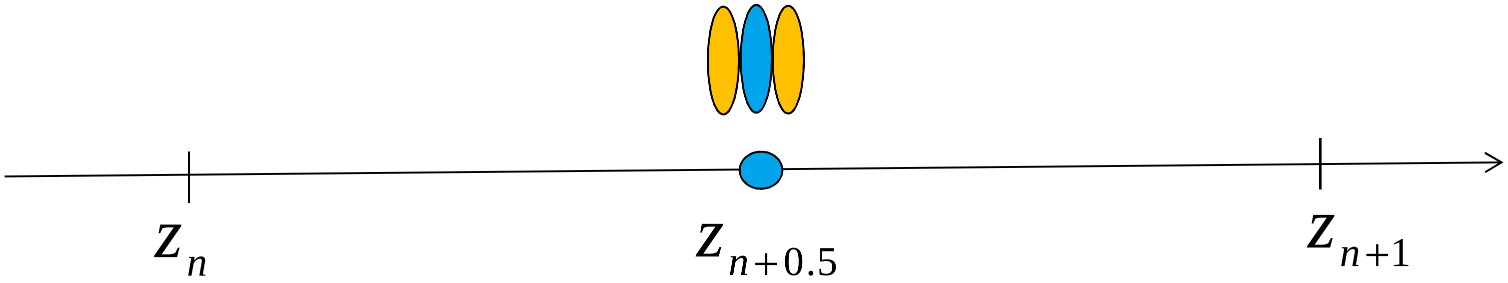

$$\frac{d}{dz}\tilde{E}\left(z_{n+0.5}, t_j(z_{n+0.5})\right) = \frac{\tilde{E}\left(z_{n+1}, t_j(z_{n+0.5}) + \frac{0.5\Delta z}{c}\right) - \tilde{E}\left(z_n, t_j(z_{n+0.5}) - \frac{0.5\Delta z}{c}\right)}{\Delta z} + O(2)$$

Time Dependent Simulations

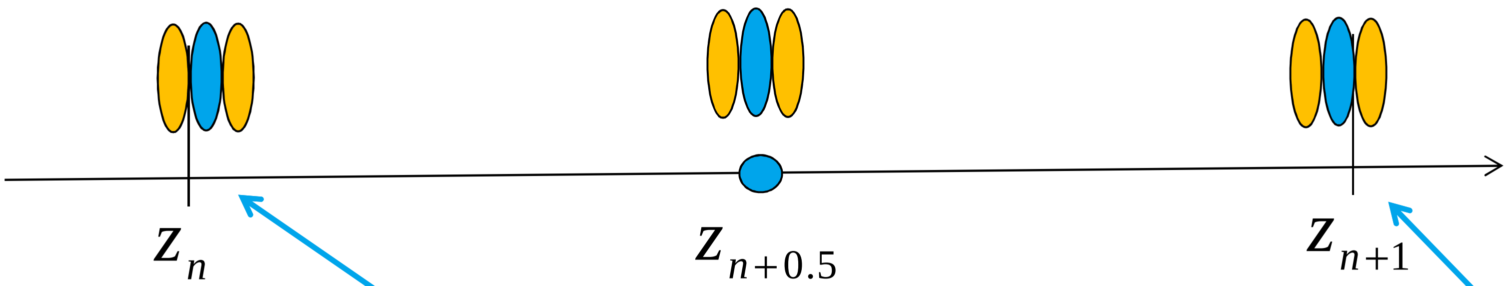

$$t_j(z_{n+0.5}) - \frac{0.5\Delta z}{c} = t_{j-0.5}(z_n) \qquad t_j(z_{n+0.5}) + \frac{0.5\Delta z}{c} = t_{j+0.5}(z_{n+1})$$

field of the current slice j

field of the previous slice j-1

$$\frac{\nabla_\perp^2}{2ik}\left(\frac{\tilde{E}_{n+1}^{j} + \tilde{E}_{n}^{j-1}}{2}\right) + \frac{\tilde{E}_{n+1}^{j} - \tilde{E}_{n}^{j-1}}{\Delta z} = F(z_{n+0,5}, t_j(z_{n+0,5}))$$

$$\tilde{E}_n^j = \tilde{E}\left(z_n, t_{j+0.5}(z_n)\right)$$

Time Dependent Simulations

Parallel algorithm

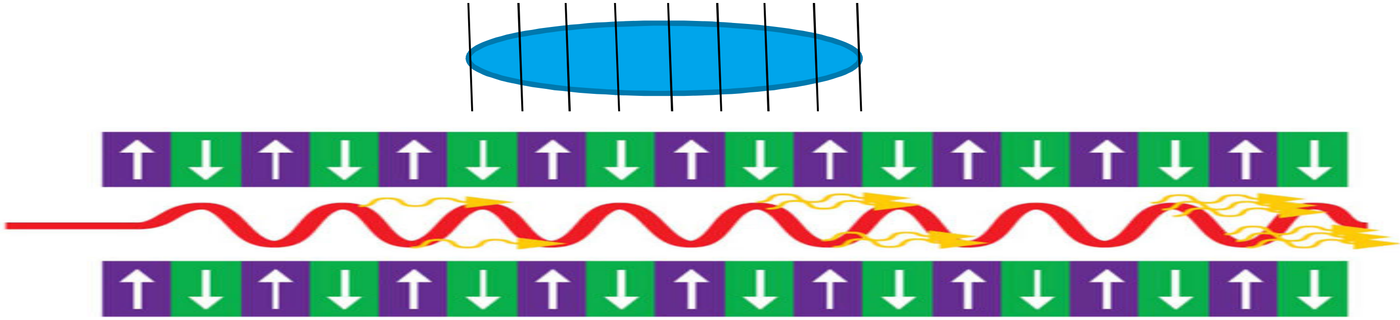

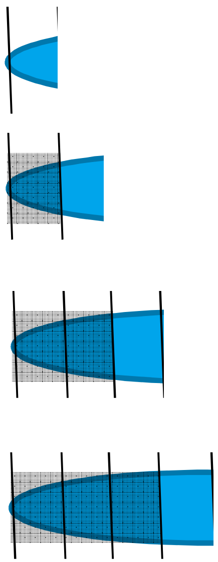

„Slice for slice"

- ❑ we start from the last slice and track the particles of this slice through the undulator; the radiated EM field is saved.
- ❑ then we track the next slice in the radiation field of the previous slices

Time Dependent Simulations

SASE in the European XFEL

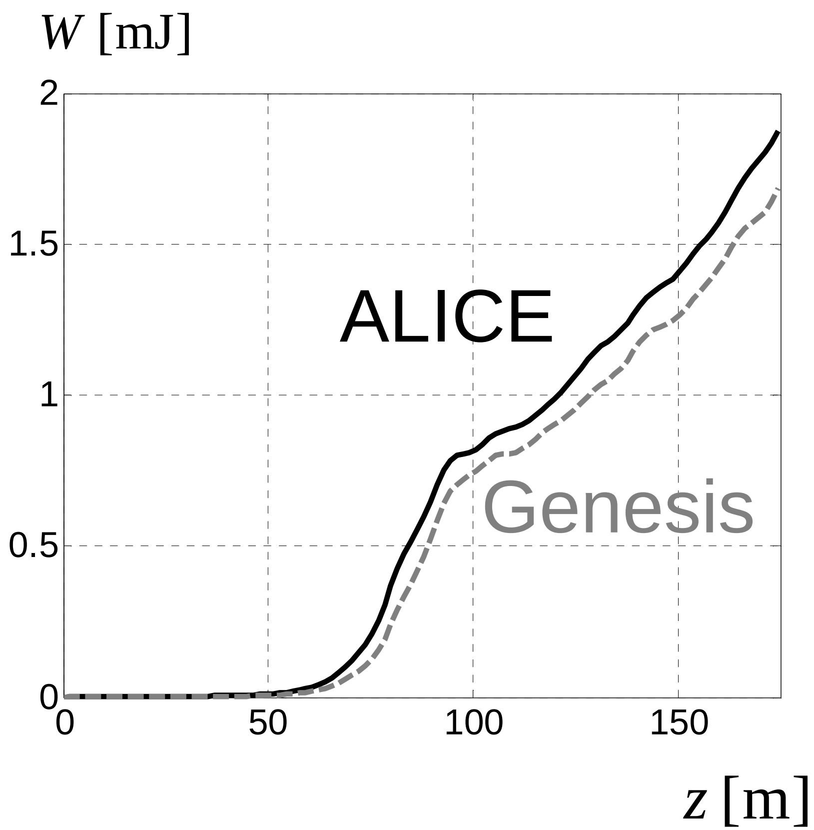

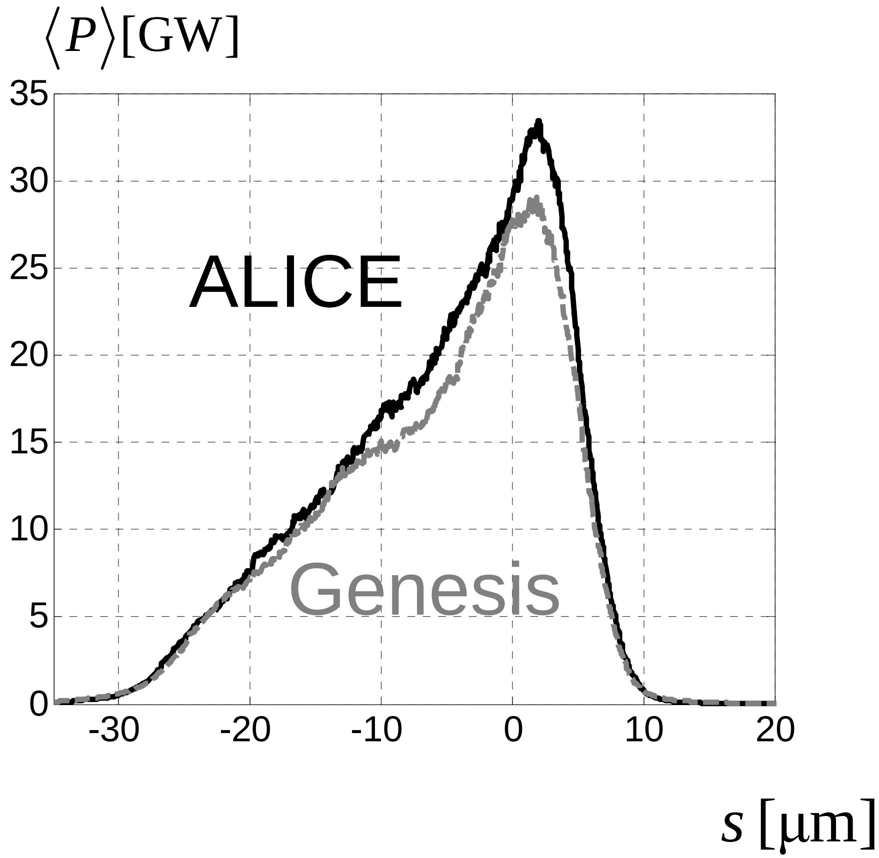

I.Zagorodnov, Ultra-short low charge operation at FLASH and the European XFEL, FEL 2010, Malmö, 2010

Problems and Challenges

Comparison with SPARC FEL experiment

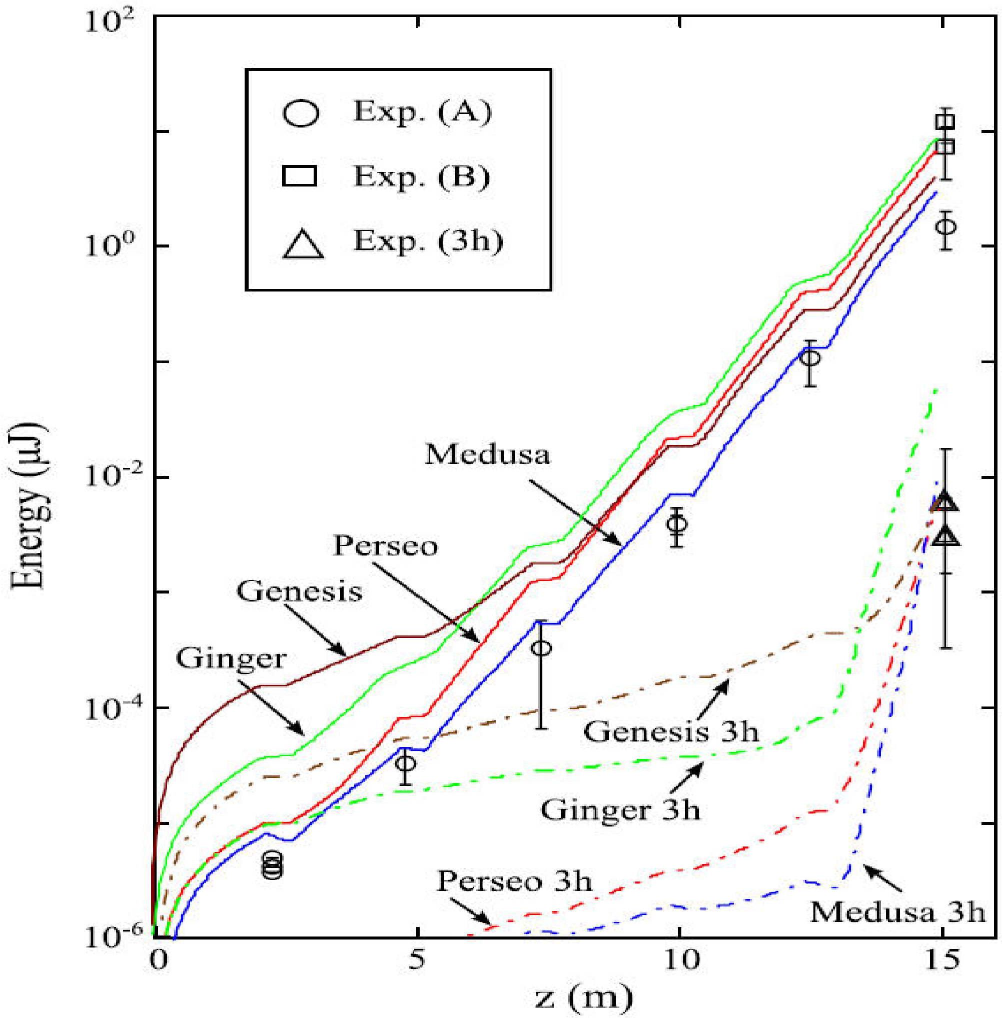

L. Giannesi et al, PR STAB 14, 060712(2011)

Medusa is a code based on non-averaged equations

Problems and Challenges

Limitations of the considered FEL model

- fast „slalom“ motion is not modeled
- only forward propagating field is considered
- macroparticles are locked in the slice with periodic boundary conditions
- only low order harmonics are simulated correctly
- macroscopic space charge, bunch shape changes are not modeled
- narrow frequency bandwidth near the resonance frequency, narrow energy spread

Problems and Challenges

“Table-Top-FEL”

M.Fuchs et al, Nature Physics **5**, 826(2009)

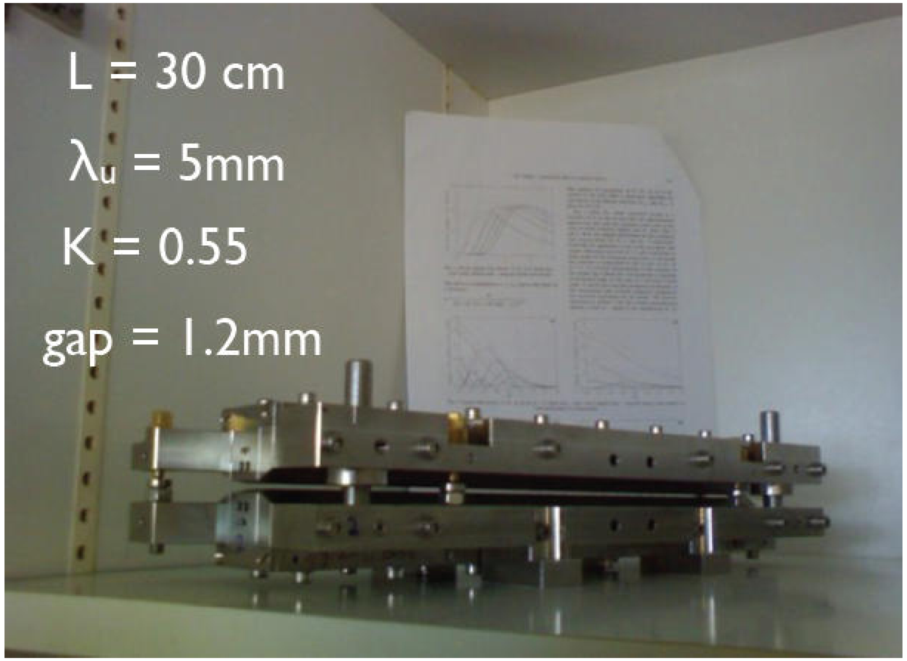

strong space charges, large energy spread

↓

fast bunch shape change

↓

- charge or macroparticles redistribution
- macroscopic space charge equation
- non-averaged modell

Problems and Challenges

- FEL codes based on averaged equations are checked by experiments
- new FEL schemes (Table Top FEL, Echo-Enabled High-Harmonic Generation etc.) require to consider more physics
- FEL codes based on non-averaged FEL equations, with macroscopic space charge are under development

H.P. Freund, S.G. Biedron, S.V. Milton, IEEE J. Quantum Electron. 36 (2000) 275. (Medusa code)

C.K.W. Nam, P. Aitken, and B.W.J. McNeil, Unaveraged three-dimensional modelling of the FEL, FEL 2008, Gyeongju, Korea, 2008

SASE for Nominal Bunch Parameters

Full 3D simulation method (200 CPU, ~10 hours)

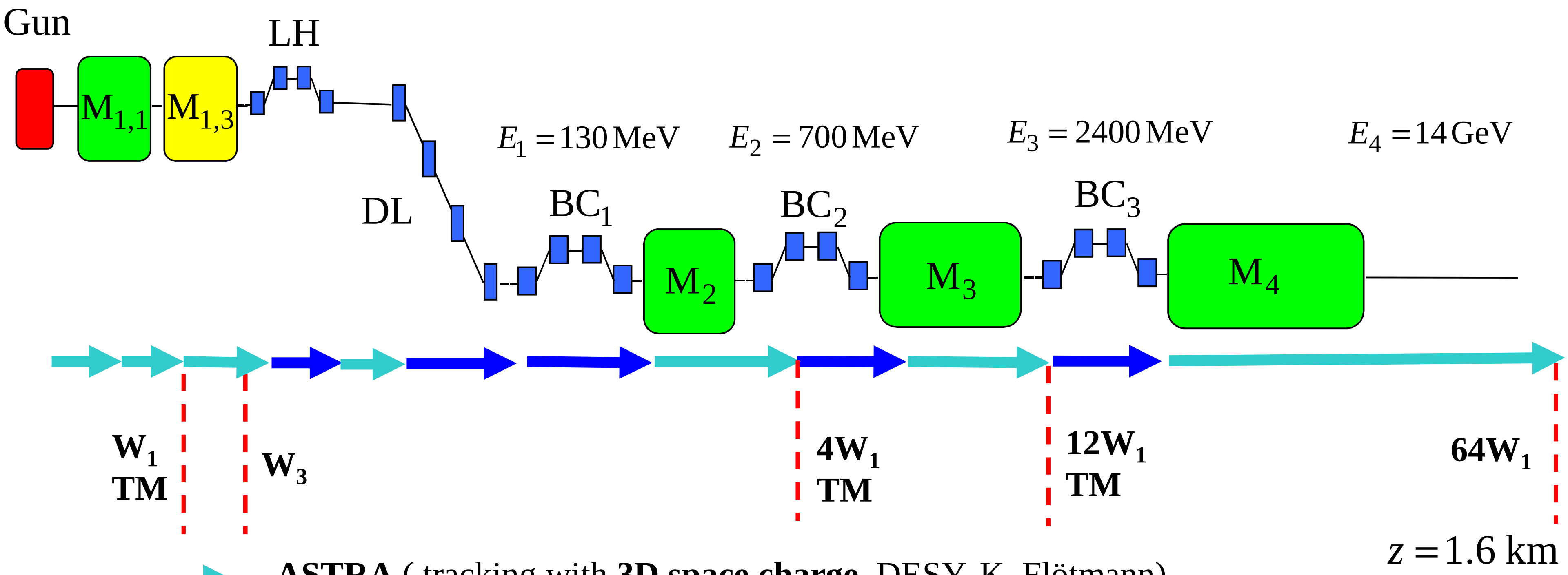

ASTRA (tracking with **3D space charge**, DESY, K. Flötmann)

CSRtrack (tracking through dipoles, DESY, M. Dohlus, T. Limberg)

W1 -TESLA cryomodule wake (TESLA Report 2003-19, DESY, 2003)

W3 - ACC39 wake (TESLA Report 2004-01, DESY, 2004)

TM - transverse matching to the design optics

SASE for Nominal Bunch Parameters

Macro-parameters

Charge Q, nC	Momentum compaction factor in BC_1 $R_{56,1}$, [mm]	Compr. in BC_1 C_1	Momentum compaction factor in BC_2 $R_{56,2}$, [mm]	Compr. in BC_2 C_2	Momentum compaction factor in BC_3 $R_{56,3}$, [mm]	Total compr. C	First derivative Z', $[m^{-1}]$	Second derivative Z'', $[m^{-2}]$
1	-100	3.5	-54	8	-20	121	0	2000
0.5	-89	3.5	-50	8	-20	217	0	1000
0.25	-78	3.5	-50	8	-20	385	0	1000
0.1	-71	3.5	-50	8	-20	870	0	1000
0.02	-67	3.5	-50	8	-20	4237	0	500

$E_1 = 130\,\mathrm{MeV}$ $\quad E_2 = 700\,\mathrm{MeV}$ $\quad E_3 = 2400\,\mathrm{MeV}$

SASE for Nominal Bunch Parameters

Q=1 nC

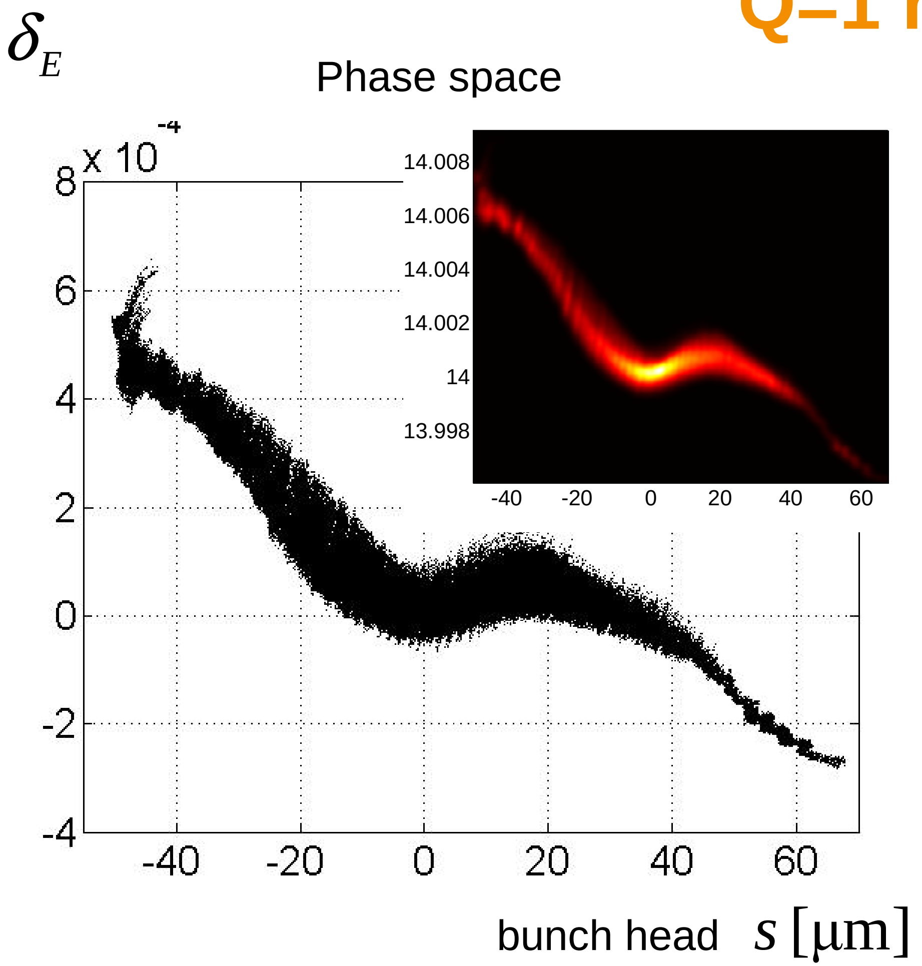

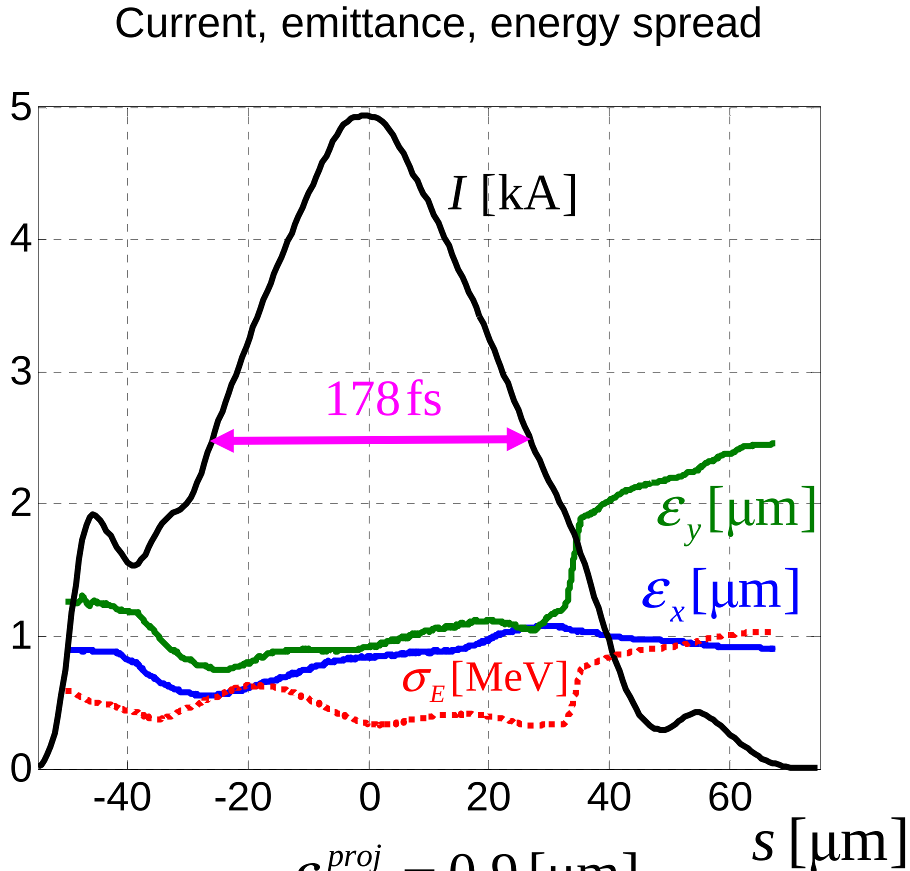

$$\varepsilon_x^{proj} = 0.9\,[\mu m]$$

$$\varepsilon_y^{proj} = 3.5\,[\mu m]$$

We have removed 6% of bad particles in the analysis

SASE for Nominal Bunch Parameters

Q=500 pC

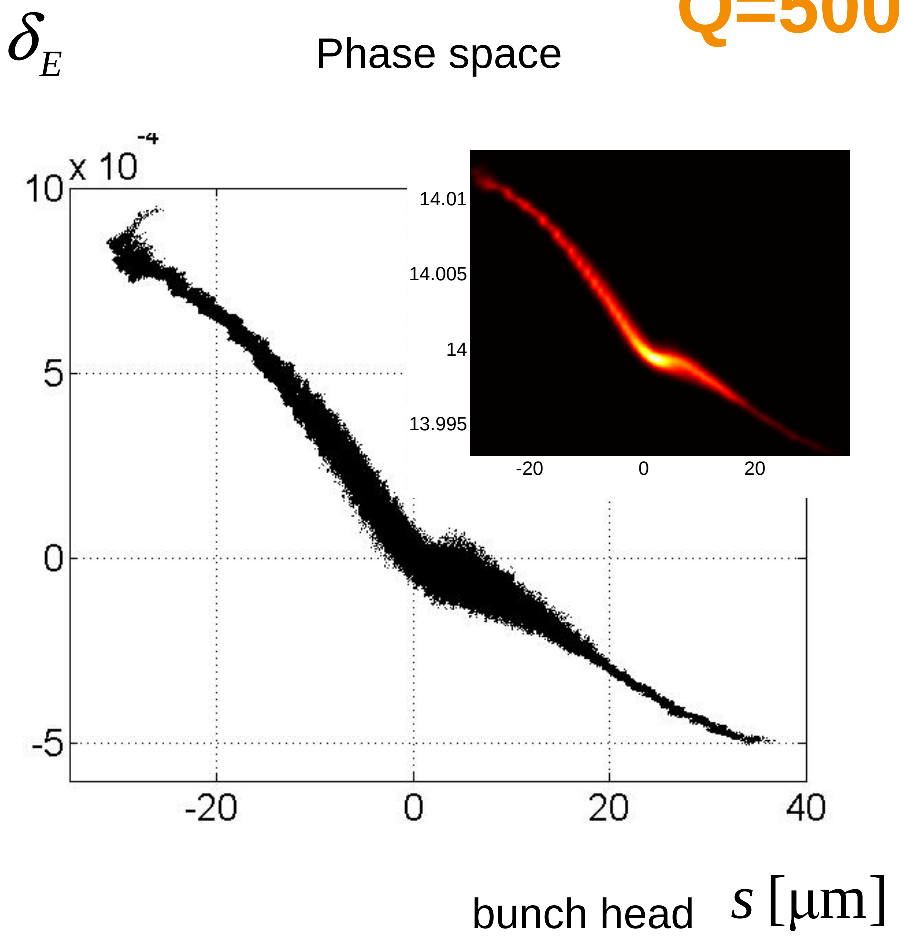

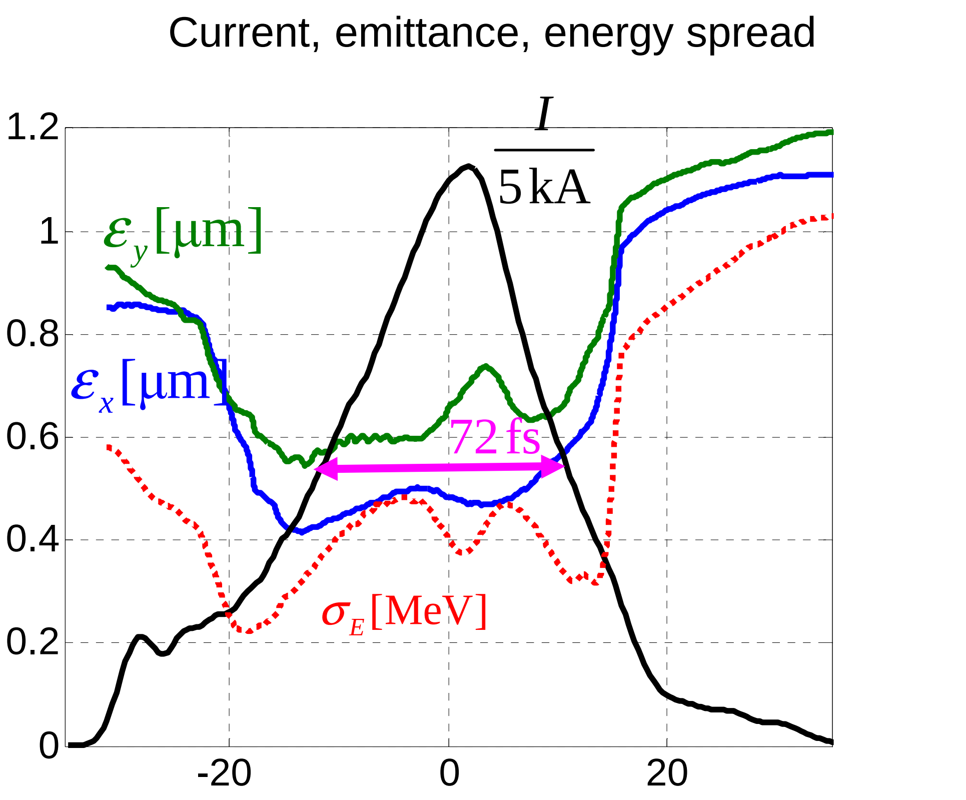

$$\varepsilon_x^{proj} = 0.7\,[\mu\text{m}]$$

$$\varepsilon_y^{proj} = 2.2\,[\mu\text{m}]$$

SASE for Nominal Bunch Parameters

Q=250 pC

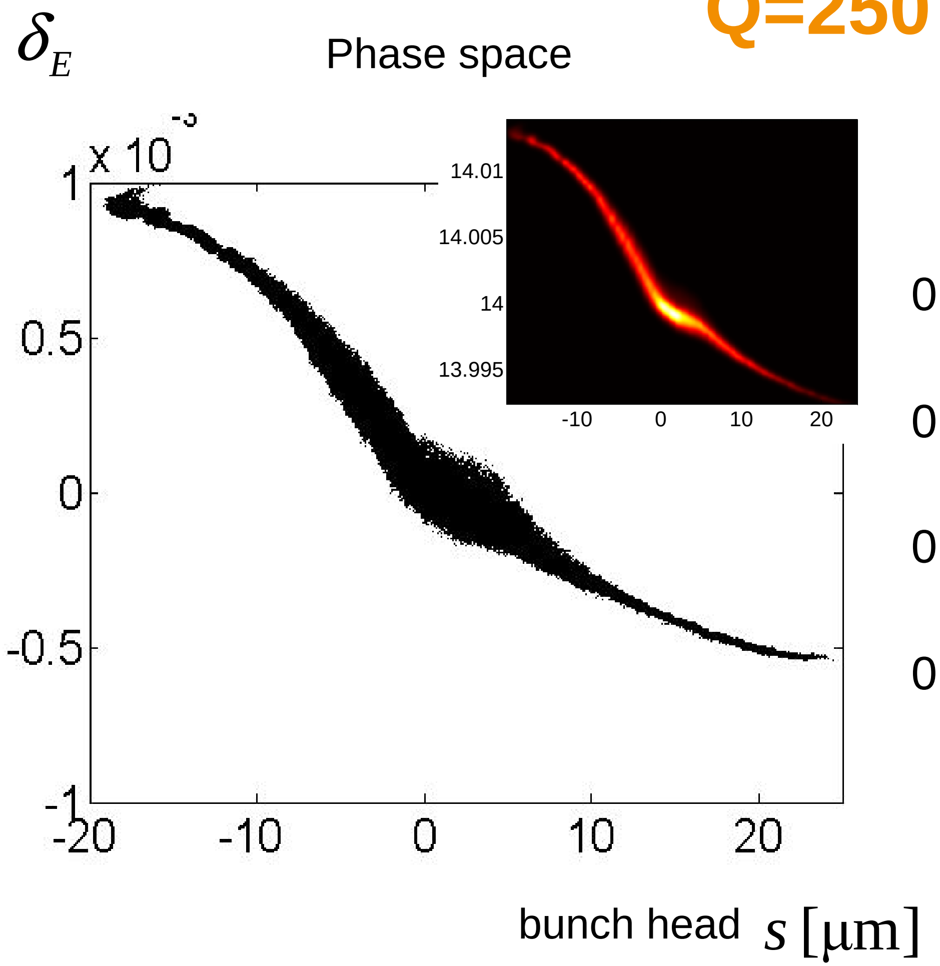

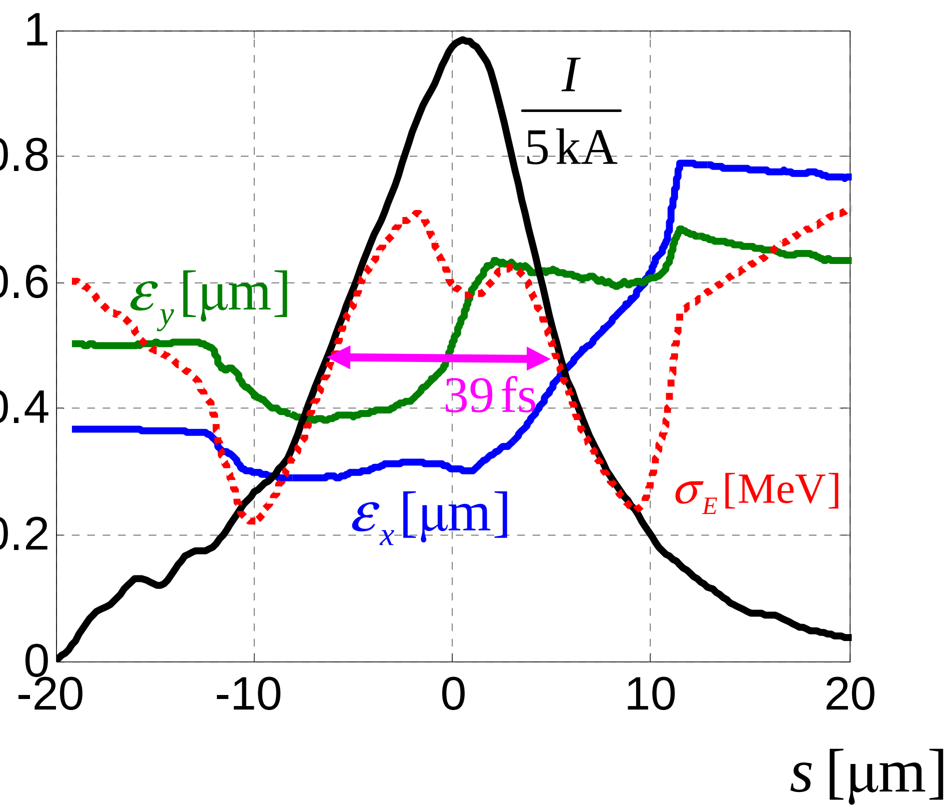

$$\varepsilon_x^{proj} = 0.45\,[\mu\mathrm{m}]$$
$$\varepsilon_y^{proj} = 1.5[\mu\mathrm{m}]$$

SASE for Nominal Bunch Parameters

Q=100 pC

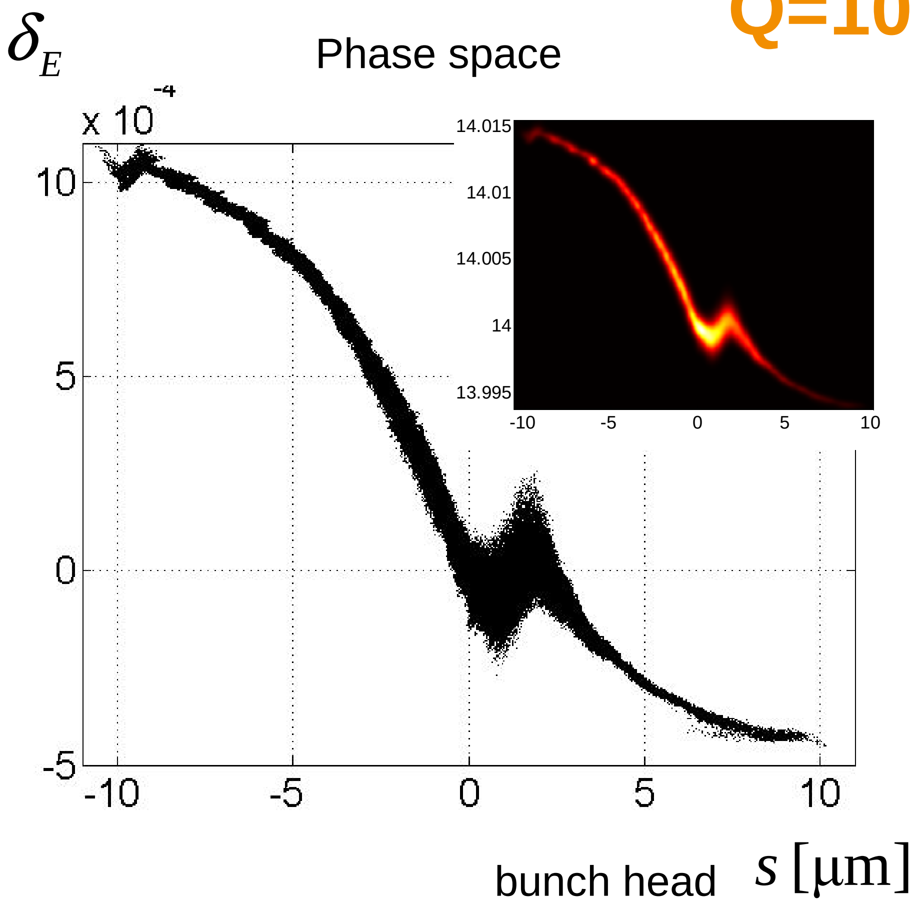

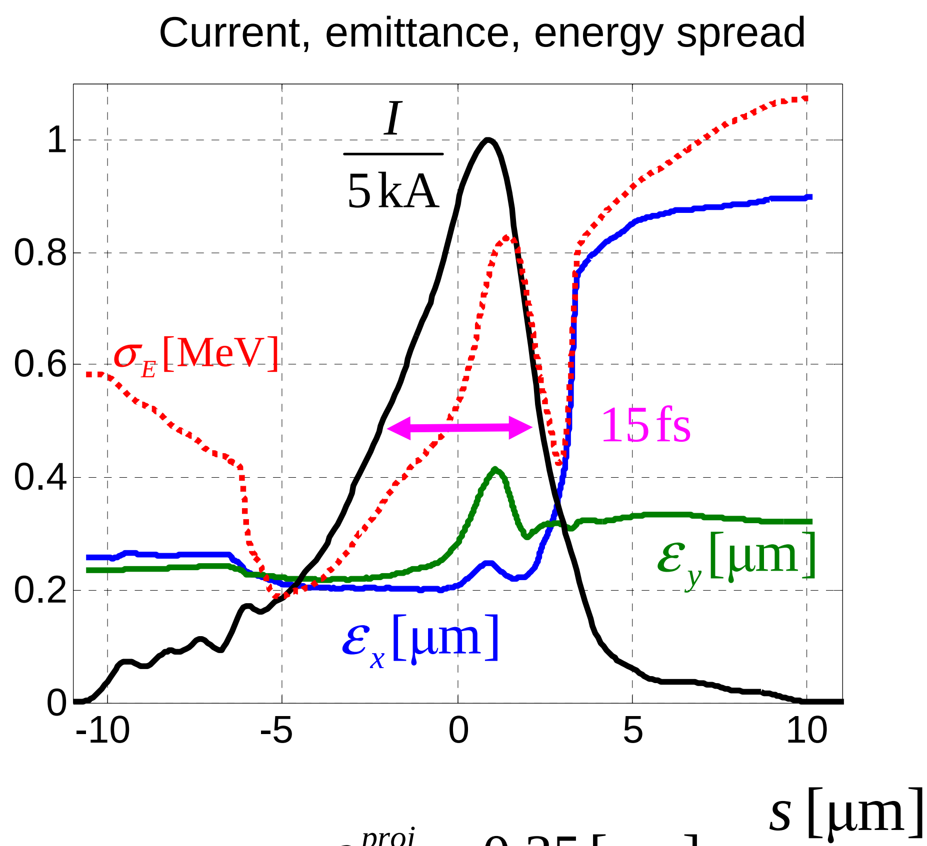

$$\varepsilon_x^{proj} = 0.35\,[\mu\mathrm{m}]$$

$$\varepsilon_y^{proj} = 0.84\,[\mu\mathrm{m}]$$

SASE for Nominal Bunch Parameters

Q=20 pC

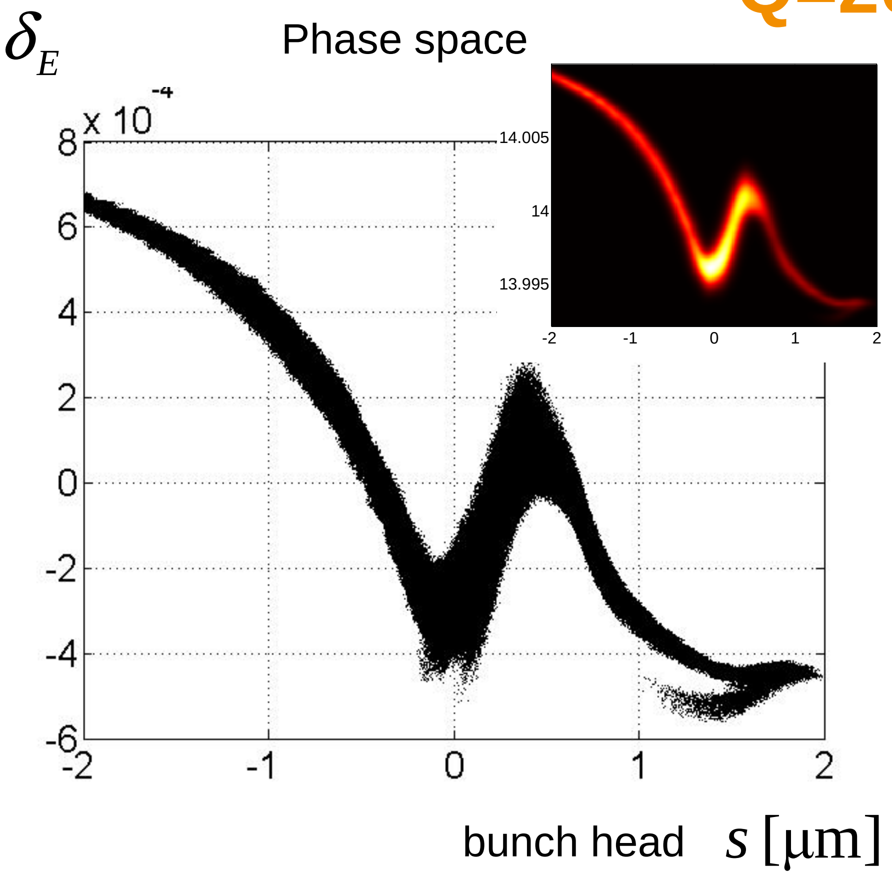

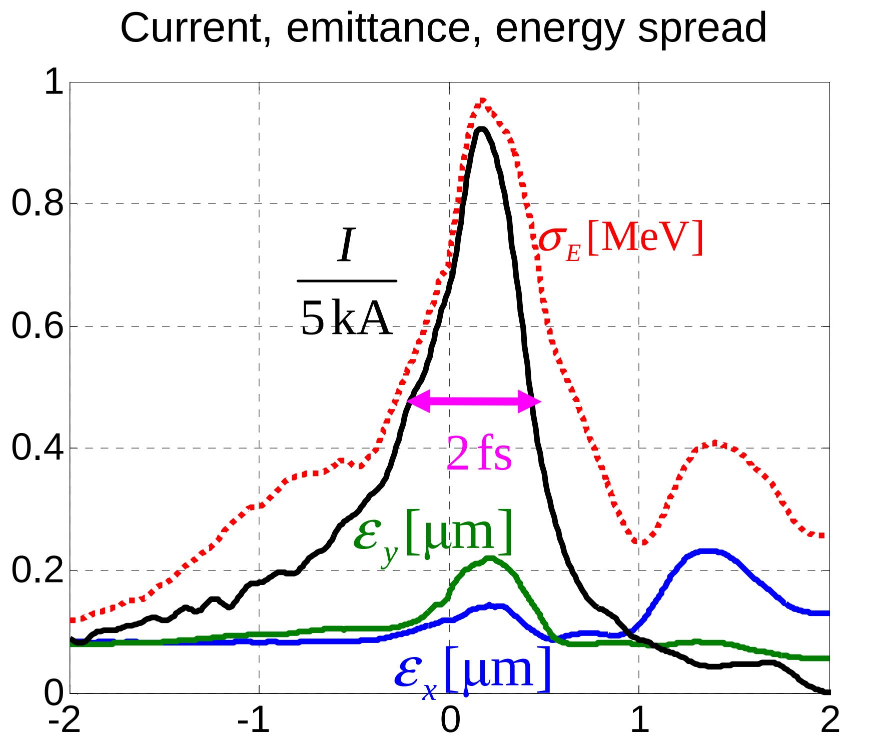

$$\varepsilon_x^{proj} = 0.14\,[\mu\mathrm{m}]$$

$$\varepsilon_y^{proj} = 0.26\,[\mu\mathrm{m}]$$

SASE for Nominal Bunch Parameters

Parameter	Unit					
Bunch charge	nC	1	0.5	0.25	0.1	0.02
Peak current (gun)	A	43	24	13.5	5.7	1.2
Bunch length (gun, FWHM)	ps	25	22	20	17	17
Slice emittance (gun)	µm	0.8	0.5	0.3	0.21	0.09
Projected emittance (gun)	µm	1	0.7	0.6	0.3	0.1
Compression		114	233	363	877	3833
Peak current	kA	**4.9**	**5.6**	**4.9**	**5**	**4.6**
Bunch length (FWHM)	fs	178	72	39	12	2.2
Slice emittance	µm	**1**	**0.7**	**0.5**	**0.3**	**0.2**
Projected emittance	µm	3.5	2.2	1.5	0.84	0.26
Slice energy spread (**laser heater off**)	MeV	0.45	0.44	0.6	0.6	0.8

SASE for Nominal Bunch Parameters

Mismatch and wake Q=1nC

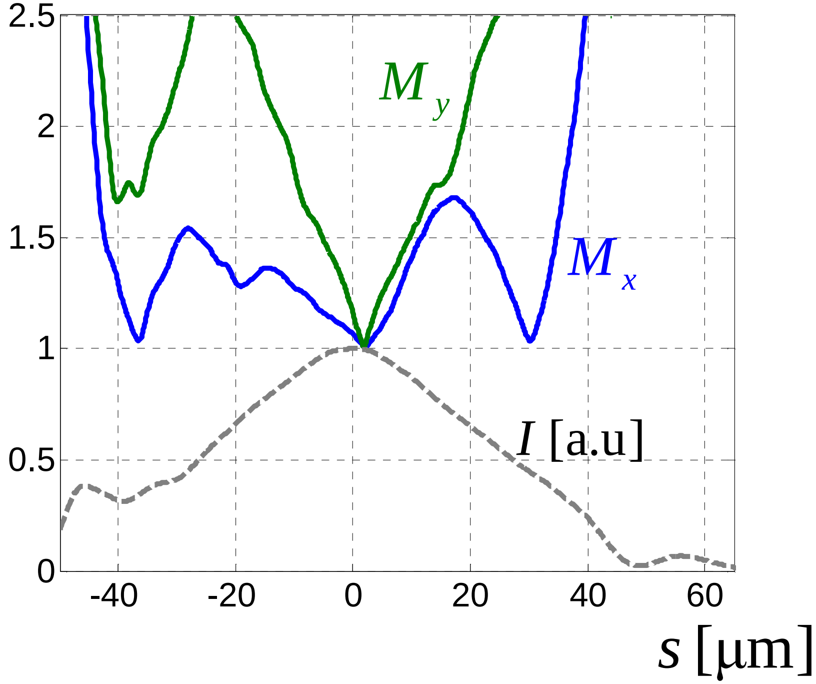

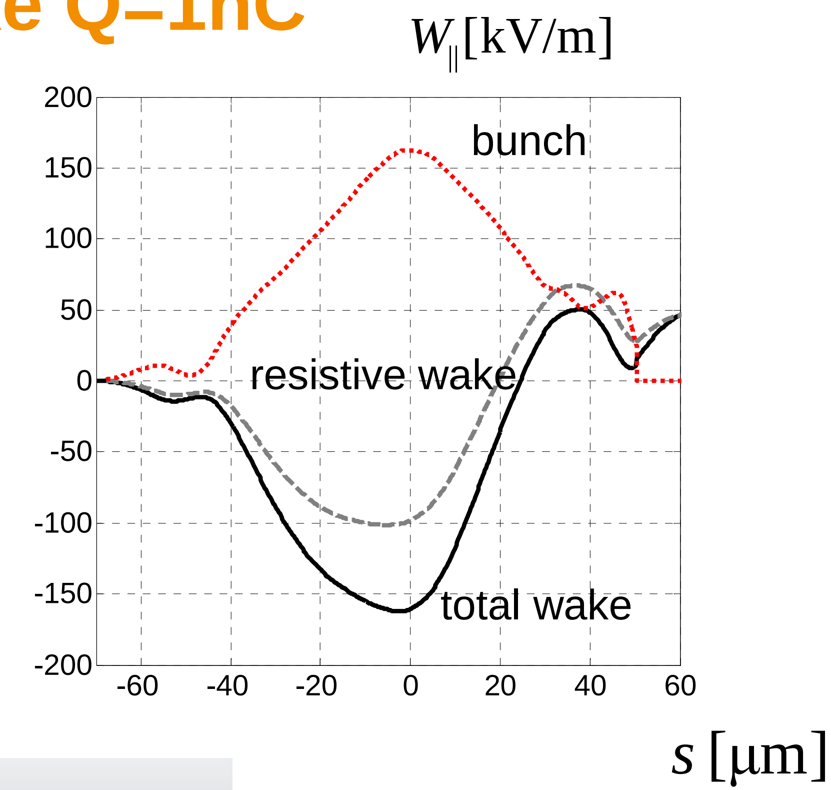

Loss, spread, peak parameters

Section	Type of element	Number	Loss (V/pC)	%	Spread (V/pC/m)	%	Peak (V/pC/m)	%
SA1	ABS	32	2.389E+03	14	8.717E+02	7	3.451E+03	12
SA1	BEL	64	1.342E+03	8	4.476E+02	3	1.803E+03	6
SA1	BPME	33	1.780E+03	11	7.243E+02	6	2.598E+03	9
SA1	PIPE	33	8.730E+03	53	1.020E+04	80	1.844E+04	62
SA1	PIPR	32	7.812E+02	5	1.157E+03	9	2.069E+03	7
SA1	PUM	32	3.025E+02	2	2.383E+02	2	5.476E+02	2
SA1	RET	32	1.228E+03	7	4.422E+02	3	1.766E+03	6
SA1			1.655E+04	100	1.283E+04	100	2.951E+04	100
			1.655E+04	100	1.283E+04	100	2.951E+04	100

SASE for Nominal Bunch Parameters

Radiation Q=1nC. SASE

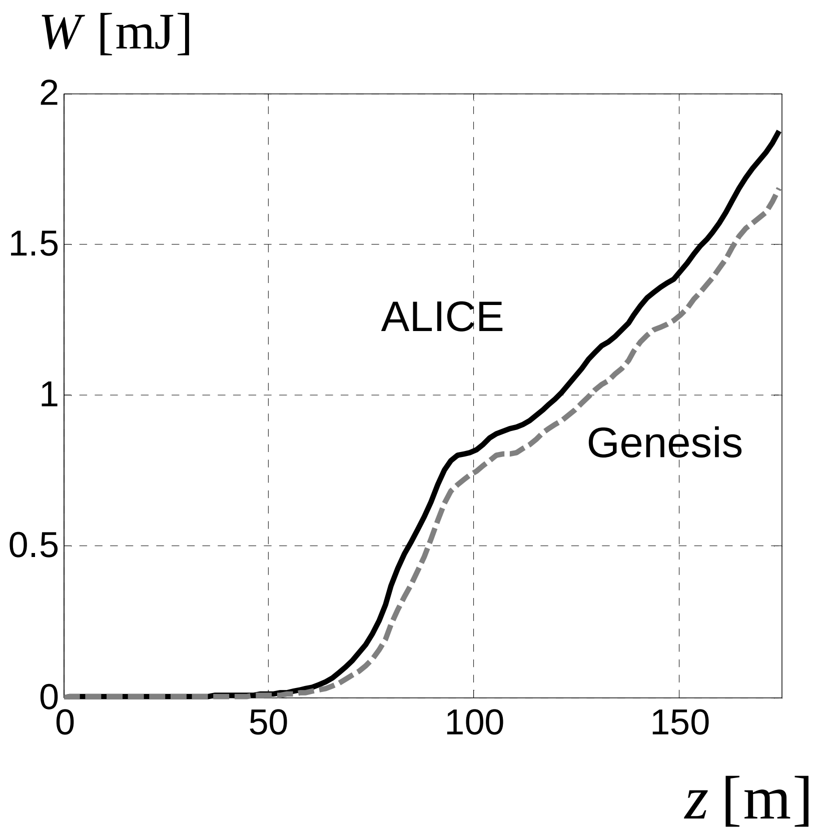

One shot from different particle distributions

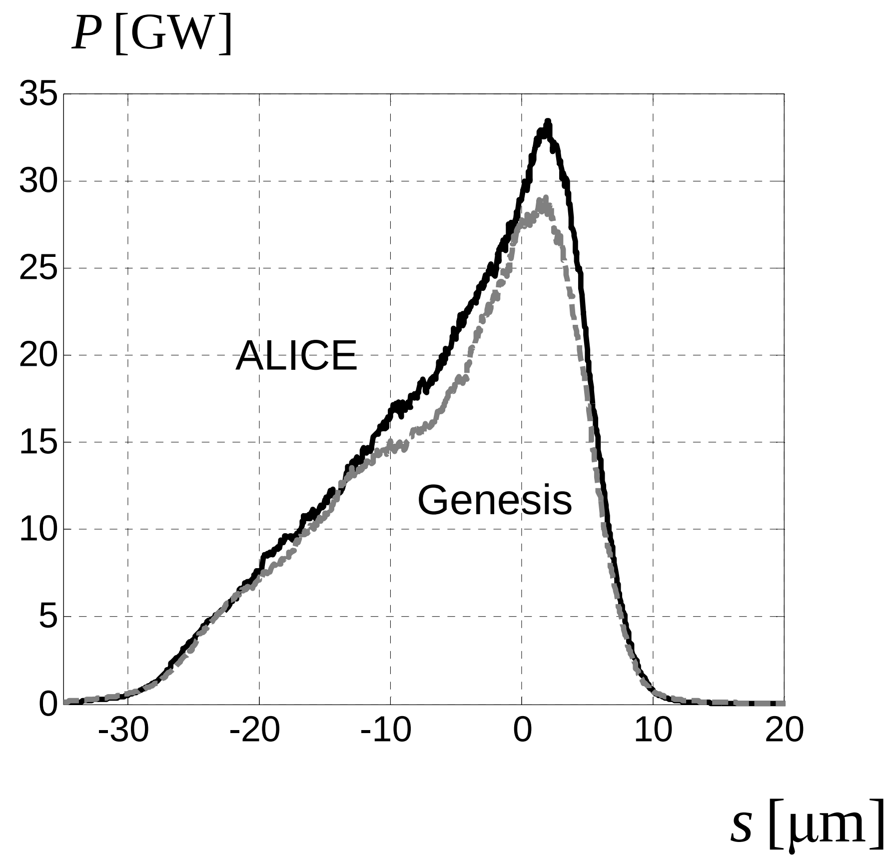

Averaged through 20000 slices

SASE for Nominal Bunch Parameters

Linear undulator tapering

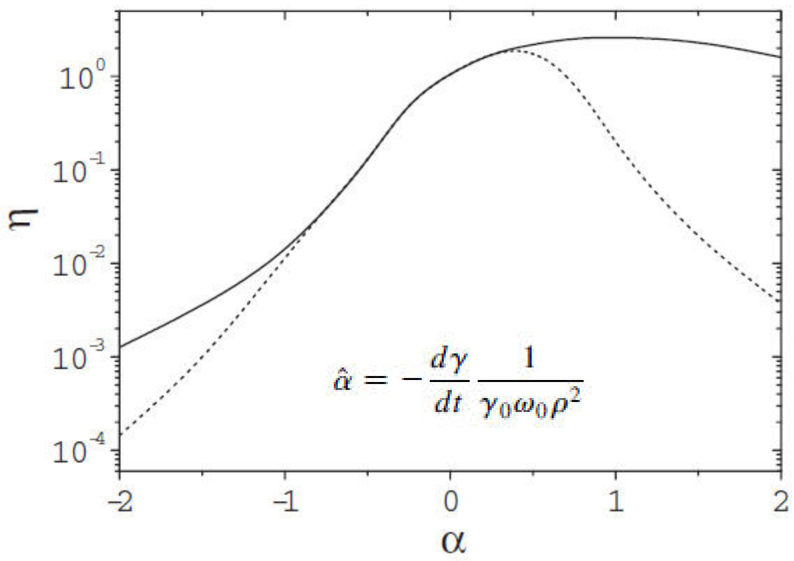

FIG. 2. Normalized output power versus parameter $\hat{\alpha}$. Solid: $\hat{z} = \hat{z}_{sat}(\hat{\alpha})$ (see Fig. 1); dashed: $\hat{z} = \hat{z}_{sat}(0) = 13$.

PHYSICAL REVIEW SPECIAL TOPICS - ACCELERATORS AND BEAMS
9, 050702 (2006)

Self-amplified spontaneous emission FEL with energy-chirped electron beam and its application for generation of attosecond x-ray pulses

E. L. Saldin, E. A. Schneidmiller, and M. V. Yurkov
Deutsches Elektronen-Synchrotron (DESY), Hamburg, Germany

(Received 17 March 2006; published 3 May 2006)

$$\hat{\alpha}_{opt} = 0.25$$

$$\hat{C}(\hat{z}) = \hat{b}\hat{z}$$

$$\hat{b}_{opt} = 0.5\alpha_{opt}$$

$$\hat{C}(\hat{z}) = 0.125\hat{z}$$

$$\frac{dK}{dz} \approx \frac{1}{kK}\left(2k_u\gamma\frac{d\gamma}{dz} - 0.5\left(k_u\rho\gamma\right)^2\right)$$

SASE for Nominal Bunch Parameters

Linear undulator tapering

$$\frac{mc^2}{e}\frac{d\gamma}{dz} = -160\,\frac{\text{keV}}{\text{m}}$$

$$\left(\frac{dK}{dz}\right)_{opt} = -4.8\cdot 10^{-5}\,\text{m}^{-1}$$

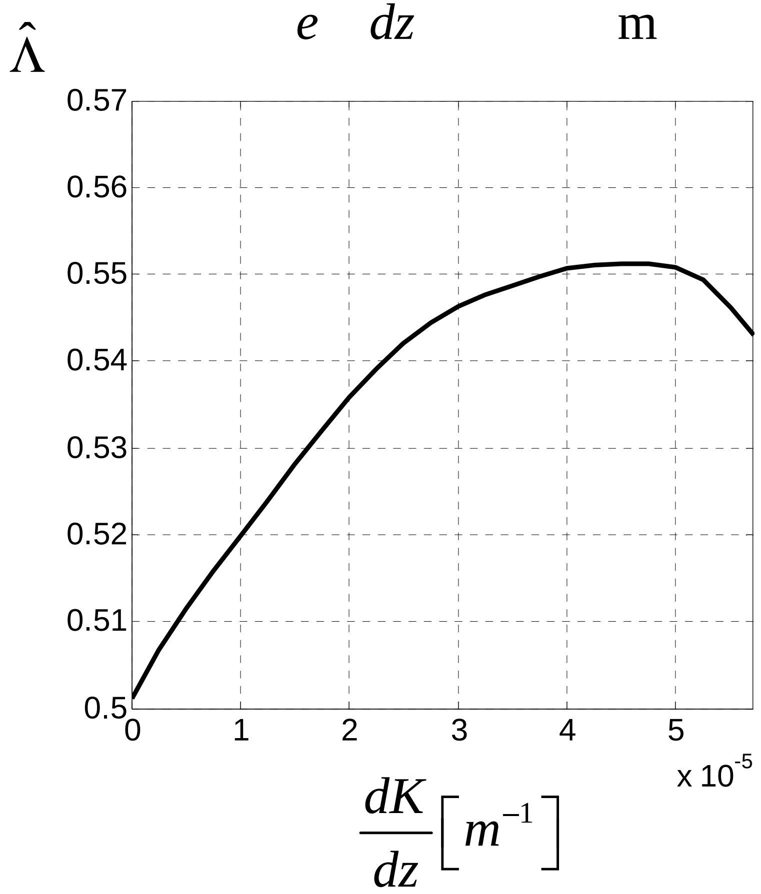

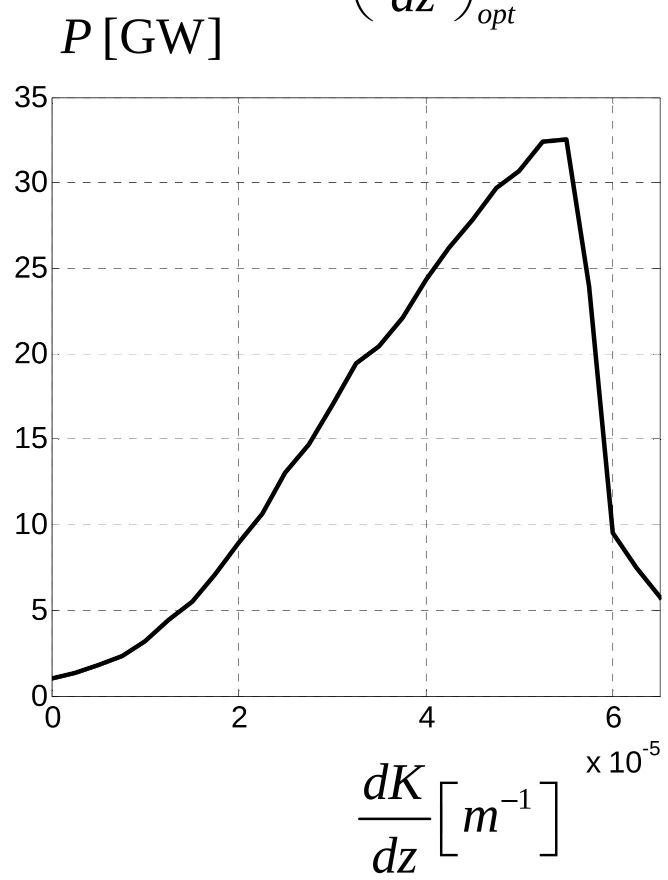

SASE for Nominal Bunch Parameters

Radiation Q=1 nC

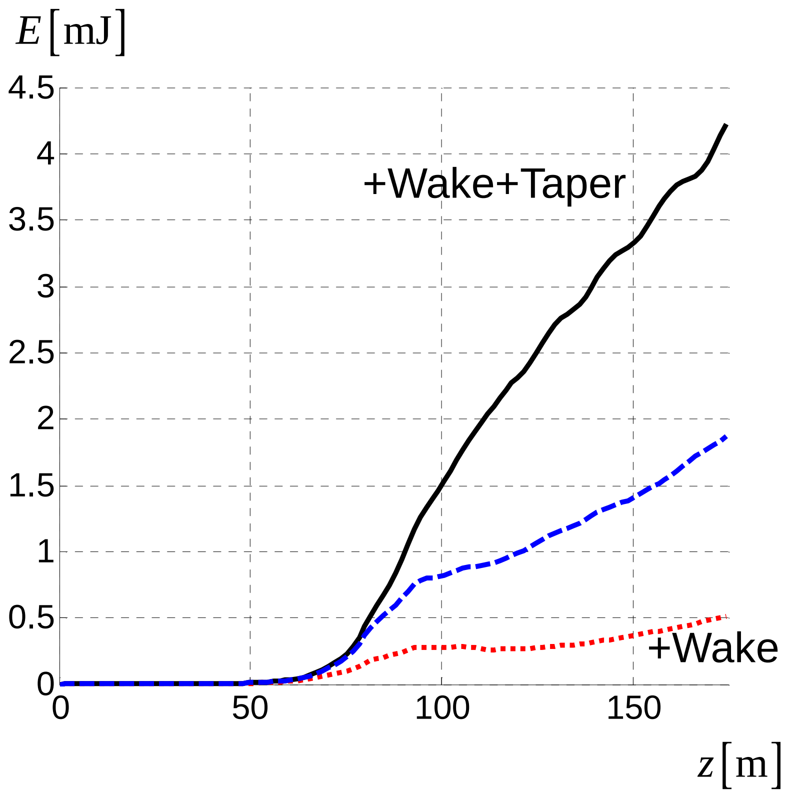

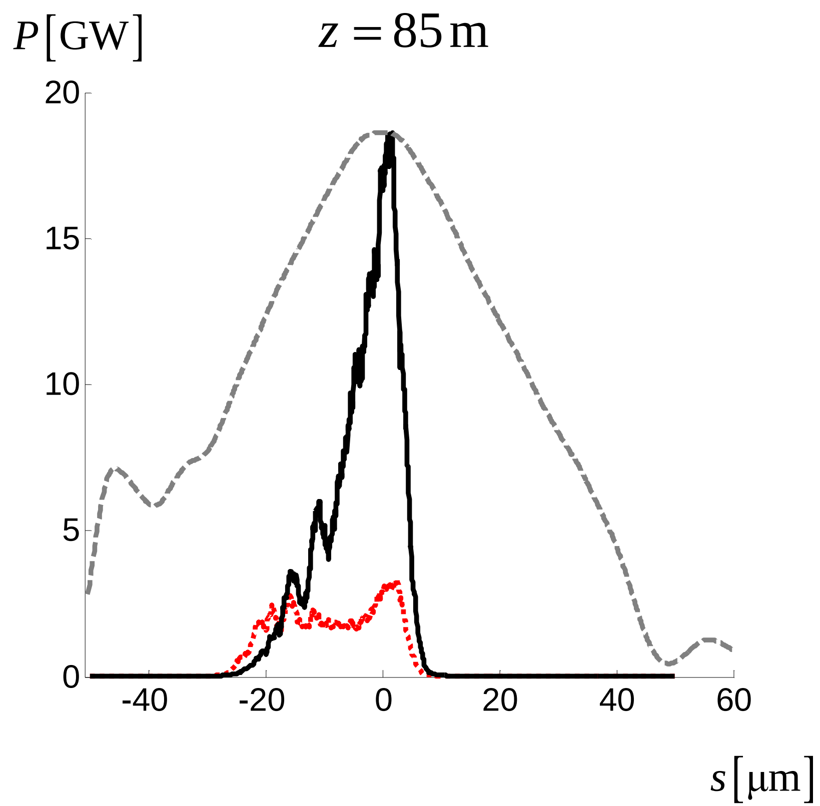

$$\left(\frac{dK}{dz}\right)_{opt} = -4.8\cdot 10^{-5}\,\mathrm{m}^{-1}$$

Averaged through 8000 slices

SASE for Nominal Bunch Parameters

Mismatch and wake Q=250 pC

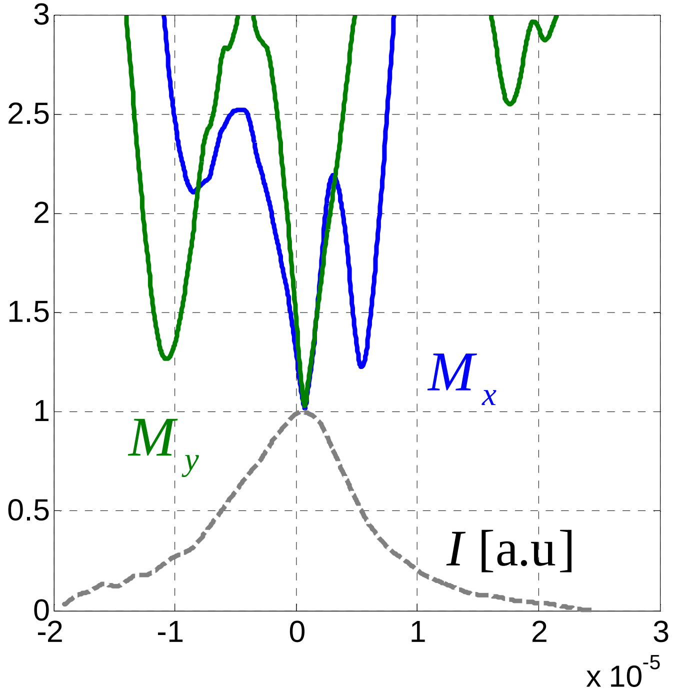

s [μm]

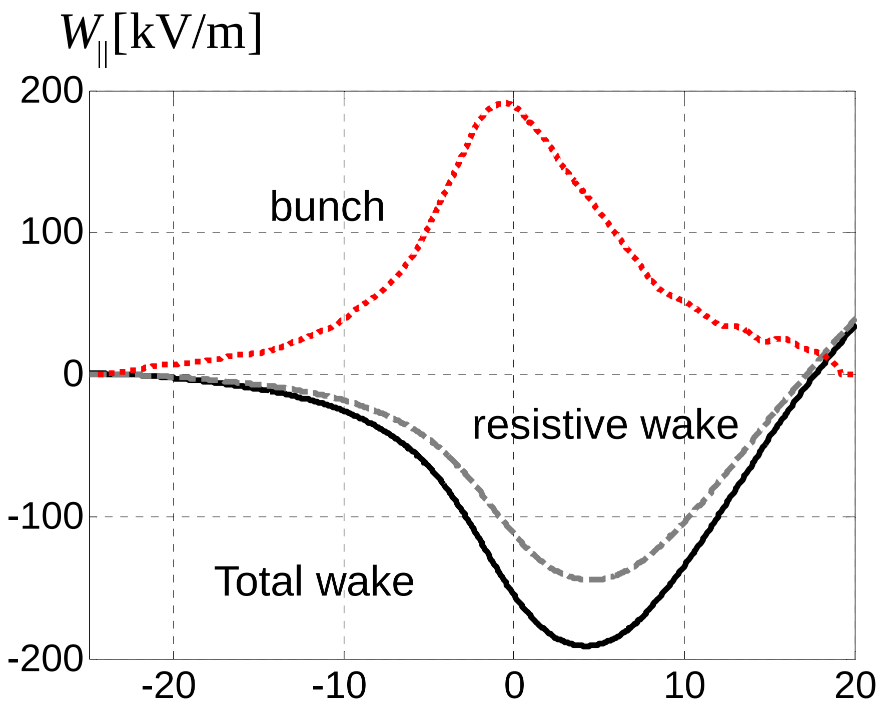

s [μm]

SASE for Nominal Bunch Parameters

Radiation Q=250 pC

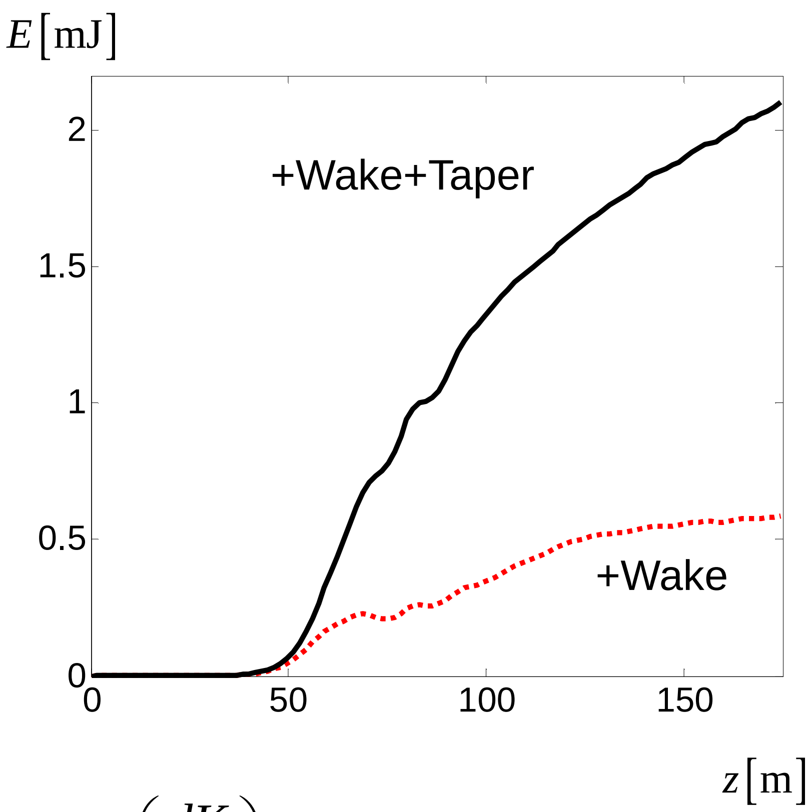

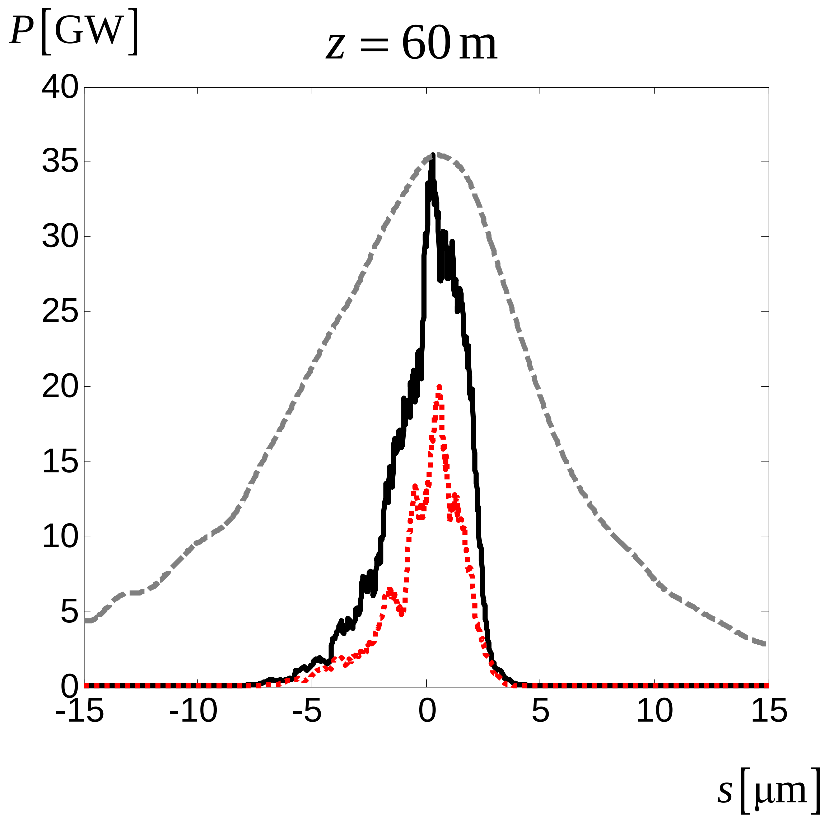

$$\left(\frac{dK}{dz}\right)_{opt} = -4.8 \cdot 10^{-5}\,\mathrm{m}^{-1}$$

Averaged through 2400 slices

SASE for Nominal Bunch Parameters

Mismatch and wake Q=20 pC

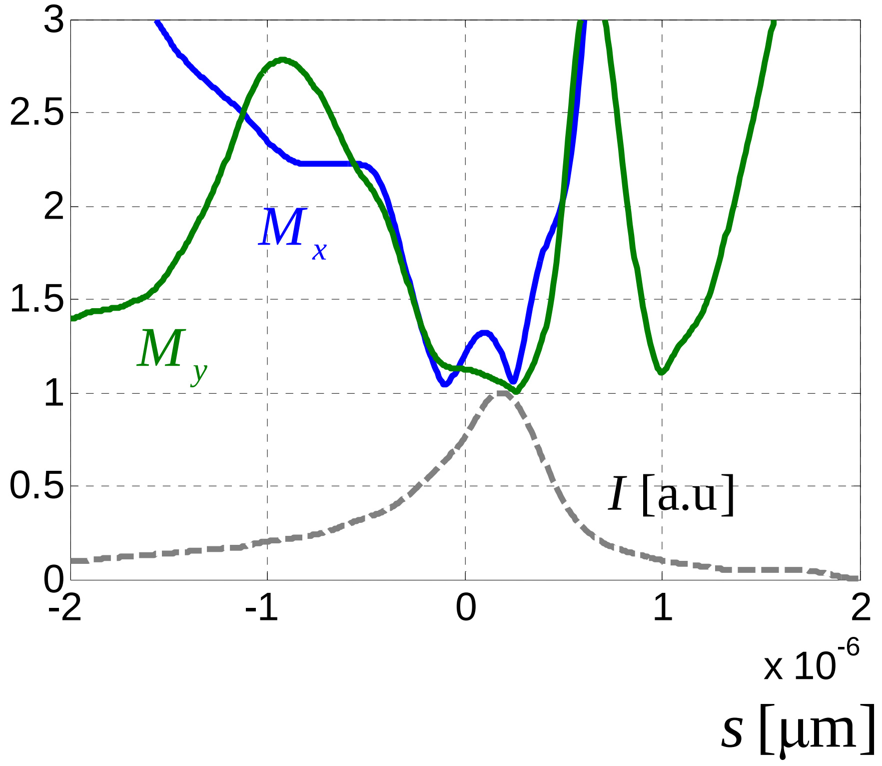

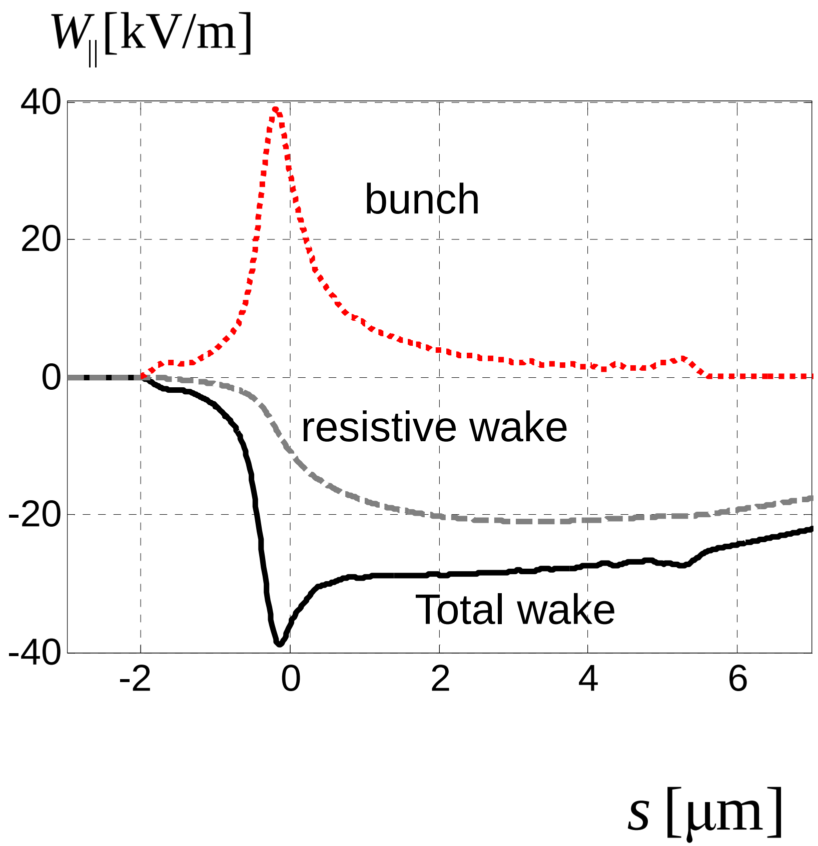

$$\frac{mc^2}{e}\frac{d\gamma}{dz} = -40\frac{\text{keV}}{\text{m}} \qquad \left(\frac{dK}{dz}\right)_{opt} = -2.2\cdot 10^{-5}\,\text{m}^{-1}$$

SASE for Nominal Bunch Parameters

Radiation Q=20 pC

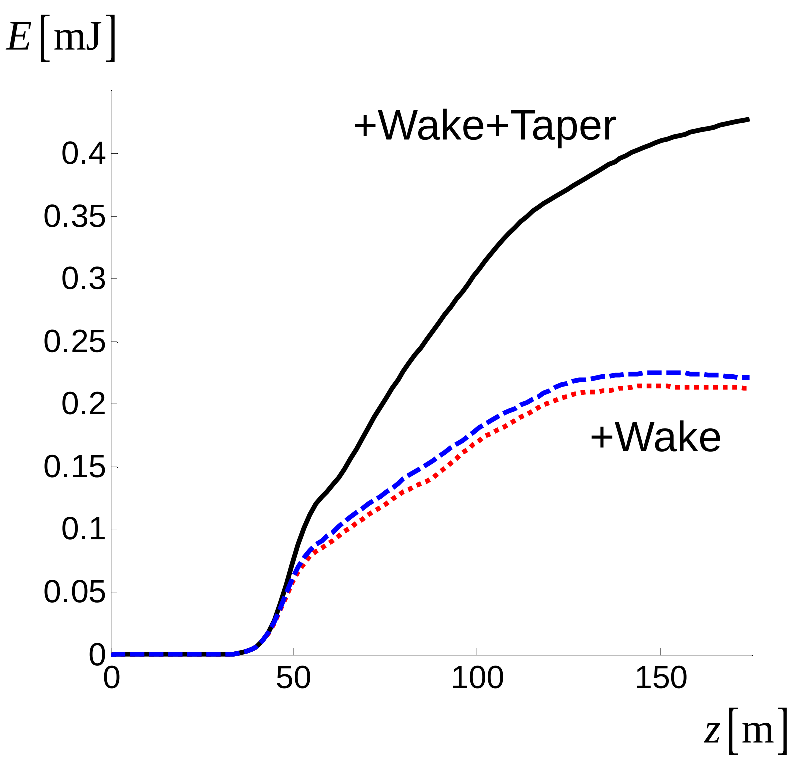

$$\left(\frac{dK}{dz}\right)_{opt} = -4.8 \cdot 10^{-5}\,\mathrm{m}^{-1}$$

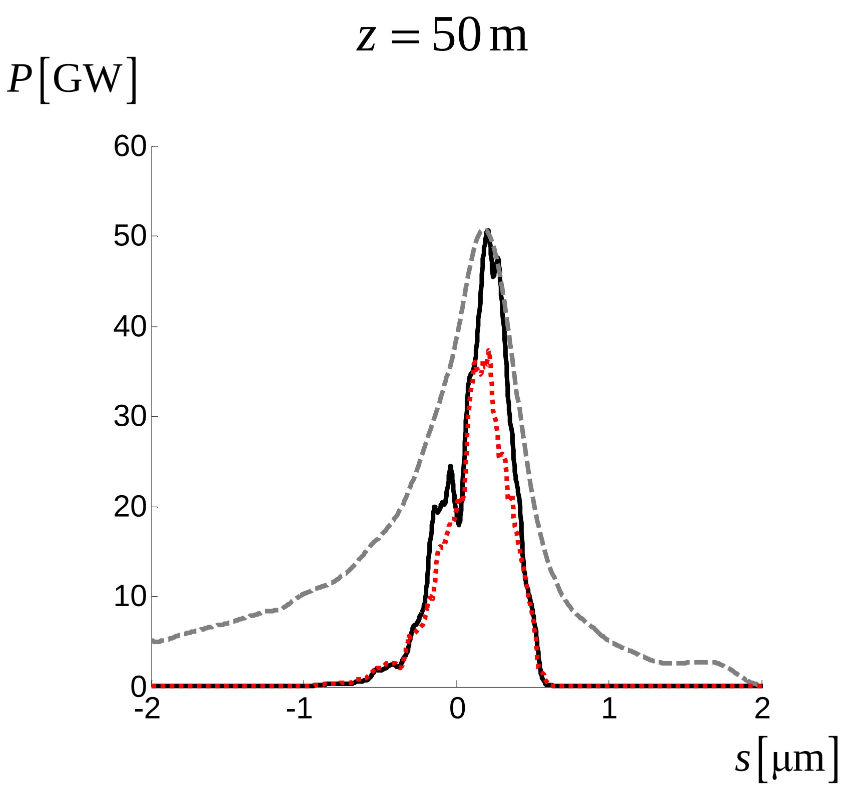

Averaged through 800 slices

SASE for Nominal Bunch Parameters

Slice parameters for SASE simulations

Slice parameters are extracted from S2E simulations for SASE simulations

$$\gamma \quad \Delta\gamma \quad \varepsilon_x \quad \varepsilon_y \quad \beta_x \quad \beta_y \quad \langle x\rangle \quad \langle y\rangle \quad \langle x'\rangle \quad \langle y'\rangle \quad \alpha_x \quad \alpha_y \quad I$$

slice emittance

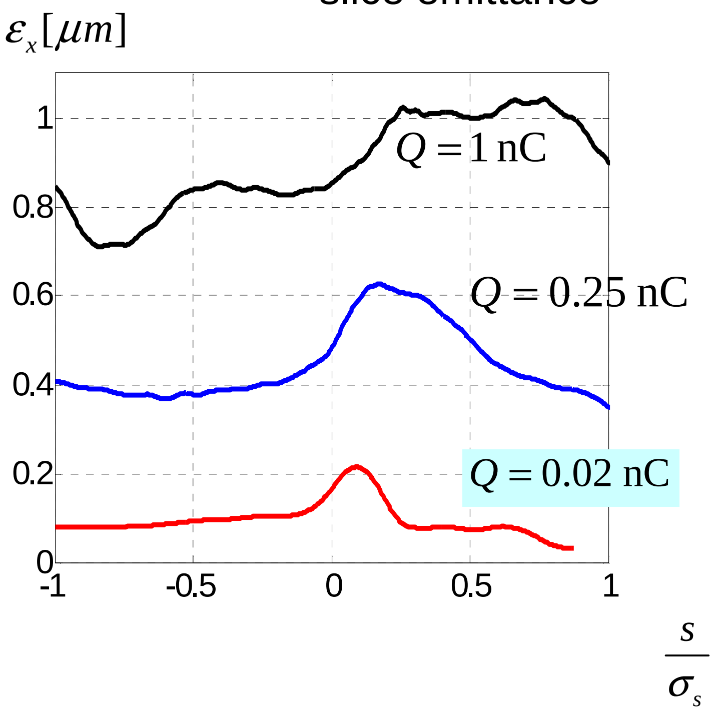

current

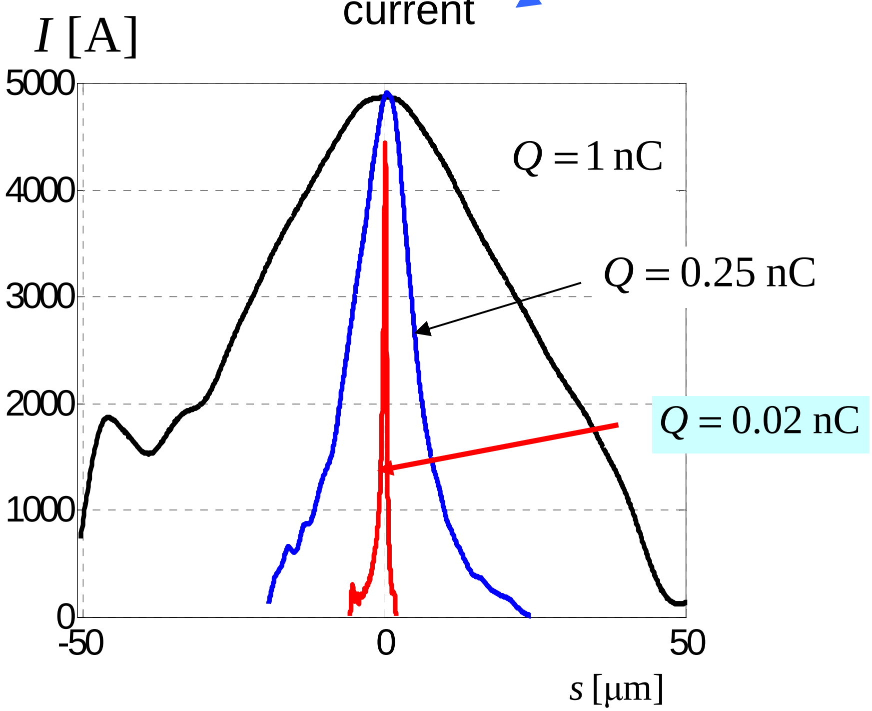

SASE for Nominal Bunch Parameters

Radiation energy statistics (1-25-120 runs)

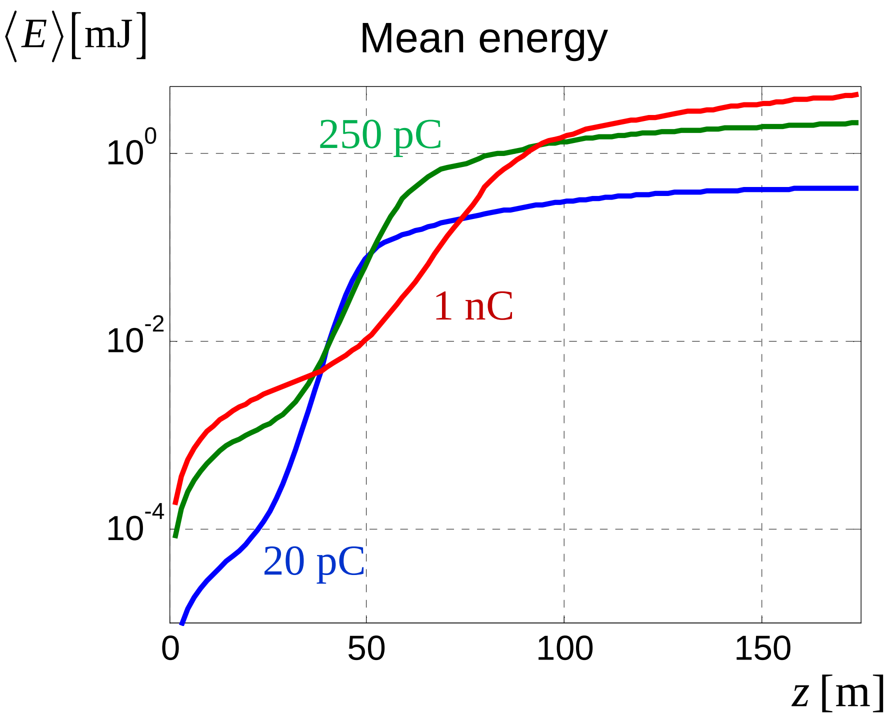

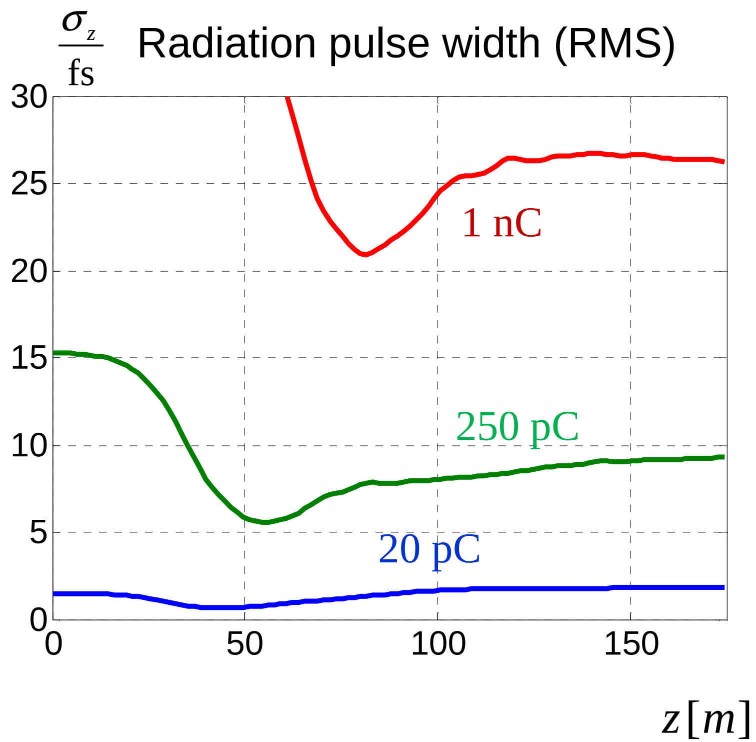

Charge, nC	1	0.25	0.02
Mean radiation energy, mJ	1-4	1-2	0.1-0.4
Pulse radiation width (FWHM), fs	**25-50**	**10-20**	**1-2**

SASE for Nominal Bunch Parameters

Radiation energy statistics

Q=20 pC (120 runs)

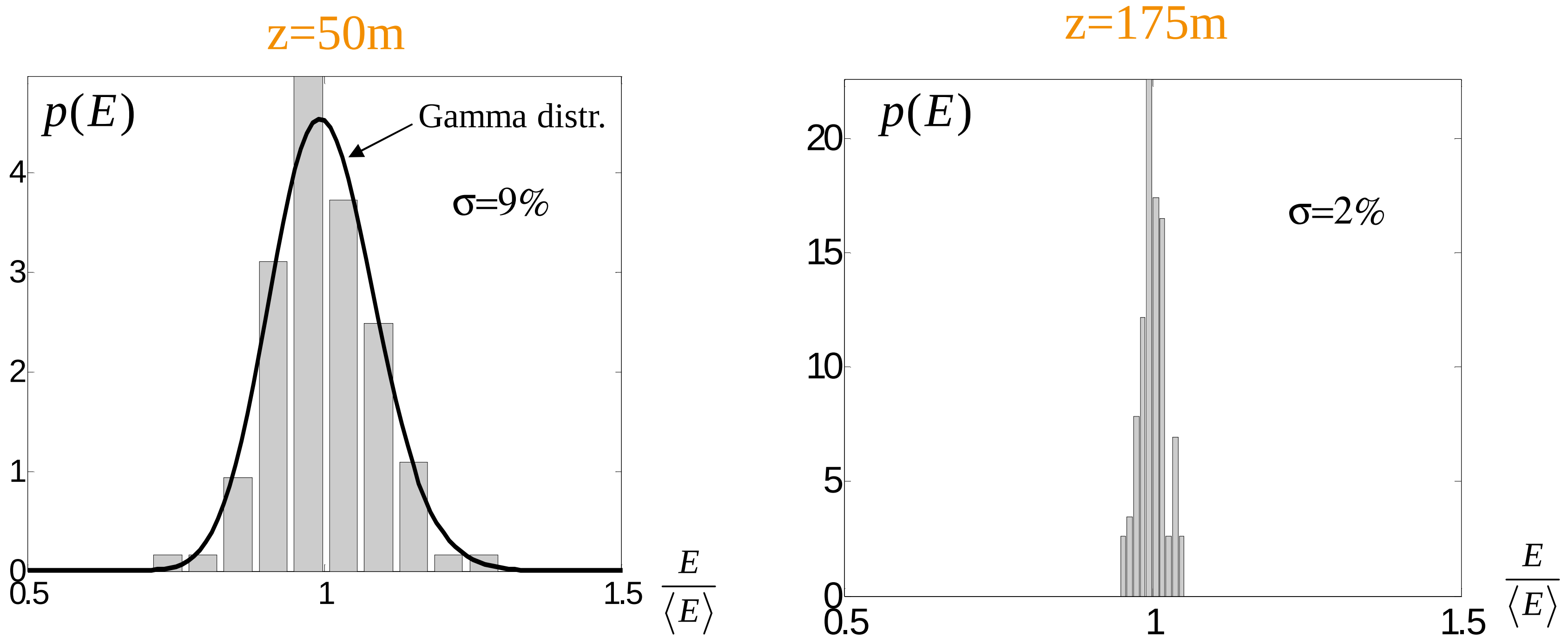

SASE for Nominal Bunch Parameters

Q= 250 pC **Temporal structure** Q=20 pC

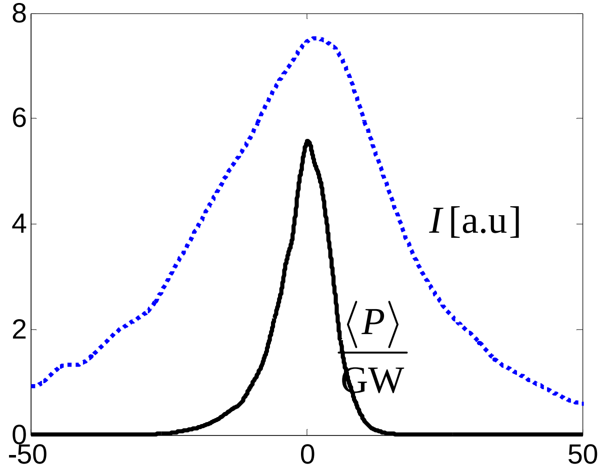

t[fs]

z=50m

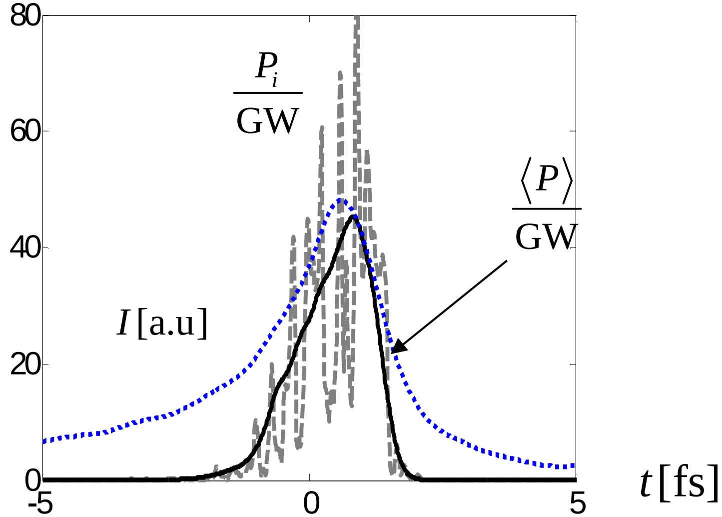

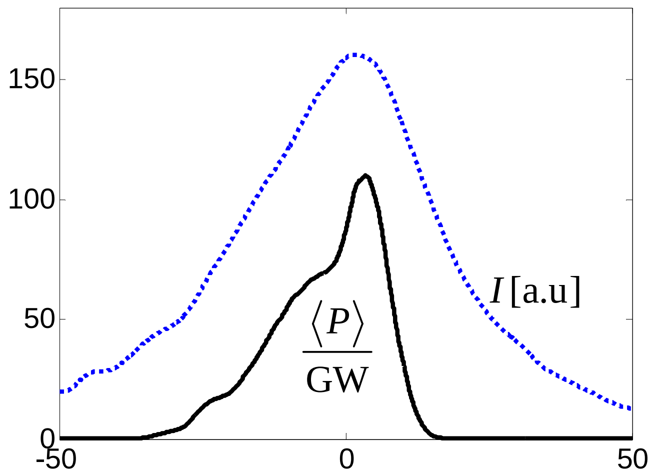

t[fs]

z=175m

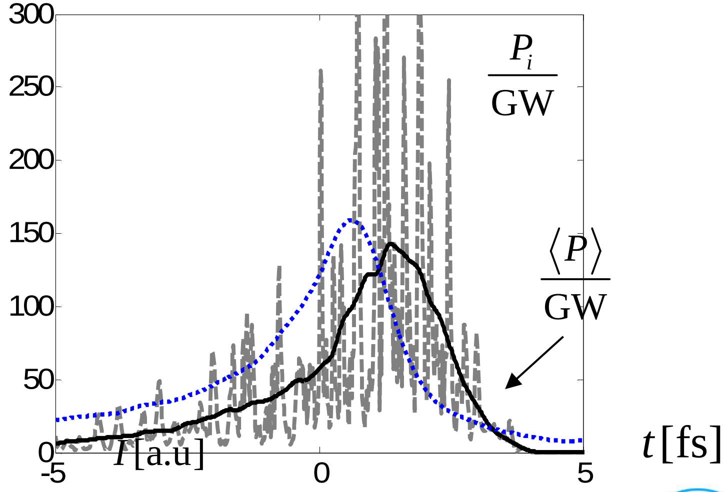

SASE for Nominal Bunch Parameters

Spectrum

Q= 250 pC

Q=20 pC

z=50m

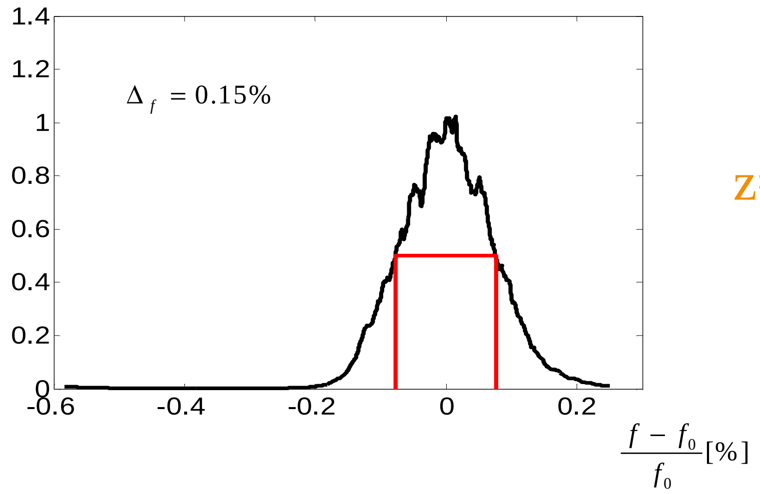

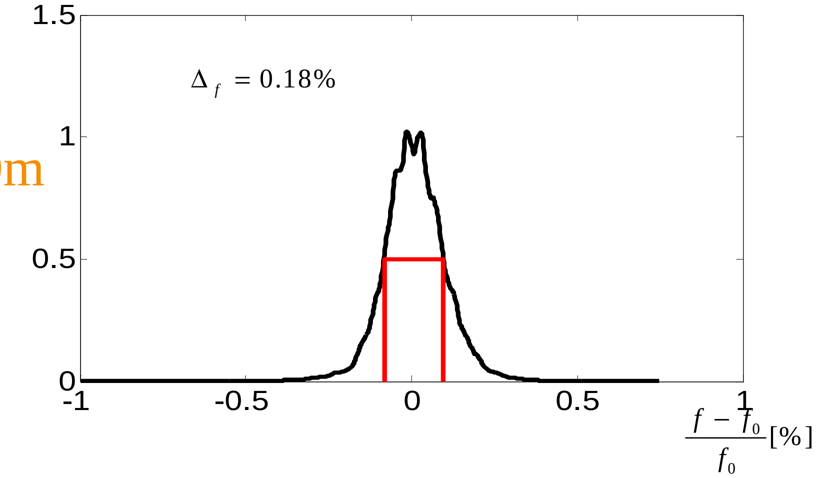

z=175m

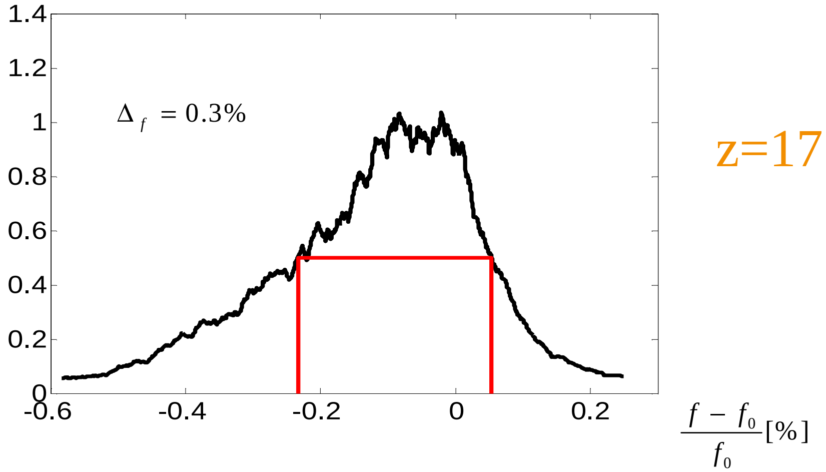

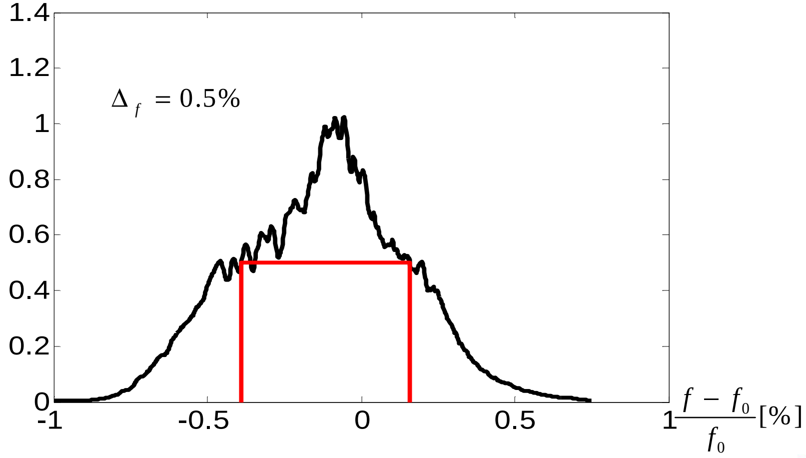

SASE for Nominal Bunch Parameters

Summary

Bunch charge, nC	1	0.25	0.02
Wavelength, nm	0.1		
Beam energy, GeV	14		
Peak current, kA	**~ 5**		
Slice emmitance,mm-mrad	**1**	**0.5**	**0.2**
Saturation length, m	**85**	**60**	**45**
Energy in the rad. pulse, mJ	1-4	1-2	0.1-0.4
Radiation pulse duration FWHM, fs	**25-50**	**10-20**	**1-2**
Averaged peak power, GW	**10-50**	**10-100**	**50-150**
Spectrum width, %		**0.15-0.3**	**0.18-0.5**

Impact of Accelerator Wakes on SASE

Impedance Budget (list of elements)

El.type	Num.	Loss (kV/nC)	%	Spread (kV/nC)	%	Peak (kV/nC)	%
BPMF	4	4.075E+01	0	1.858E+01	0	5.804E+01	0
COL	7	6.725E+03	19	3.373E+03	22	1.058E+04	21
KICK	3	3.645E+03	10	1.459E+03	9	5.283E+03	10
PIP20	1	5.116E+03	14	3.661E+03	24	8.959E+03	18
PUMCL	78	5.605E+02	2	2.363E+02	2	7.946E+02	2
CAV	808	1.481E+04	42	8.842E+03	57	2.814E+04	56
CAV3	8	8.084E+01	0	3.010E+01	0	1.117E+02	0
FLANG	500	1.330E+03	4	5.610E+02	4	1.886E+03	4
TDS	8	1.507E+03	4	7.348E+02	5	2.174E+03	4
OTRB	8	1.584E+02	0	7.251E+01	0	2.254E+02	0
STEP1	1	3.010E+00	0	5.969E-01	0	3.441E+00	0
BPMA	107	5.654E+02	2	2.896E+02	2	8.670E+02	2
OTRA	12	3.078E+02	1	1.274E+02	1	4.494E+02	1
BPMC	56	4.431E+01	0	2.138E+01	0	6.805E+01	0
BPMR	26	2.993E+02	1	1.304E+02	1	4.501E+02	1
DCM	4	1.644E+01	0	7.479E+00	0	2.315E+01	0
BPMB	27	5.744E-02	0	1.587E-01	0	6.023E-01	0
BAM	5	3.319E+00	0	1.494E+00	0	4.768E+00	0
TORA	3	3.147E+01	0	1.609E+01	0	4.763E+01	0
TORAO	6	1.856E+02	1	7.684E+01	0	2.700E+02	1
		3.530E+04	100	1.540E+04	100	5.037E+04	100

Accelerator wakes. Q=1nC

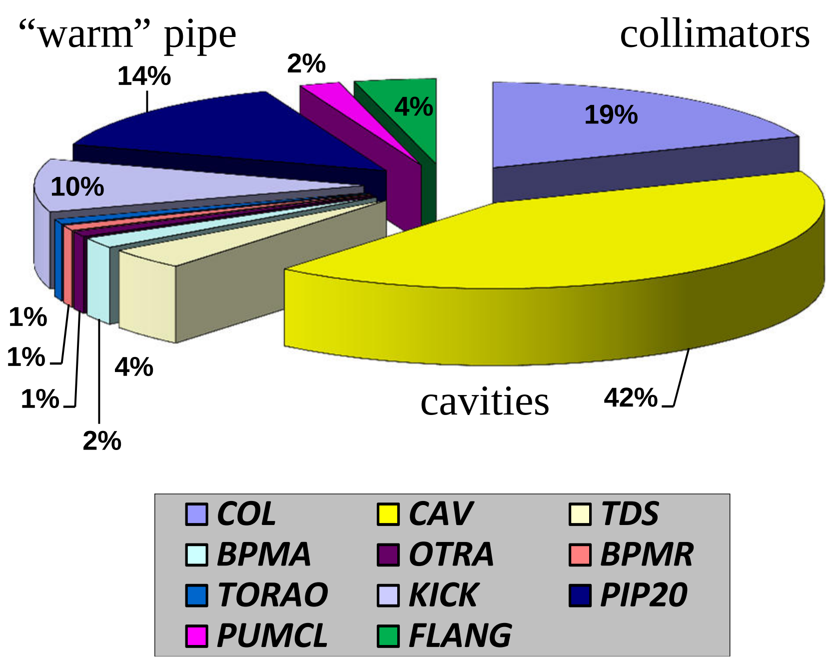

Impact of Accelerator Wakes on SASE

Accelerator wakes. Q=1nC

$W_{\|}\,[\mathrm{MV}]$

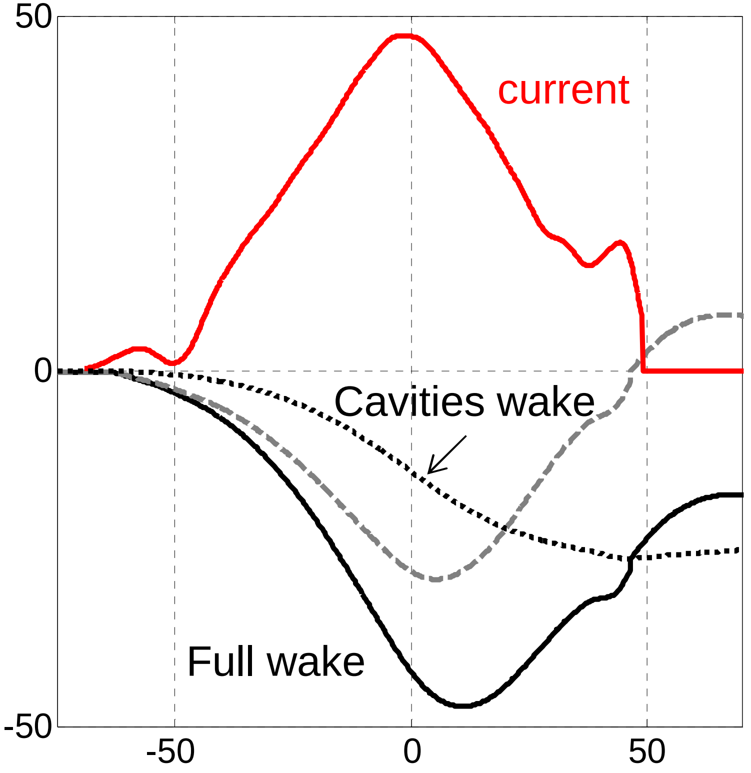

$s\,[\mu\mathrm{m}]$

$$\frac{E-E_0}{E_0\rho} \qquad \rho = 5.3e-4$$

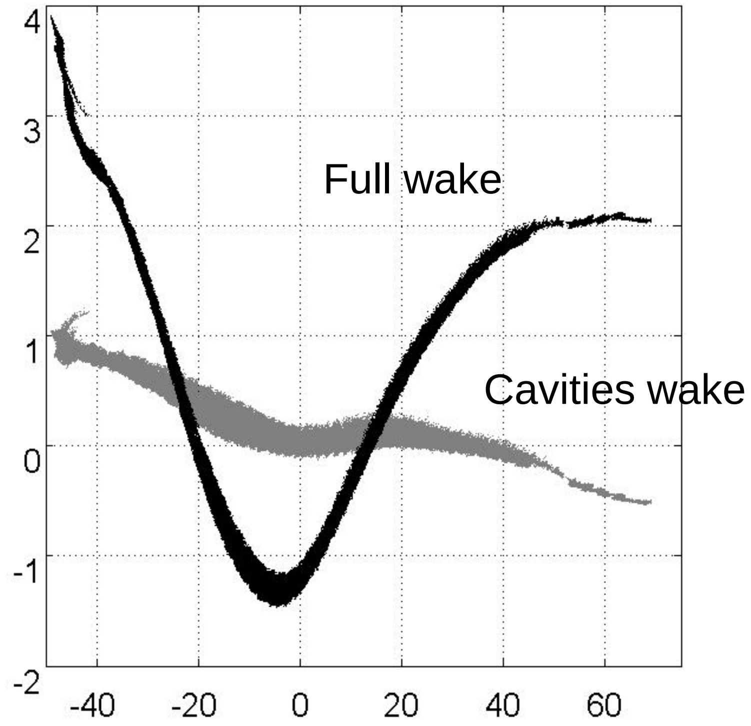

$s\,[\mu\mathrm{m}]$

Impact of Accelerator Wakes on SASE

“Artificially” matched beam. Q=1nC

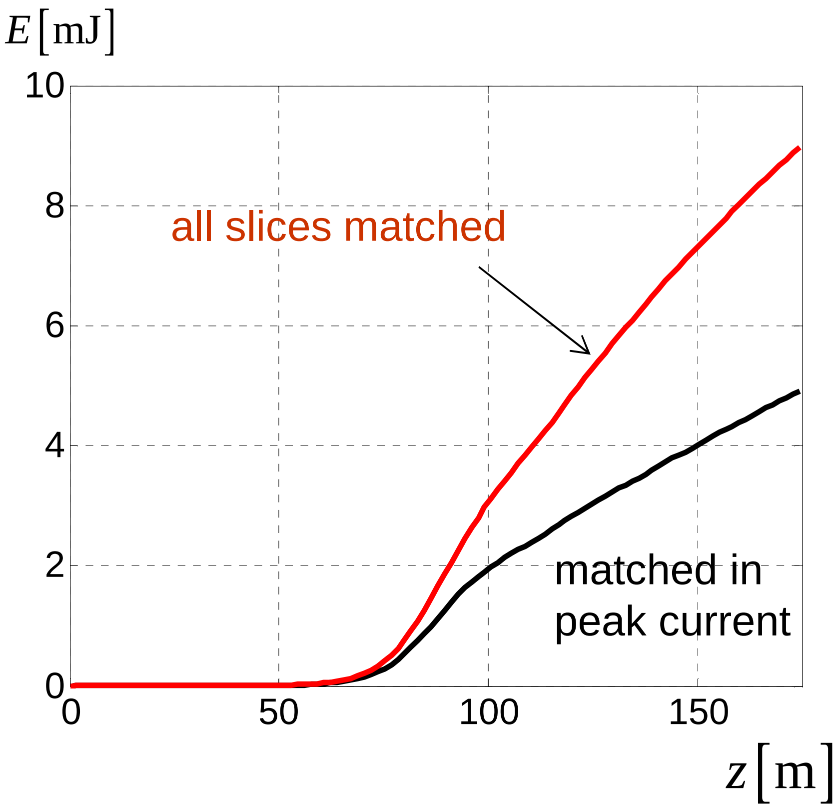

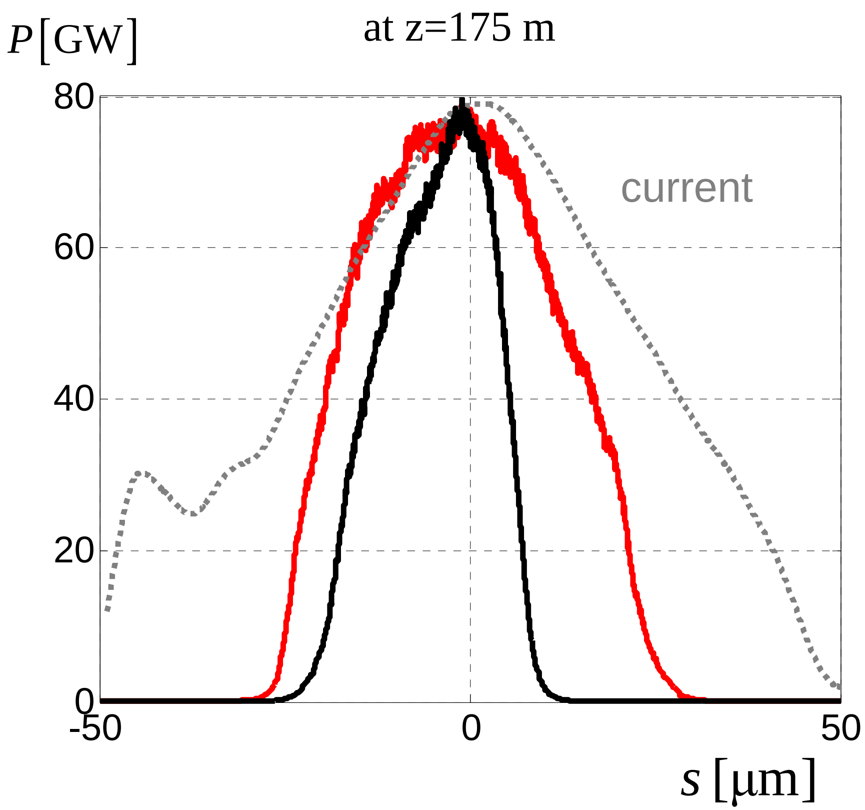

With full accelerator and undulator wake

$$\left(\frac{dK}{dz}\right)_{opt} = -4.8\cdot 10^{-5}\,\mathrm{m}^{-1}$$

Impact of Accelerator Wakes on SASE

Beam matched in the peak current. Q=1nC

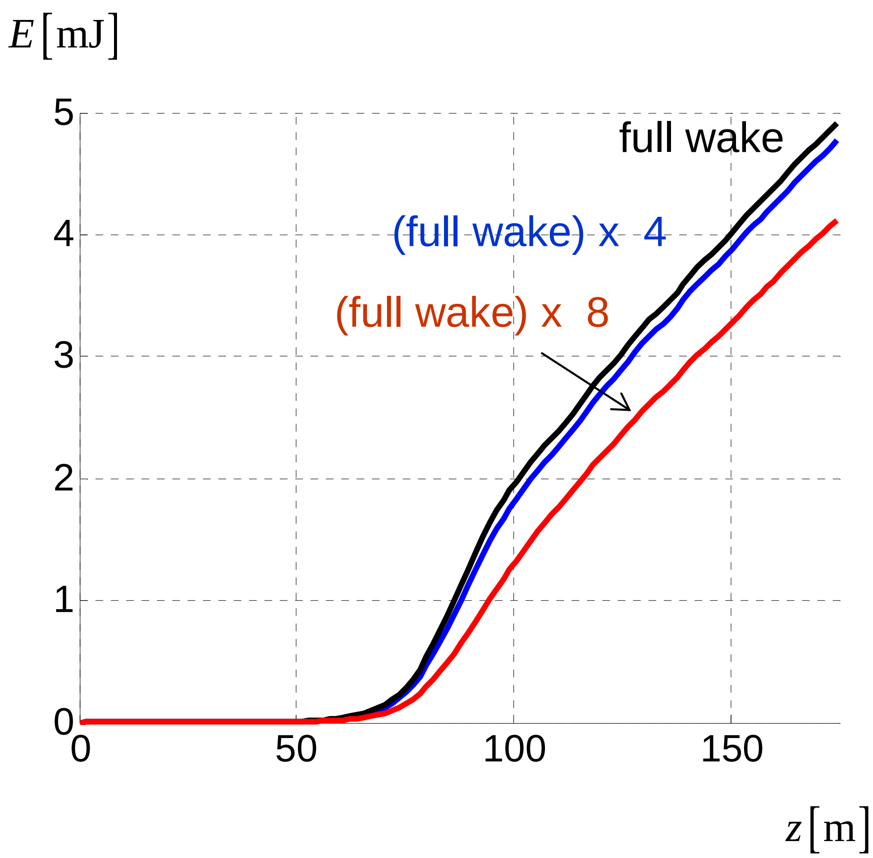

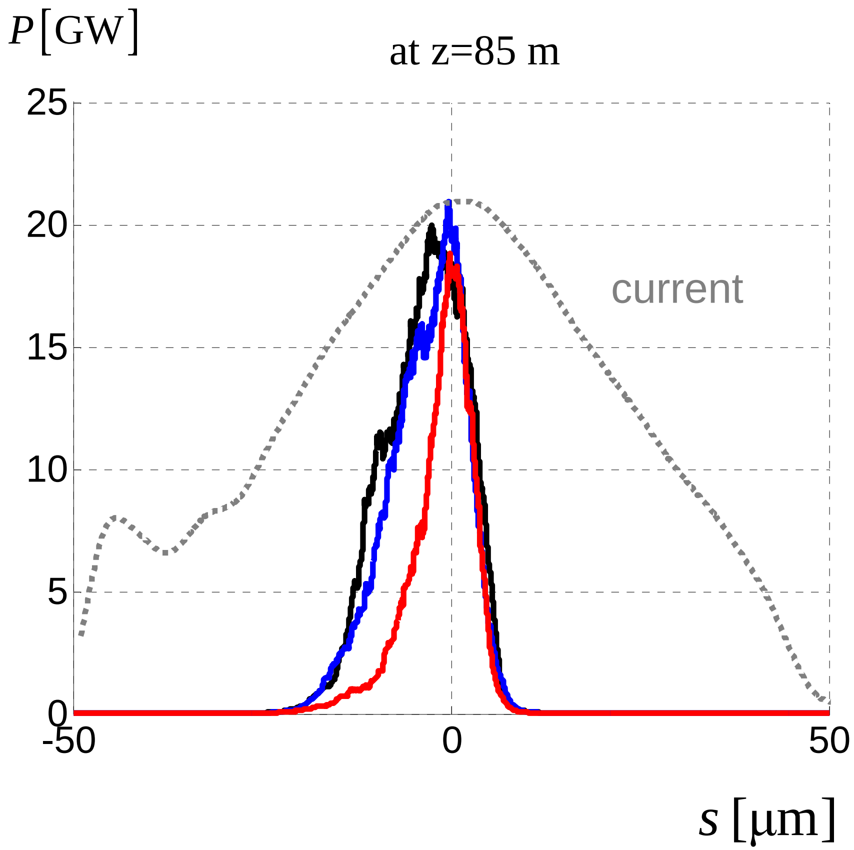

Impact of Accelerator Wakes on SASE

Beam matched in the peak current. Q=1nC

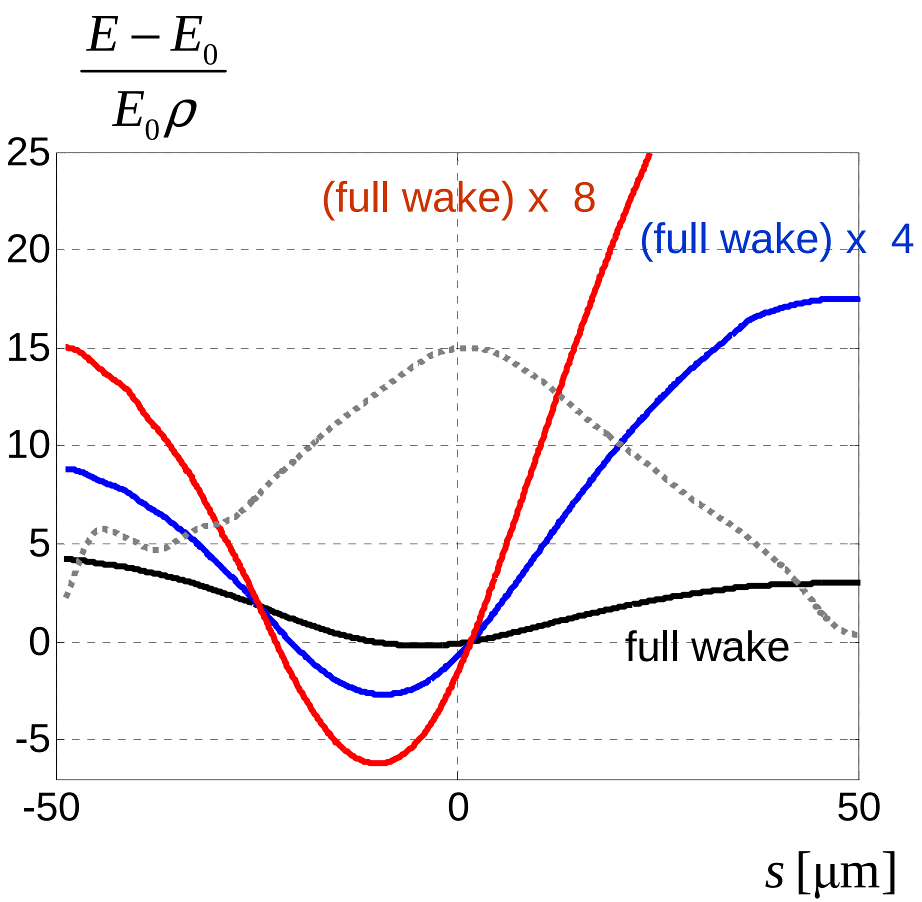

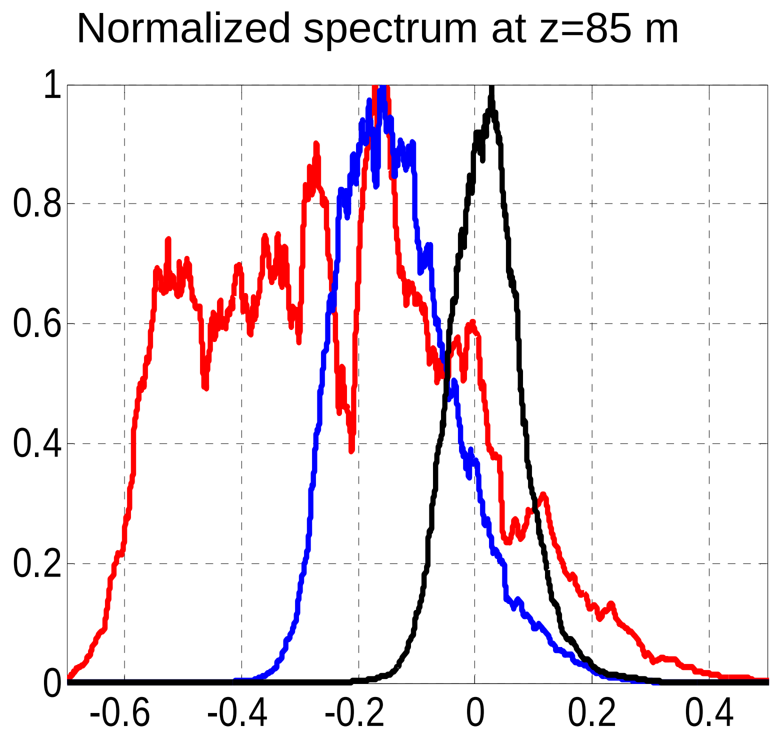

FWHM=0.14%

$\frac{\omega-\omega_0}{\omega_0}[\%]$

FWHM=0.23%

FWHM=0.6%

Impact of Accelerator Wakes on SASE

El.type	*Num.*	*Loss (kV/nC)*	*%*	*Spread (kV/nC)*	*%*	*Peak (kV/nC)*	*%*
BPMF	4	6.150E+01	0	2.891E+01	0	8.933E+01	0
COL	7	2.283E+04	32	1.022E+04	31	3.452E+04	35
KICK	3	7.893E+03	11	3.100E+03	9	1.052E+04	11
PIP20	1	1.652E+04	23	8.512E+03	26	2.730E+04	27
PUMCL	78	1.103E+03	2	4.743E+02	1	1.574E+03	2
CAV	808	1.574E+04	22	9.440E+03	29	2.987E+04	30
CAV3	8	9.280E+01	0	3.590E+01	0	1.316E+02	0
FLANG	500	2.619E+03	4	1.126E+03	3	3.736E+03	4
TDS	8	2.506E+03	4	1.229E+03	4	3.677E+03	4
OTRB	8	2.428E+02	0	1.137E+02	0	3.510E+02	0
STEP1	1	3.825E+00	0	6.815E-01	0	4.293E+00	0
BPMA	107	7.317E+02	1	4.231E+02	1	1.265E+03	1
OTRA	12	1.698E+02	0	8.118E+01	0	2.474E+02	0
BPMC	56	7.912E+01	0	4.531E+01	0	1.348E+02	0
BPMR	26	1.523E+02	0	7.506E+01	0	2.241E+02	0
DCM	4	2.533E+01	0	1.160E+01	0	3.612E+01	0
BPMB	27	1.247E-01	0	1.976E-01	0	7.440E-01	0
BAM	5	4.474E+00	0	2.180E+00	0	6.820E+00	0
TORA	3	4.681E+01	0	2.515E+01	0	7.275E+01	0
TORAO	6	1.107E+02	0	5.175E+01	0	1.598E+02	0
		7.063E+04	100	3.285E+04	100	1.000E+05	100

Accelerator wakes. Q=250 pC.

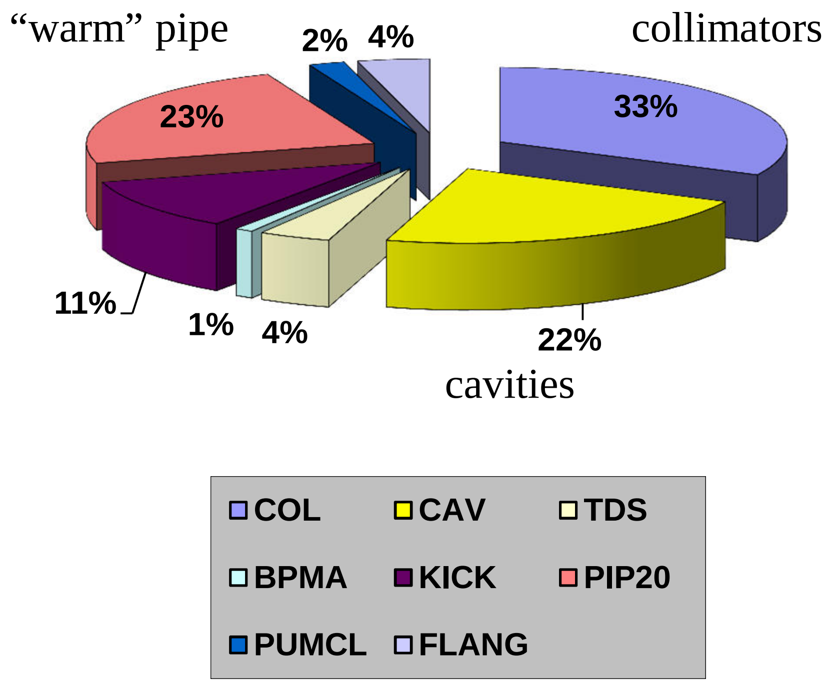

Impact of Accelerator Wakes on SASE

Accelerator wakes. Q=250 pC.

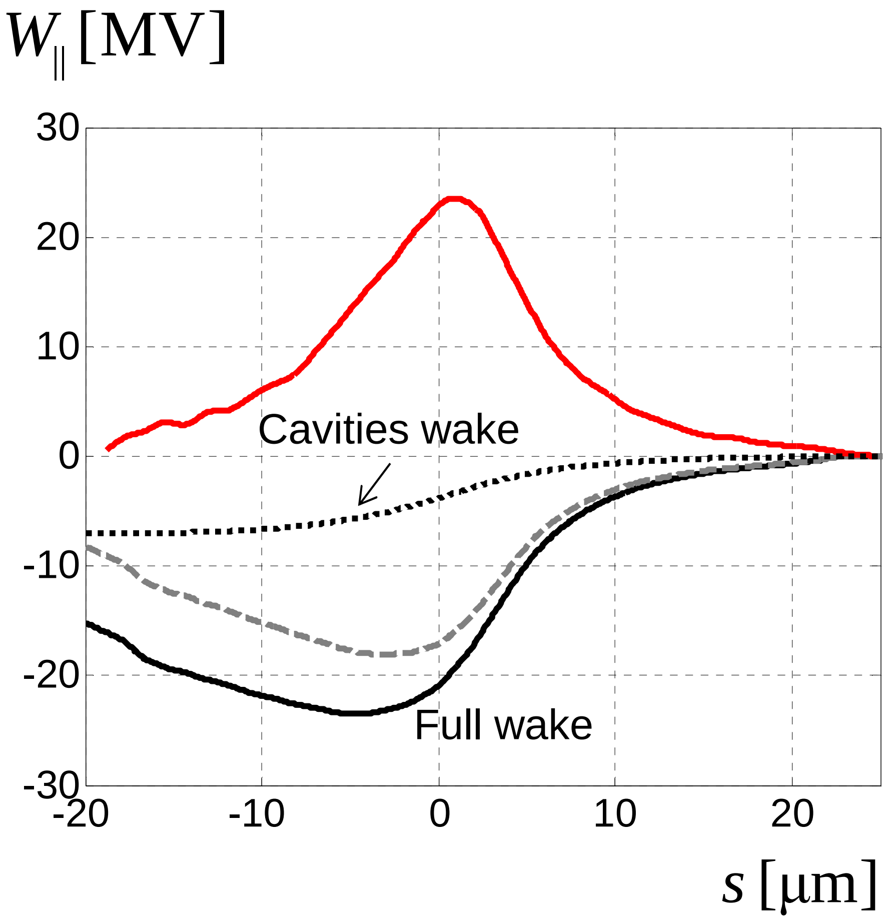

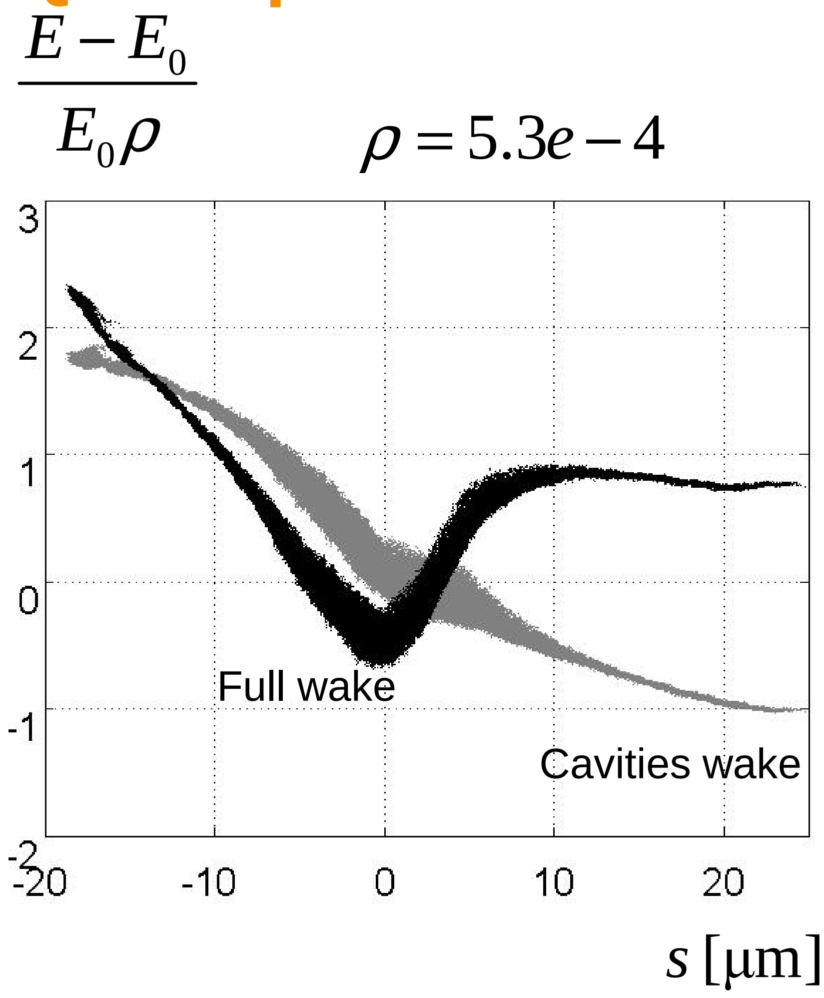

Impact of Accelerator Wakes on SASE

Beam matched in the peak current. Q=250 pC

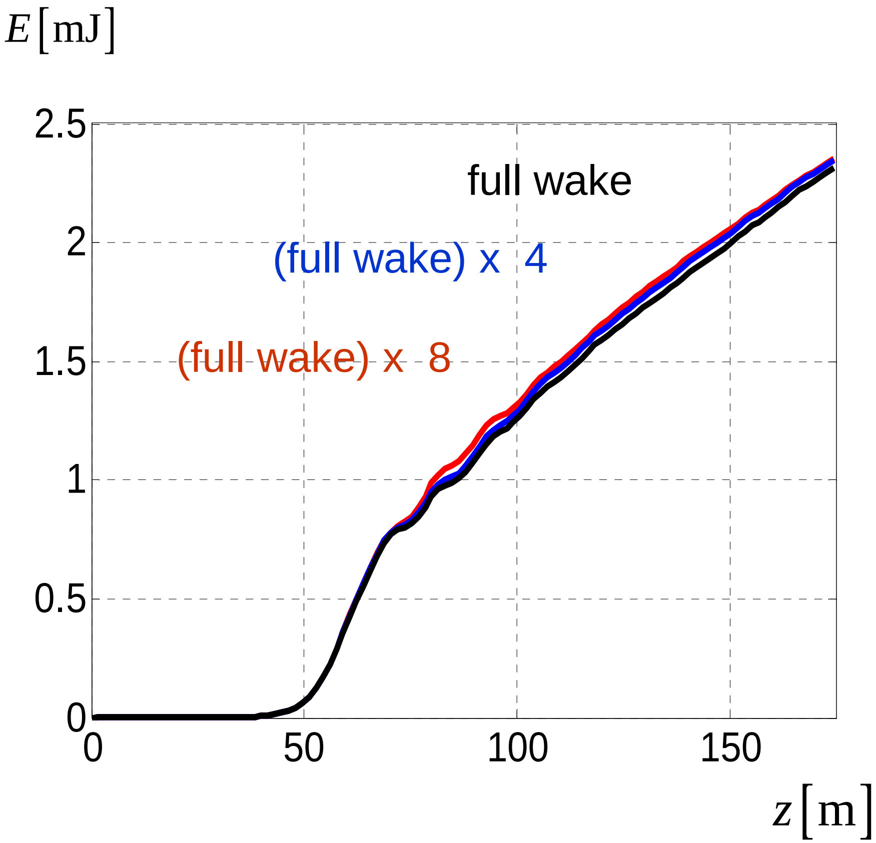

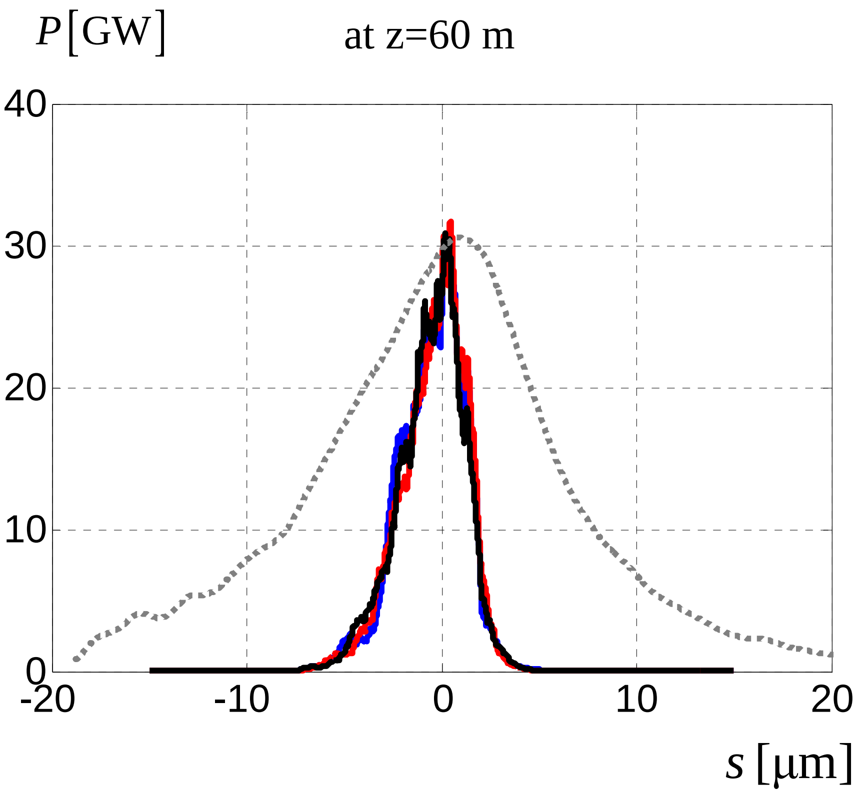

Impact of Accelerator Wakes on SASE

Beam matched in the peak current. Q=250 pC

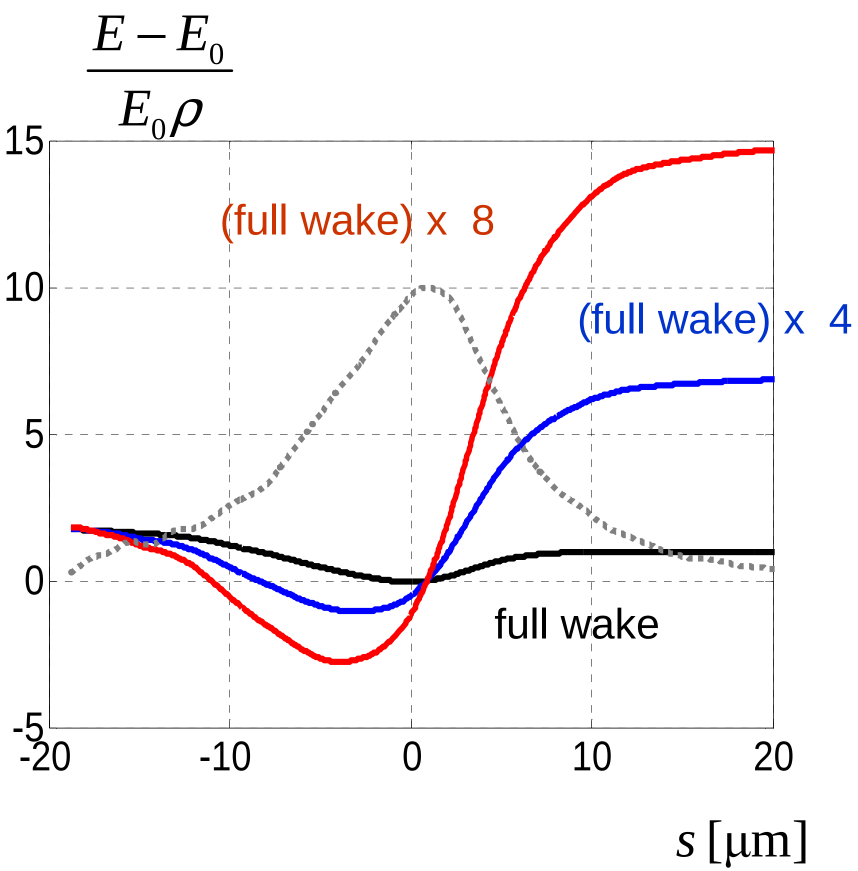

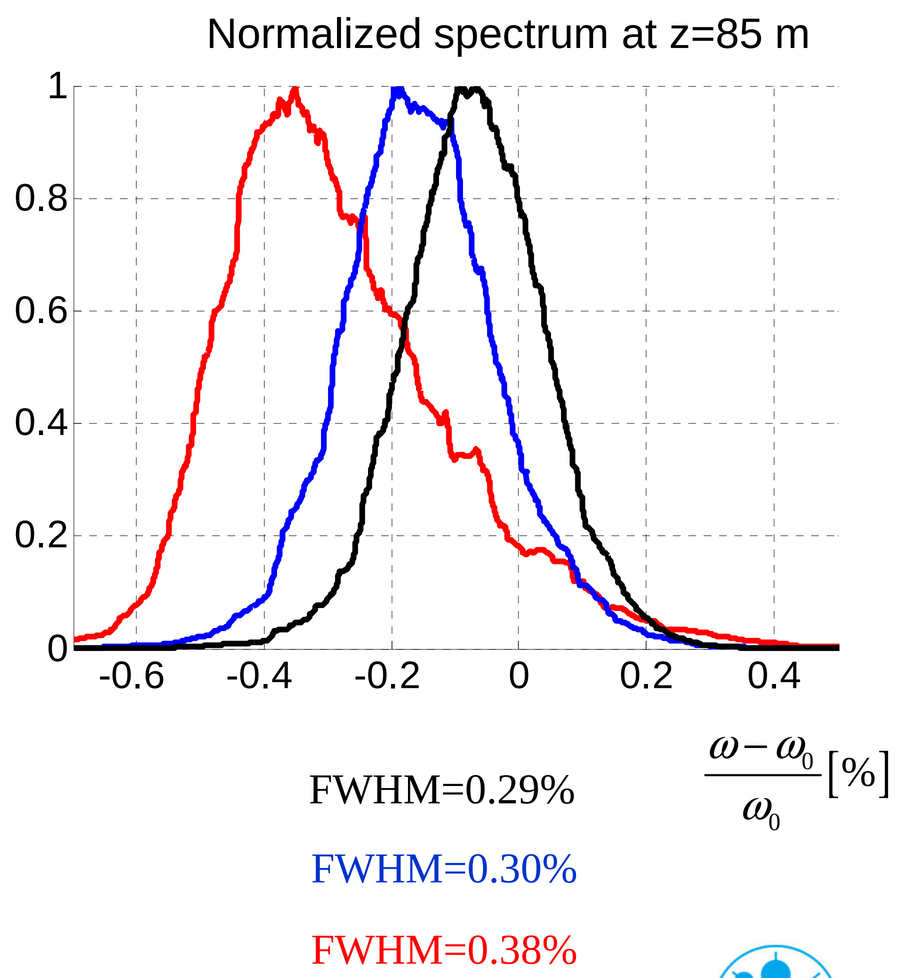

Impact of Accelerator Wakes on SASE

El.type	*Num.*	*Loss (kV/nC)*	*%*	*Spread (kV/nC)*	*%*	*Peak (kV/nC)*	*%*
BPMF	4	1.028E+02	0	4.822E+01	0	1.602E+02	0
COL	7	1.040E+05	57	8.502E+04	83	2.999E+05	75
KICK	3	3.017E+04	17	1.808E+04	18	6.233E+04	16
PIP20	1	1.975E+04	11	1.126E+04	11	3.789E+04	9
PUMCL	78	2.666E+03	1	1.237E+03	1	4.514E+03	1
CAV	808	1.670E+04	9	9.809E+03	10	3.109E+04	8
CAV3	8	9.994E+01	0	3.871E+01	0	1.424E+02	0
FLANG	500	6.328E+03	3	2.937E+03	3	1.072E+04	3
TDS	8	4.847E+03	3	2.648E+03	3	8.072E+03	2
OTRB	8	4.257E+02	0	2.010E+02	0	6.740E+02	0
STEP1	1	4.406E+00	0	7.830E-01	0	4.846E+00	0
BPMA	107	7.840E+02	0	4.502E+02	0	1.352E+03	0
OTRA	12	3.035E+02	0	1.468E+02	0	4.863E+02	0
BPMC	56	8.884E+01	0	5.119E+01	0	1.636E+02	0
BPMR	26	3.036E+02	0	1.547E+02	0	5.074E+02	0
DCM	4	4.672E+01	0	2.190E+01	0	7.487E+01	0
BPMB	27	1.755E-01	0	2.488E-01	0	7.636E-01	0
BAM	5	5.023E+00	0	2.364E+00	0	7.486E+00	0
TORA	3	6.546E+01	0	3.326E+01	0	9.760E+01	0
TORAO	6	1.989E+02	0	9.429E+01	0	3.173E+02	0
		1.810E+05	100	1.019E+05	100	4.004E+05	100

Accelerator wakes. Q=20 pC

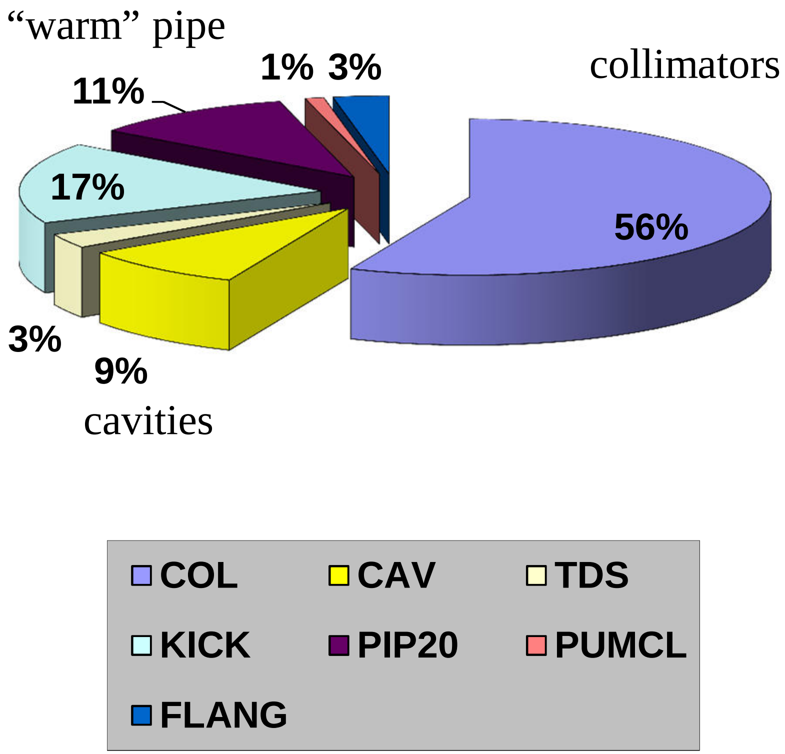

Impact of Accelerator Wakes on SASE

Accelerator wakes. Q=20 pC

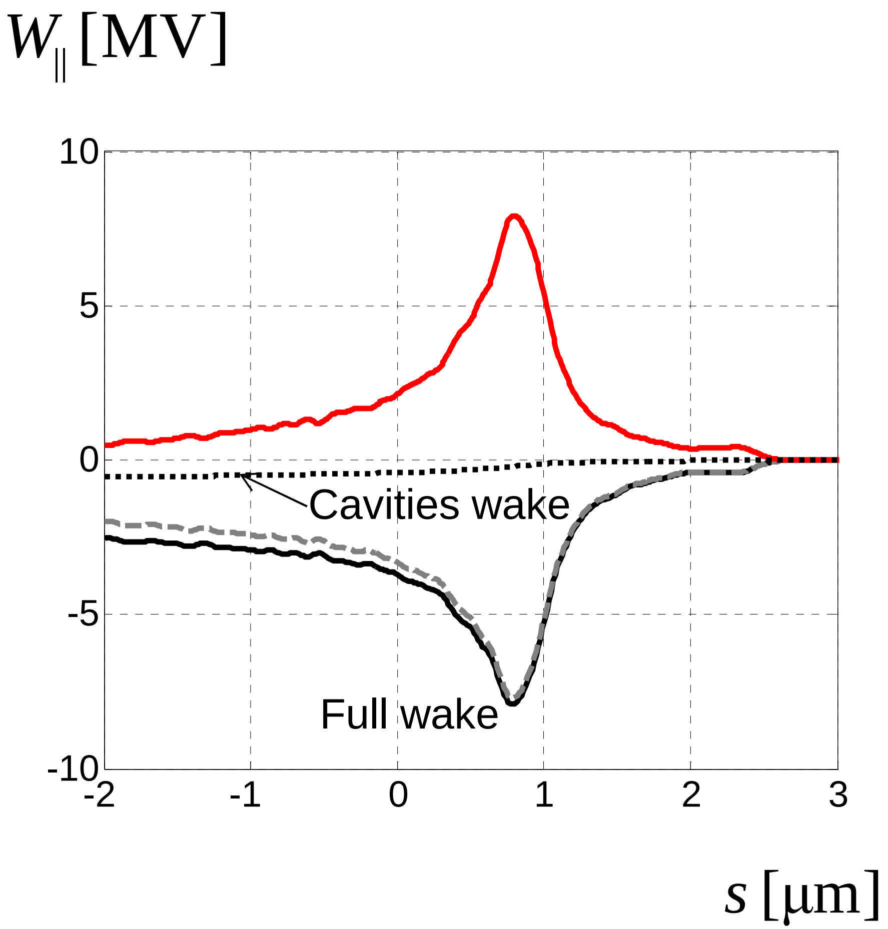

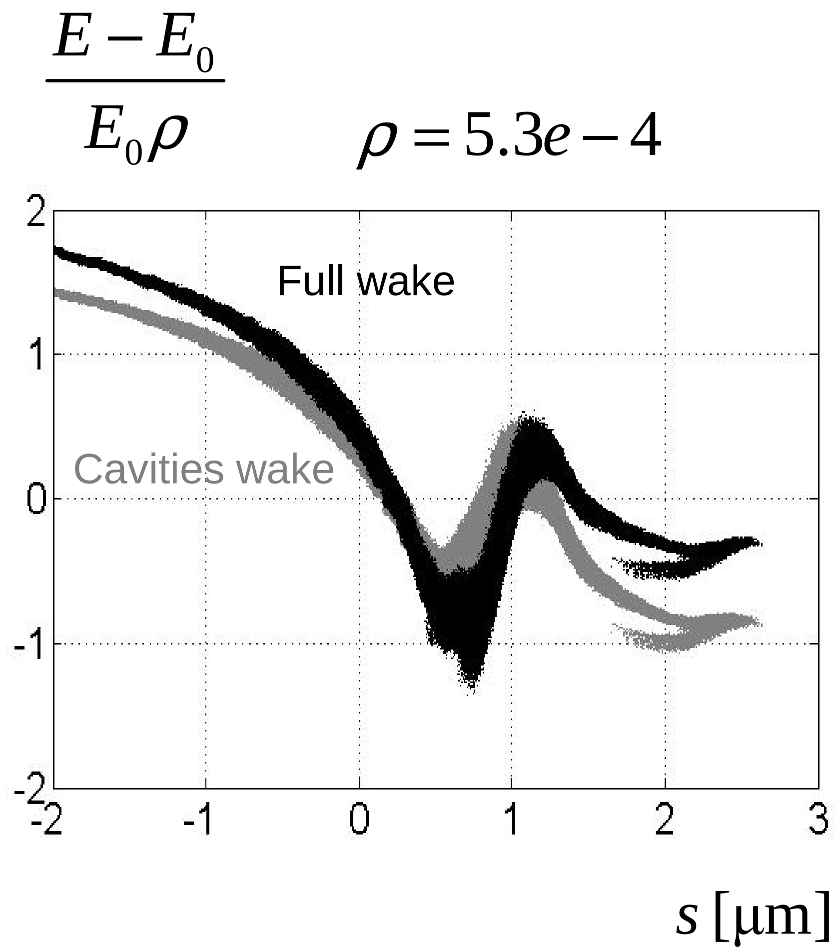

Impact of Accelerator Wakes on SASE

Beam matched in the peak current. Q=20 pC

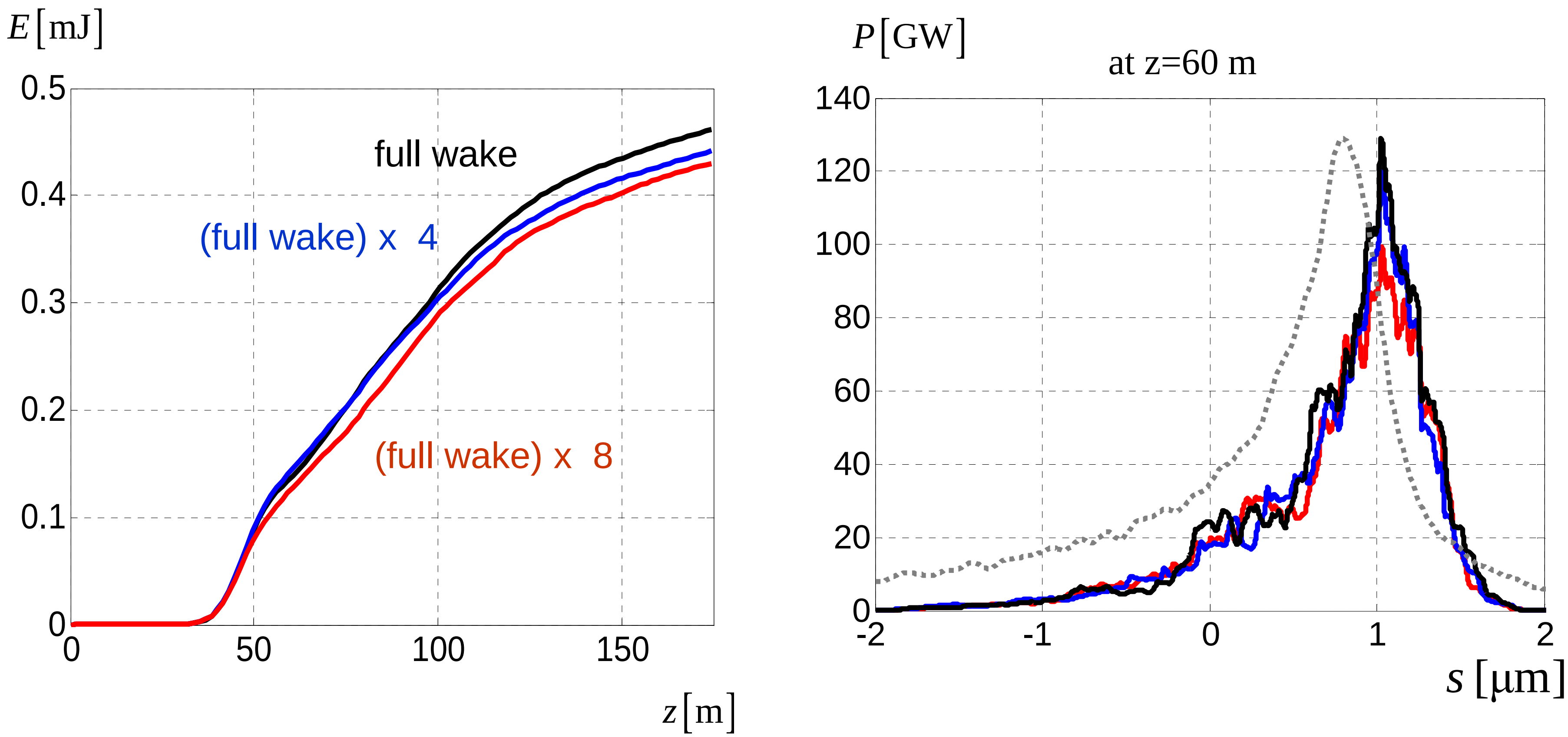

Impact of Accelerator Wakes on SASE

Beam matched in the peak current. Q=20 pC

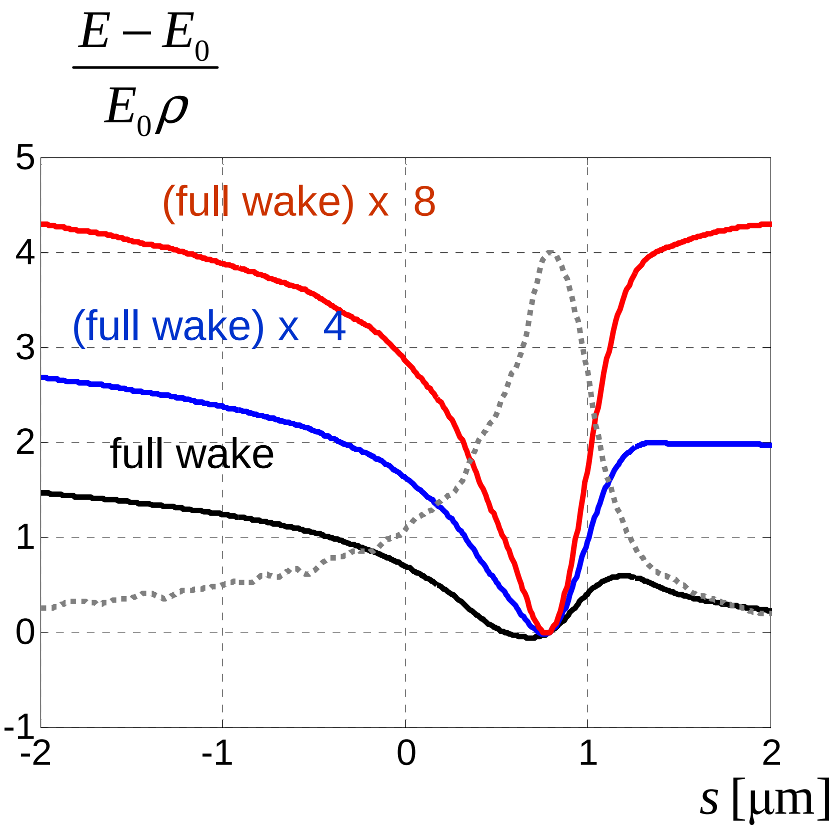

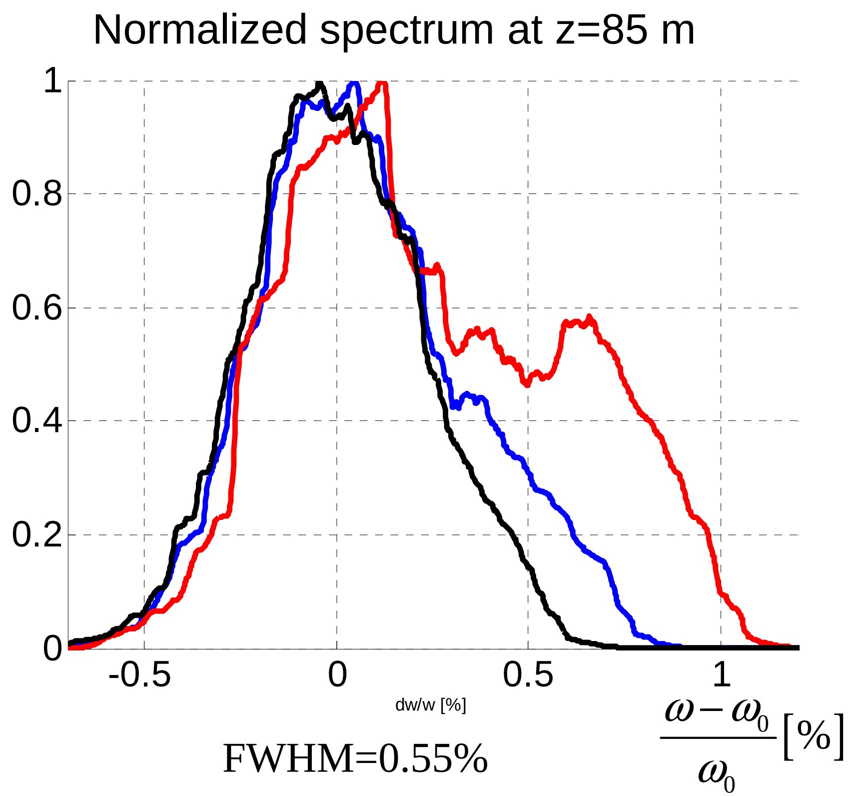

FWHM=0.55%

FWHM=0.58%

FWHM=1.0%

Impact of Accelerator Wakes on SASE

Summary

	Accelerator wake	Bunch charge, nC		
		1	0.25	0.02
Energy in the radiation pulse at z=175 m, mJ	x1	9	2.3	0.46
	x4	8	2.3	0.44
	x8	6	2.3	0.43
Spectrum width at z=85m, %	x1	0.14	0.29	0.55
	x4	0.23	0.30	0.58
	x8	0.6	0.38	1.0

We have considered only the **longitudinal** wake in a quite coarse model (adding the accelerator wake at the undulator entrance).
The **transverse** wakes are neglected.

Self-Seeding Schemes for TW Power

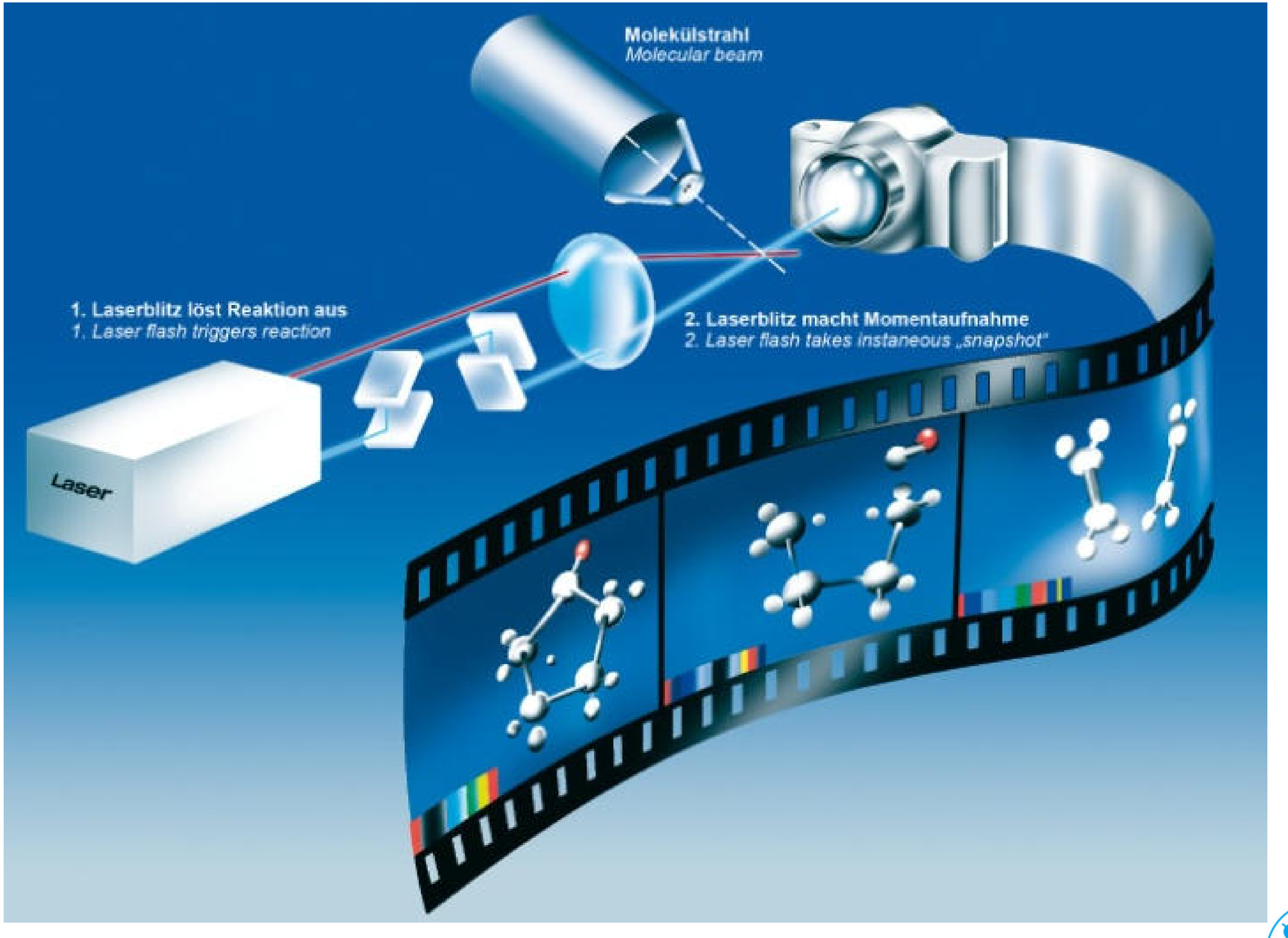

Self-Seeding Schemes for TW Power

Requirements for bio-imaging

- the imaging method “diffraction before destruction” requires pulses containing enough photons to produce measurable diffraction patterns and short enough to outrun radiation damage
- the higher is intensity, the stronger is the diffracted signal and the higher resolution can be achieved
- bio-imaging capabilities can be obtained by reducing the pulse duration to 10 fs or less and simultaneously increasing the number of photons per pulse to about 10^{14}
- Key metric is photon power. Ideally ~ 10 TW (10^{14} photons at ~3.5 keV is ~ 60 mJ and in 10 fs ~ 6 TW)

E.Saldin , Perspectives of imaging of single macromolecular complexes at the European XFEL, CFEL Seminar, Hamburg, 8.05. 2013

DESY

Self-Seeding Schemes for TW Power

Calculated scattering from a single molecule

It is confirmed by simulations that, with 10^{14} photons per 10 fs pulse at 3.5 keV photon energy in a 100 nm focus, one can achieve diffraction to the desired resolution. This is exemplified using photosystem-I membrane protein as a case study

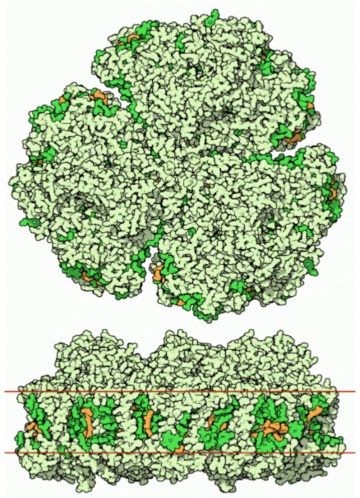

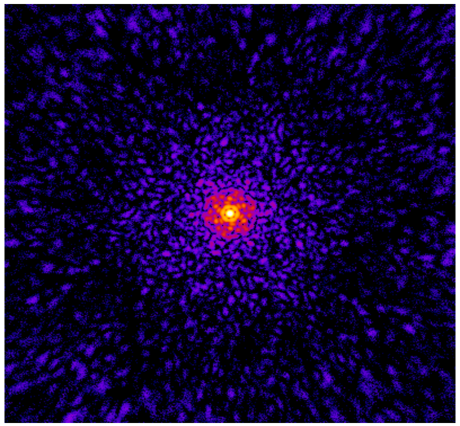

E.Saldin , Perspectives of imaging of single macromolecular complexes at the European XFEL, CFEL Seminar, Hamburg, 8.05. 2013

Simulated diffraction pattern

Courtesy of S. Serkez and O. Yefanov

Self-Seeding Schemes for TW Power

Self-seeding and undulator tapering

According to the present design of EXFEL, SASE power saturates at ~ 50 GW. This is very far from 10 TW-power level required for imaging of single bio-molecules.

There is cost-effective way to improve the output power:

Self-seeding and undulator tapering greatly improves FEL efficiency

Cost of self-seeding setup with single crystal monochromator is ~ 2 MEUR. Undulator tapering is based on the used the baseline tunable gap undulator and can be implemented without additional cost.

E.Saldin , Perspectives of imaging of single macromolecular complexes at the European XFEL, CFEL Seminar, Hamburg, 8.05. 2013

Self-Seeding Schemes for TW Power

Strong Compression for Q=1 nC

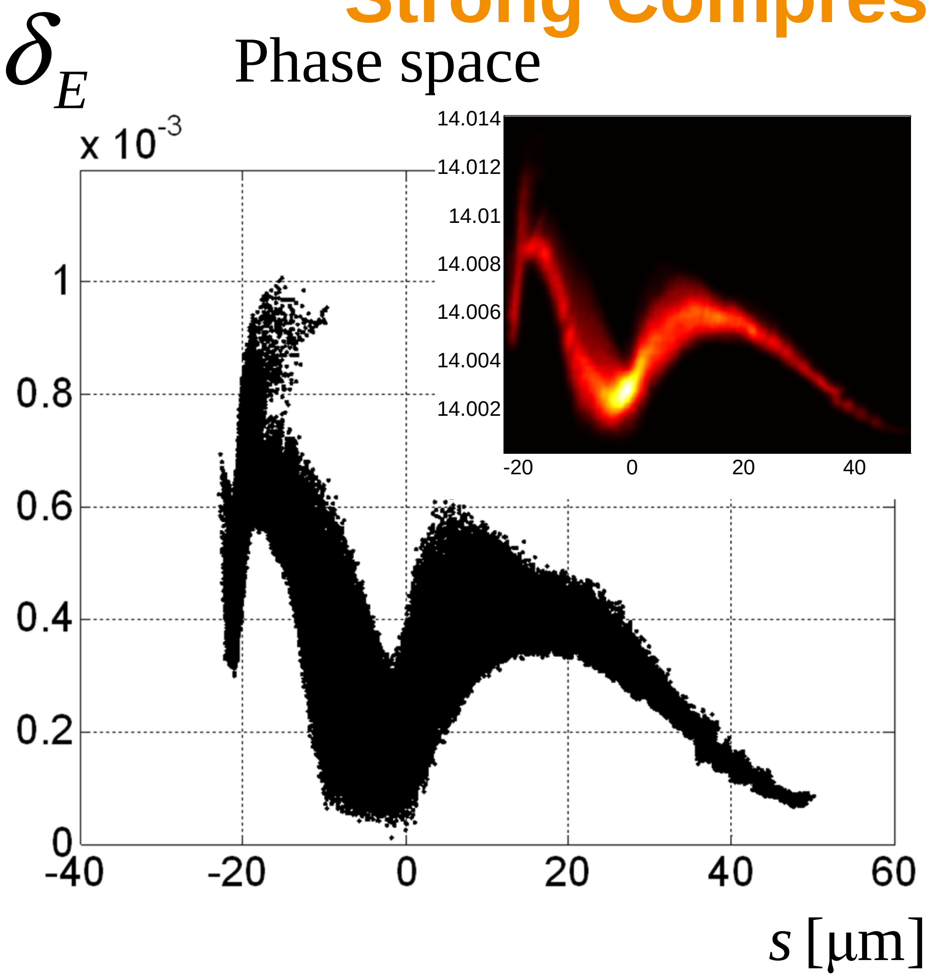

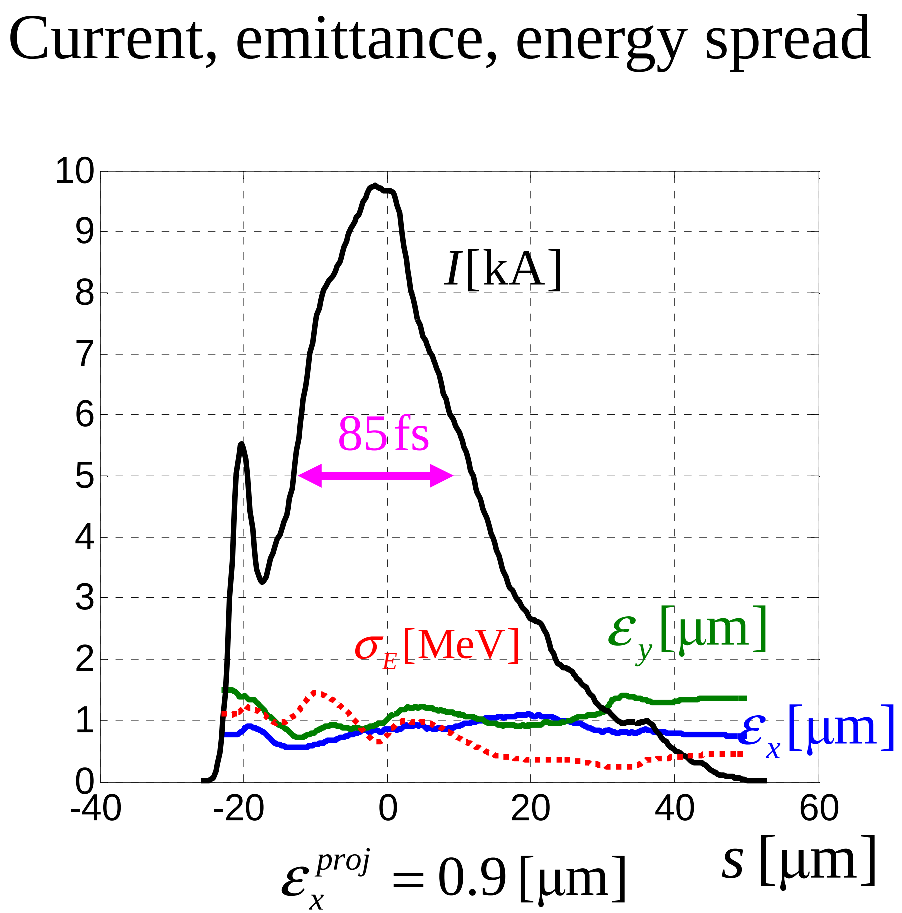

$$\varepsilon_x^{proj} = 0.9\,[\mu m]$$

$$\varepsilon_y^{proj} = 8\,[\mu m]$$

Self-Seeding Schemes for TW Power

Aluminum Foil in BC

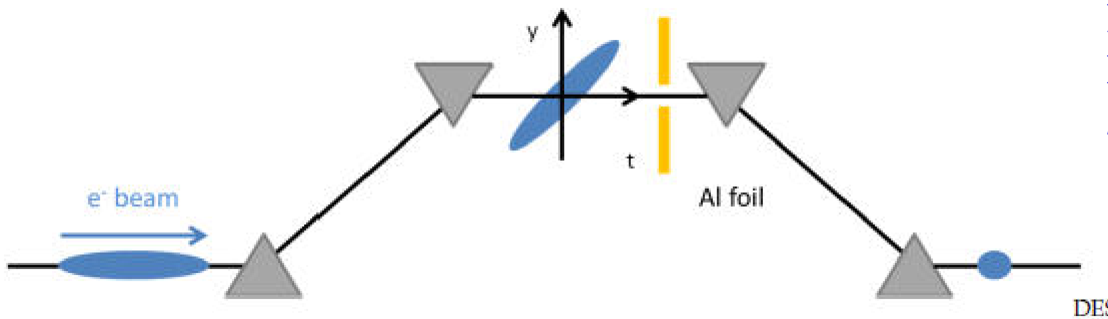

P. Emma, M. Cornacchia, K. Bane, Z. Huang, H. Schlarb, G. Stupakov, D. Walz, *PRL* **92**, 074801. 2004, (SLAC)

DESY 13-101

June 2013

Svitozar Serkez[a], Vitali Kocharyan[a], Evgeni Saldin[a], Igor Zagorodnov[a], Gianluca Geloni[b], and Oleksander Yefanov[c]

Proposal for a scheme to generate 10 TW-level femtosecond x-ray pulses for imaging single protein molecules at the European XFEL

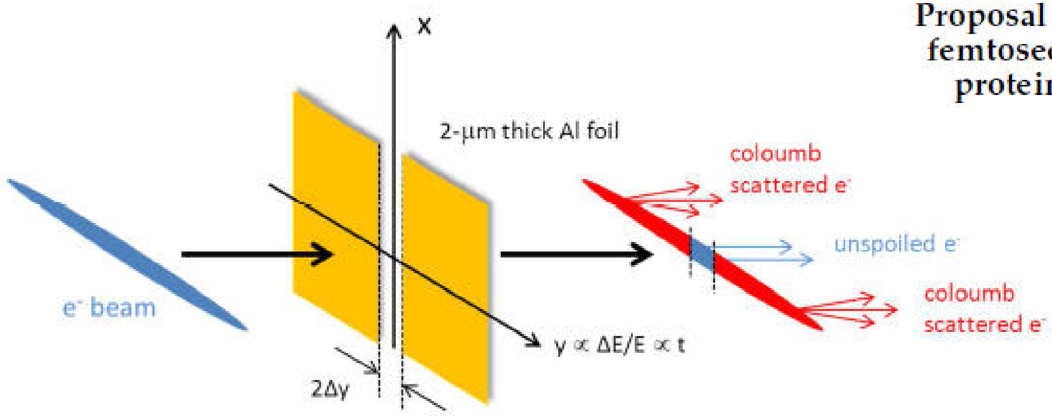

Fig. 2. The slotted foil at chicane center generates a narrow, unspoiled beam center

Self-Seeding Schemes for TW Power

Aluminum Foil in BC

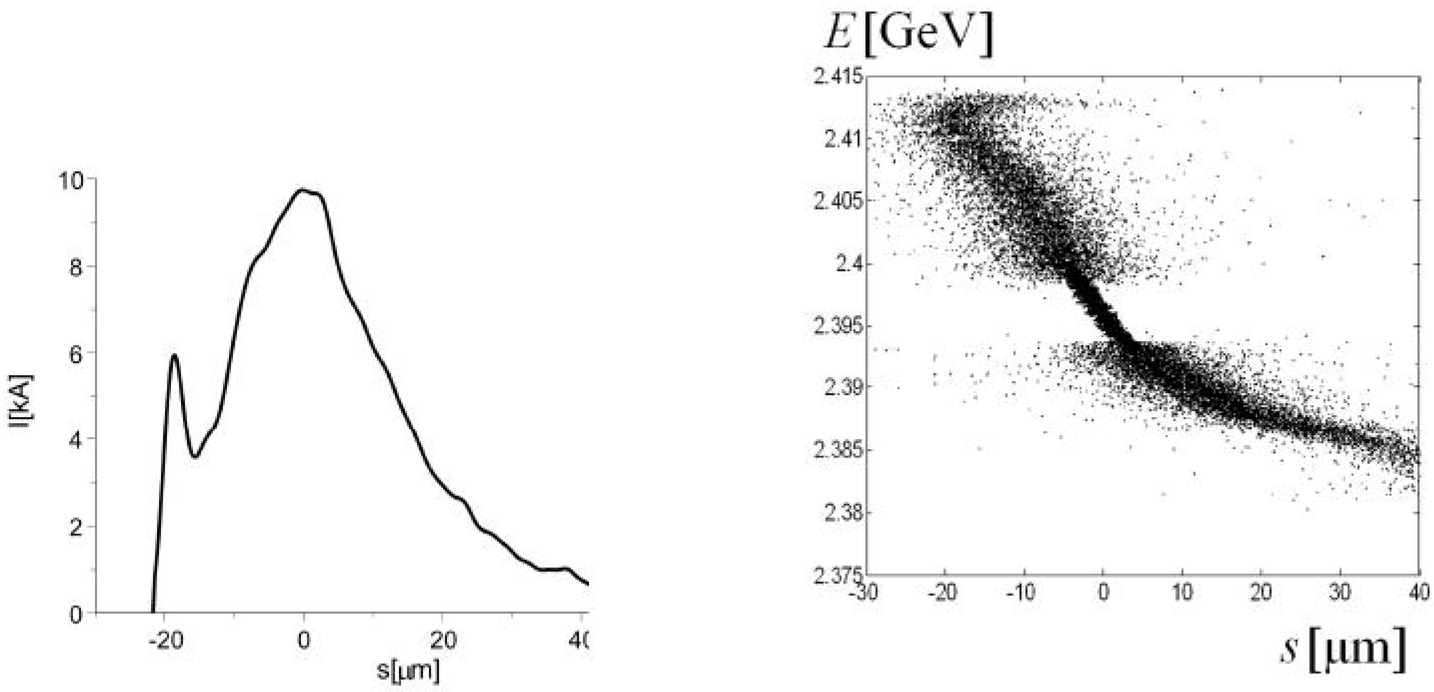

Fig. 3. Left plot: Current profile after BC3 without foil. Right plot: Longitudinal phase space distribution of the particles after BC3, with foil. The simulation includes multiple Coulomb scattering in a 2μm thin aluminum foil with a slot width of 0.7 mm.

Self-Seeding Schemes for TW Power

Aluminum Foil in BC

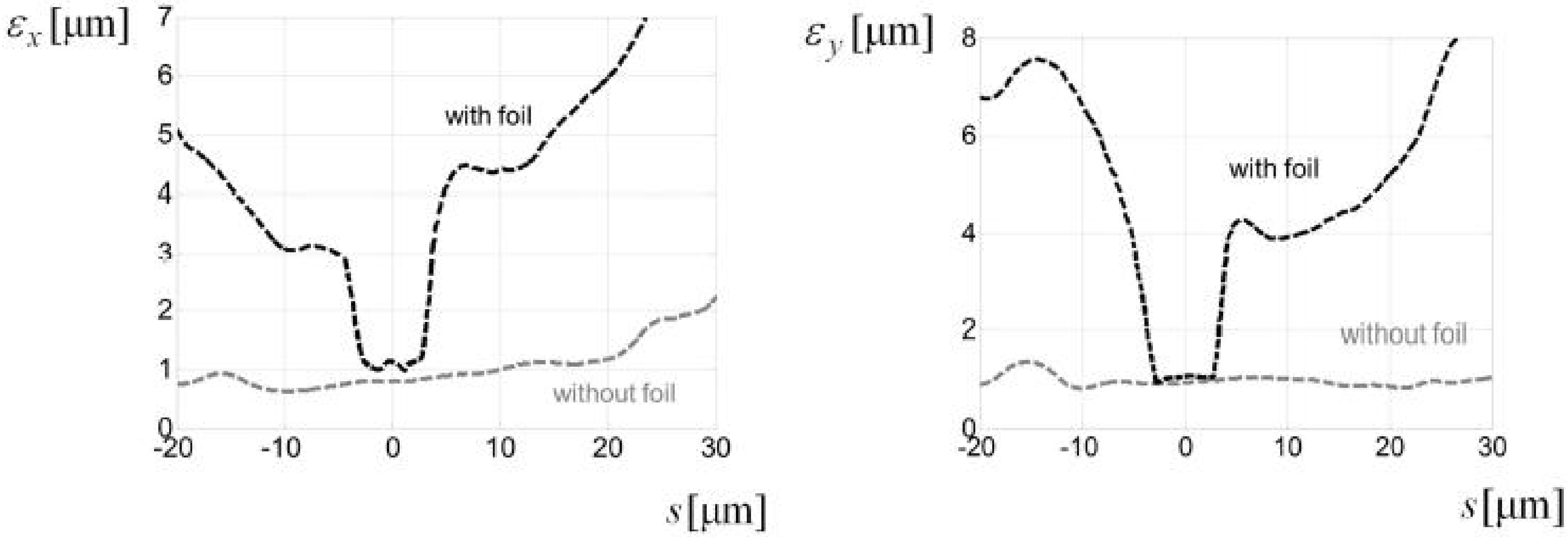

Fig. 4. Left plot: Vertical normalized emittance as a function of the position inside the electron bunch after BC3. The grey dashed curve is from particle tracking without foil. The black dashed curve is from particle tracking with foil. Right plot: Horizontal emittance as a function of the position inside the electron bunch after BC3. The grey dashed curve is from particle tracking without foil. The black dashed curve is from particle tracking with foil. (In both plots we removed 6 % of strongly scattered particles from the analysis.)

Self-Seeding Schemes for TW Power

Self-seeding

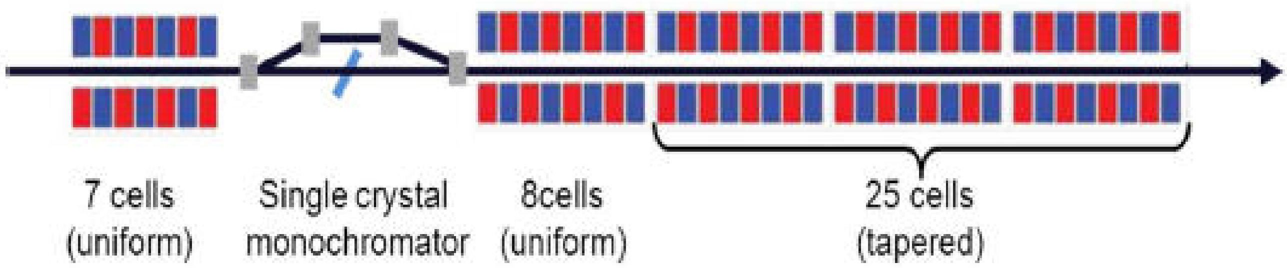

Fig. 5. Scheme for a 10 TW-power level undulator source. Self-seeding and undulator tapering greatly improve the FEL efficiency. X-ray pulse length control is obtained using a slotted foil in the last bunch compressor. The magnetic chicane accomplishes three tasks by itself. It creates an offset for single crystal monochromator, it removes the electron microbunching produced in the upstream undulator, and it acts as a magnetic delay line.

Self-Seeding Schemes for TW Power

Self-seeding

Courtesy V.Kocharyan

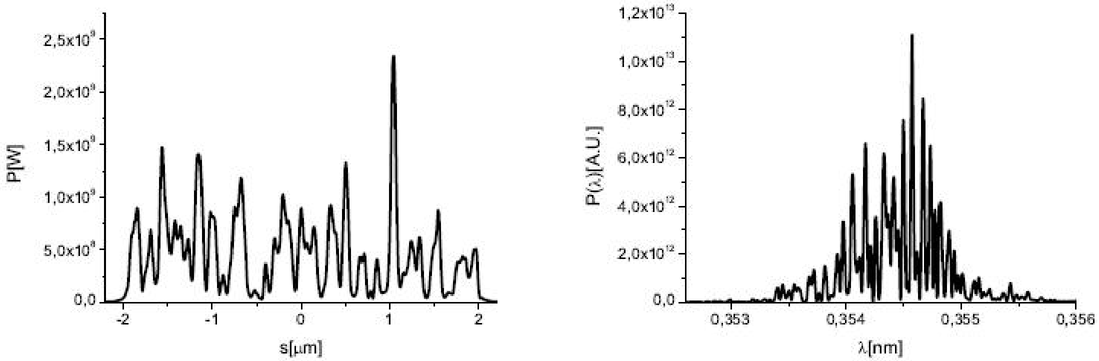

Fig. 9. Power distribution and spectrum of the SASE x-ray pulse at the exit of the first undulator.

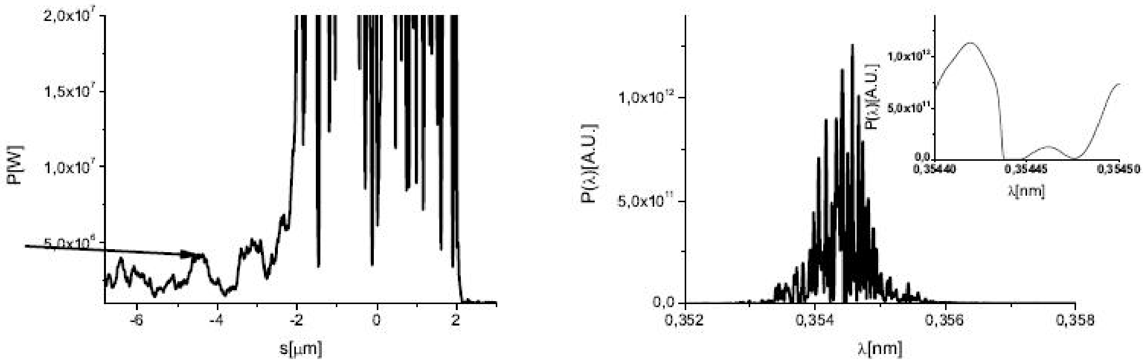

Fig. 10. Power distribution and spectrum of the SASE x-ray pulse at after the wake monochromator. The seed pulse is indicated by an arrow in the left plot.

Self-Seeding Schemes for TW Power

Self-seeding and tapering

Courtesy
V.Kocharyan

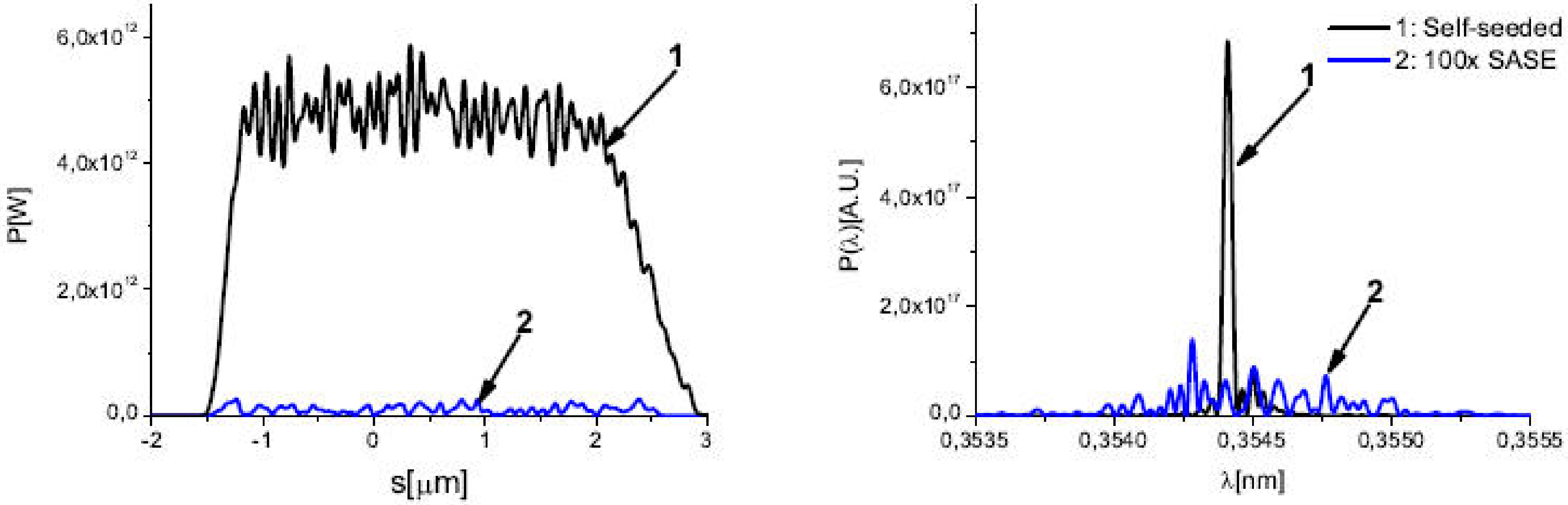

Fig. 12. Power distribution and spectrum of the output radiation pulse. The self--seeded line 1 is compared with the SASE line 2, showing the advantages of our method. The SASE spectrum is magnified of a factor 100, to make it visible in comparison with the self-seeded spectrum.

Self-Seeding Schemes for TW Power

Self-seeding and tapering

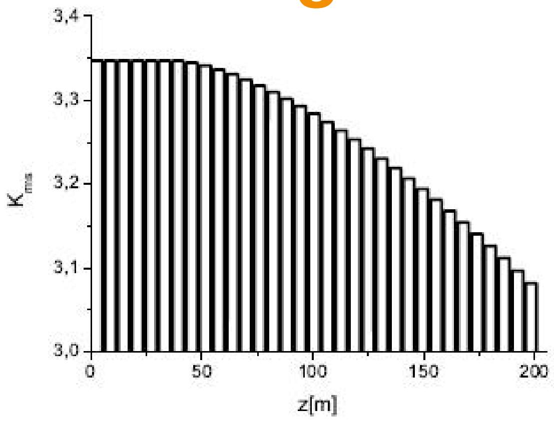

Fig. 11. Taper configuration for high-power mode of operation at 0.35 nm.

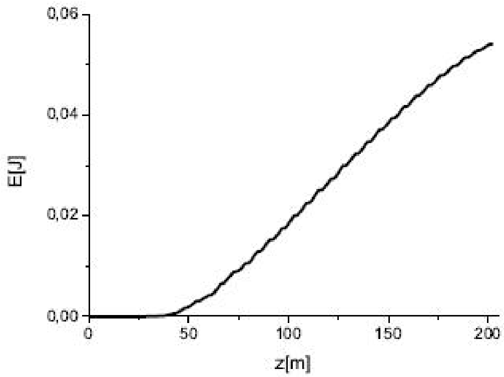

Fig. 13. Energy of the seeded FEL pulse as a function of the distance inside the output undulator.

Strong Bunch Compresion for TW Power

Strong compression and undulator tapering

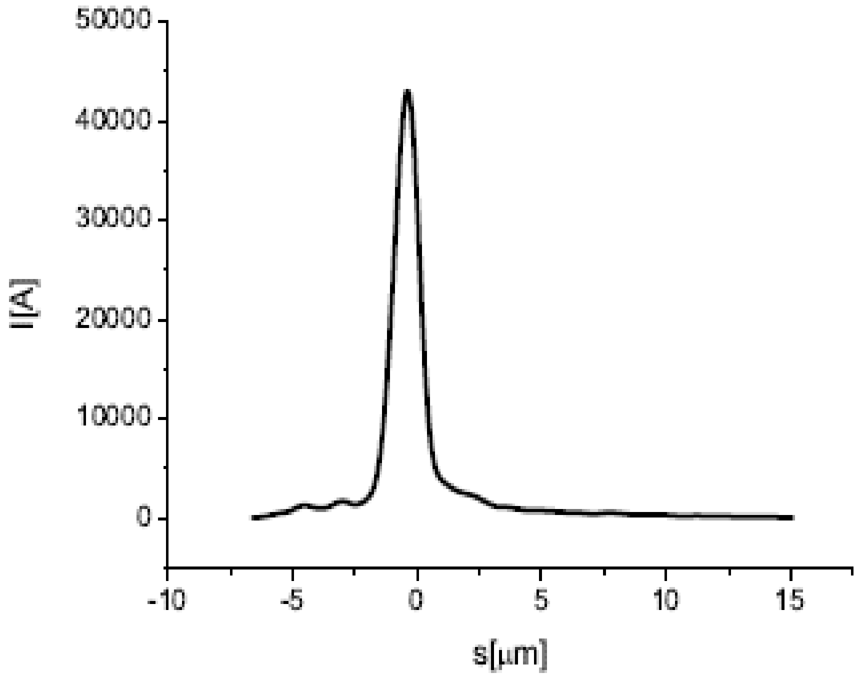

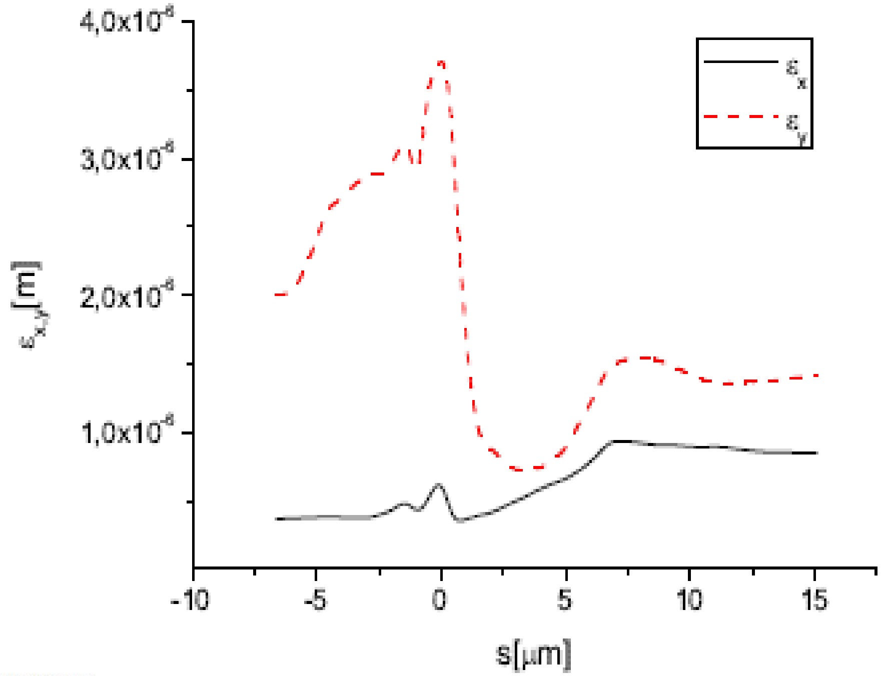

DESY 13-109

June 2013

Svitozar Serkez[a], Vitali Kocharyan[a], Evgeni Saldin[a], Igor Zagorodnov[a], Gianluca Geloni[b], and Oleksander Yefanov[c]

Extension of SASE bandwidth up to 2% as a way to increase the efficiency of protein structure determination by x-ray nanocrystallography at the European XFEL

DESY 13-138

August 2013

Svitozar Serkez[a], Vitali Kocharyan[a], Evgeni Saldin[a], Igor Zagorodnov[a], Gianluca Geloni[b]

Proposal to generate 10 TW level femtosecond x-ray pulses from a baseline undulator in conventional SASE regime at the European XFEL

Strong Bunch Compresion for TW Power

Strong compression and undulator tapering

Courtesy
V.Kocharyan

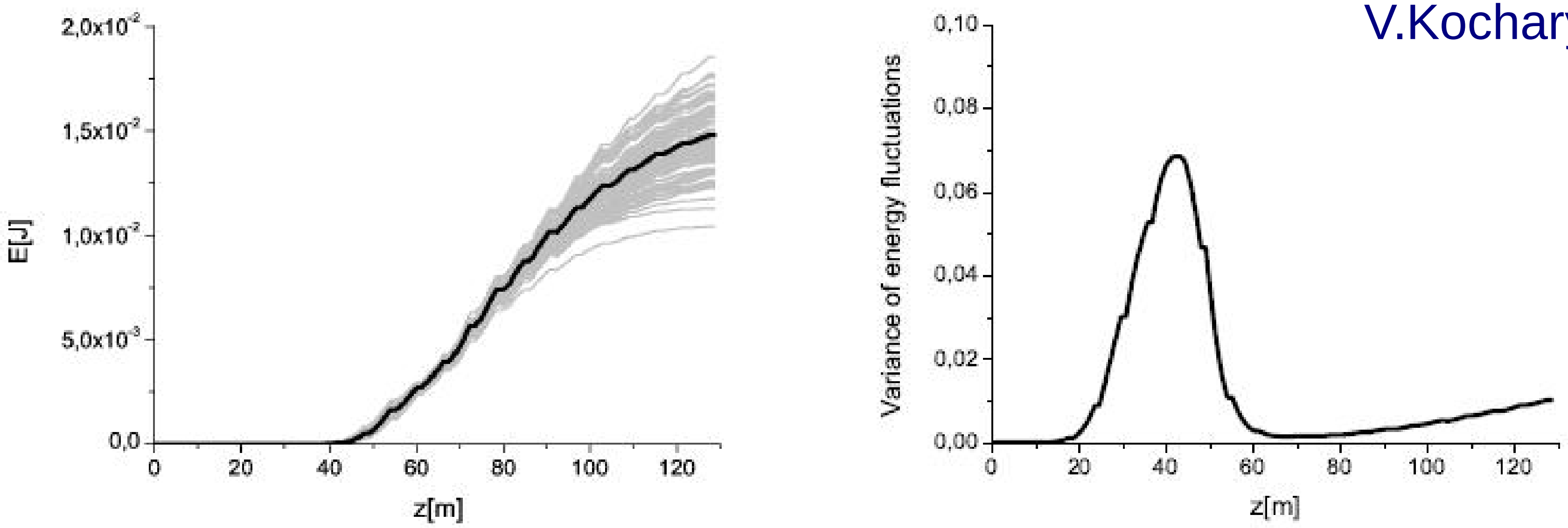

Fig. 7. Evolution of the output energy in the photon pulse and of the variance of the energy fluctuation as a function of the distance inside the output undulator, with tapering. Grey lines refer to single shot realizations, the black line refers to the average over a hundred realizations.

Strong Bunch Compresion for TW Power

Strong compression and undulator tapering

Courtesy
V.Kocharyan

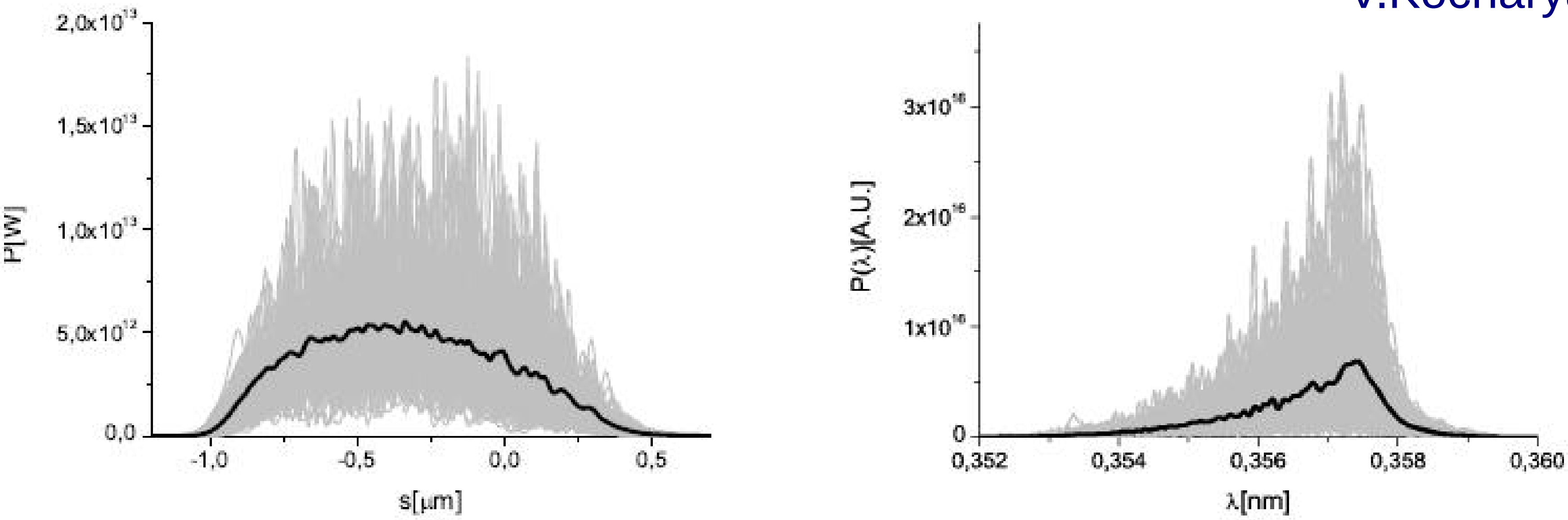

Fig. 5. Power and spectrum produced in the SASE mode at saturation with undulator tapering. Grey lines refer to single shot realizations, the black line refers to the average over a hundred realizations.

Non-linear Tapering in Nominal Regime

Current and taper for Q=250 pC

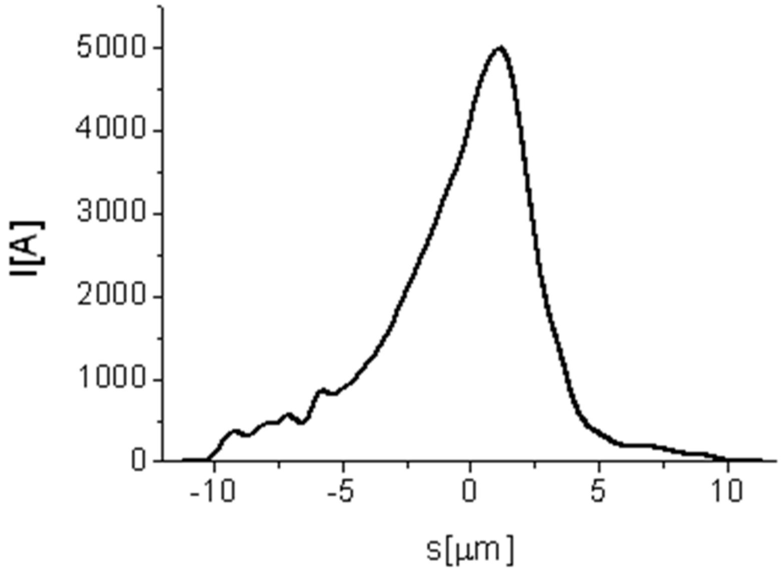

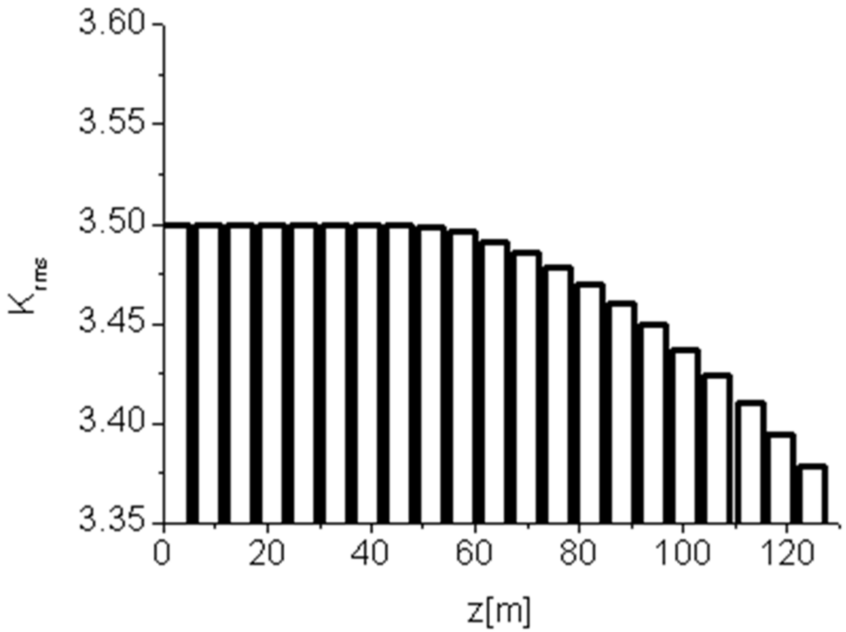

Non-linear Tapering in Nominal Regime

SASE ALICE and Genesis (v. 2.0) with intersections, quantum fluctations, taper and wake

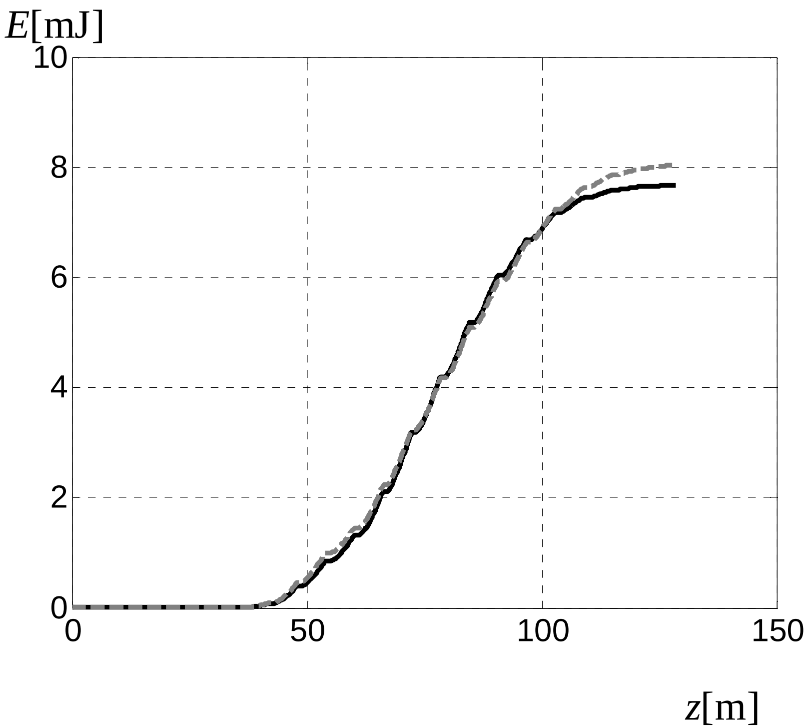

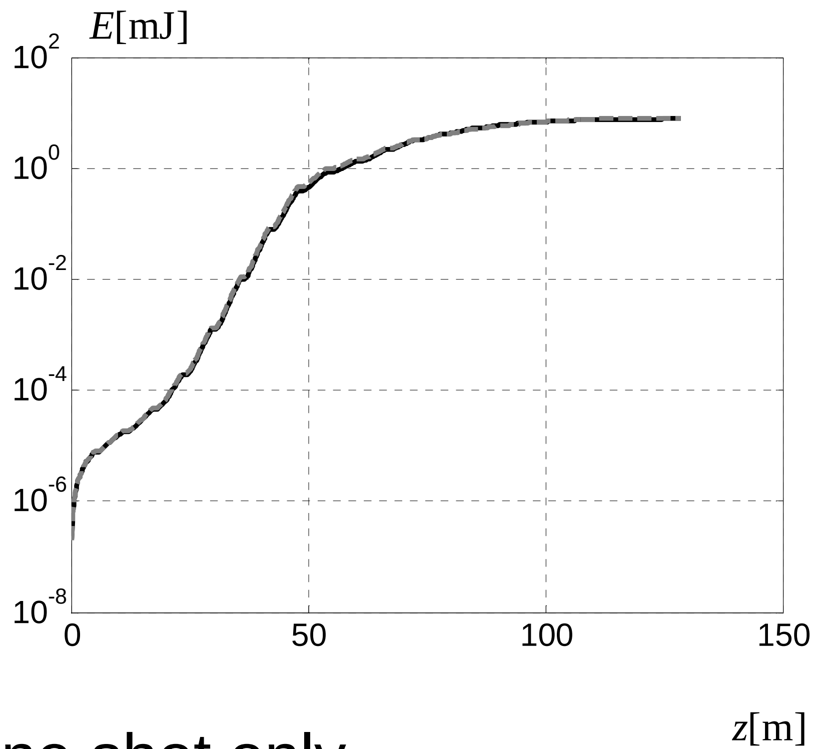

one shot only

Non-linear Tapering in Nominal Regime

SASE ALICE and Genesis (v. 2.0) with intersections, quantum fluctations, taper and wake

at z=128 m

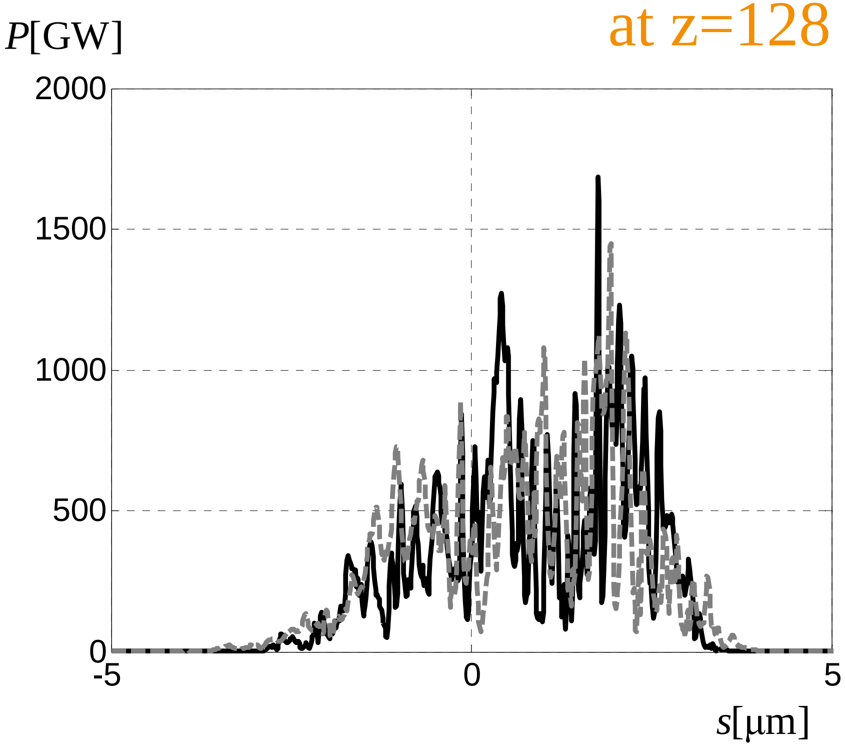

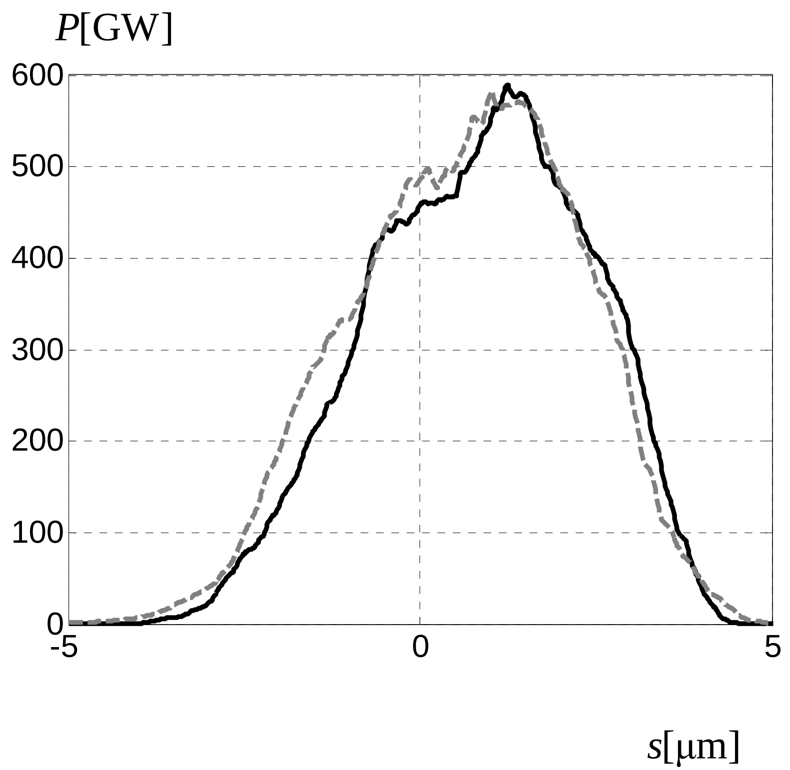

one shot only averaged over 2000 slices

Harmonic Lasing and pSASE

B. W. J. McNeil *et al.*, Phys. Rev. Lett. **96**, 084801 (2006).

E. A. Schneidmiller and M. V. Yurkov, Phys. Rev. ST Accel. Beams 15, 080702 (2012).

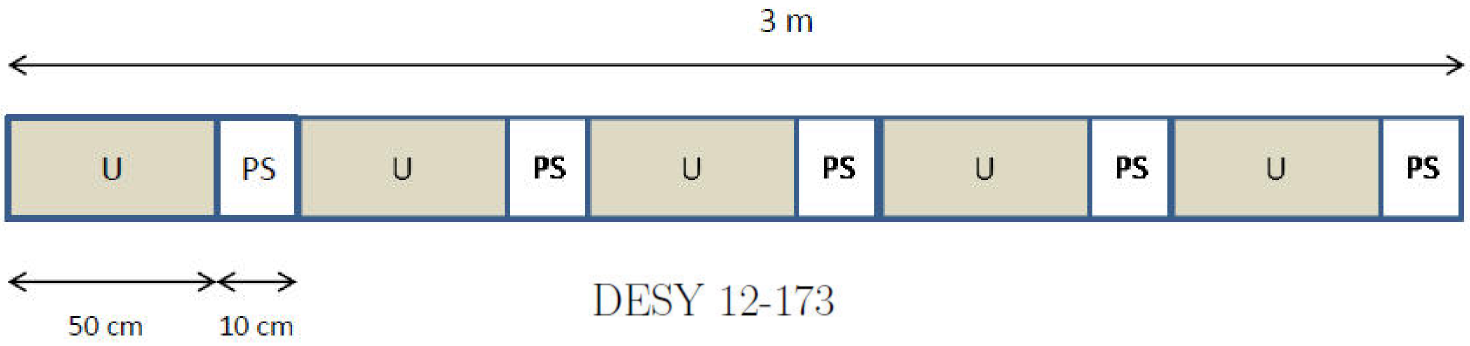

DESY 12-173

October 2012

A possible upgrade of FLASH for harmonic lasing down to 1.3 nm

E.A. Schneidmiller and M.V. Yurkov

Harmonic Lasing and pSASE

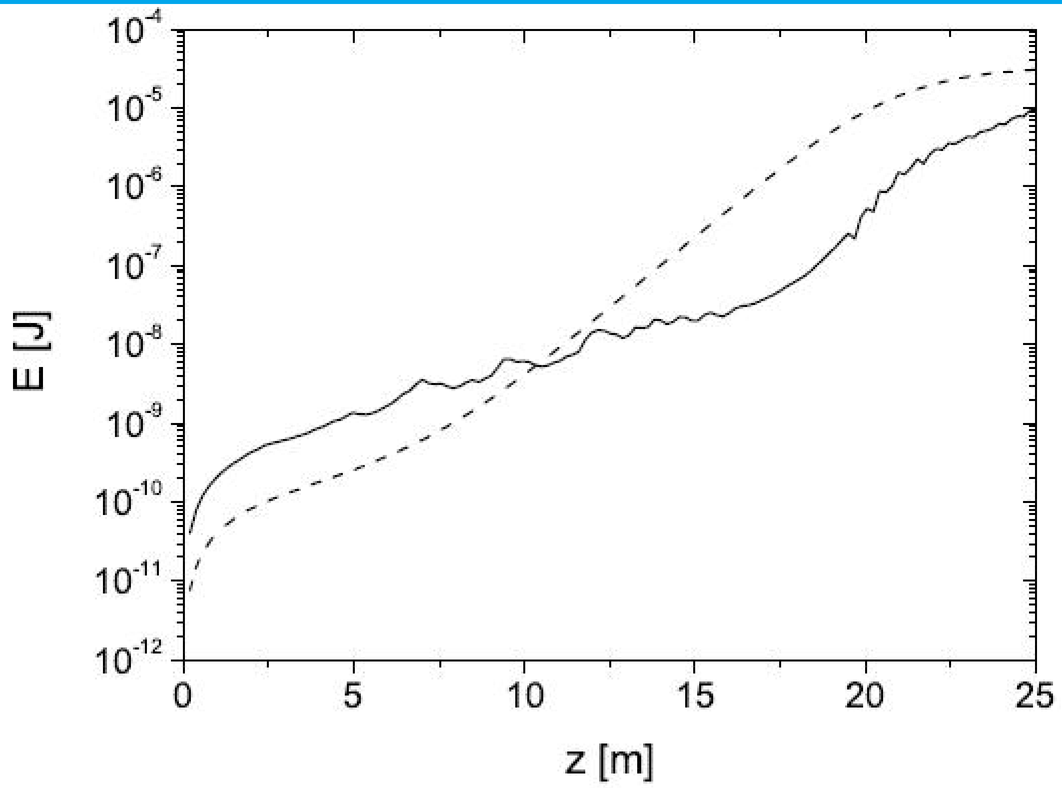

Fig. 4. Pulse energy versus magnetic length of the undulator for the fundamental (solid) and the 3rd harmonic (dash). Electron beam and undulator parameters are given in Table 1. Phase shifters are located after every 0.5 m long section of the undulator. The phase shift is $4\pi/3$ after sections 1-4, 6-9, 11-13, 18, 23, 39-49, and $2\pi/3$ after sections 5, 10, 14-17, 19-22, 24-27.

Harmonic Lasing and pSASE

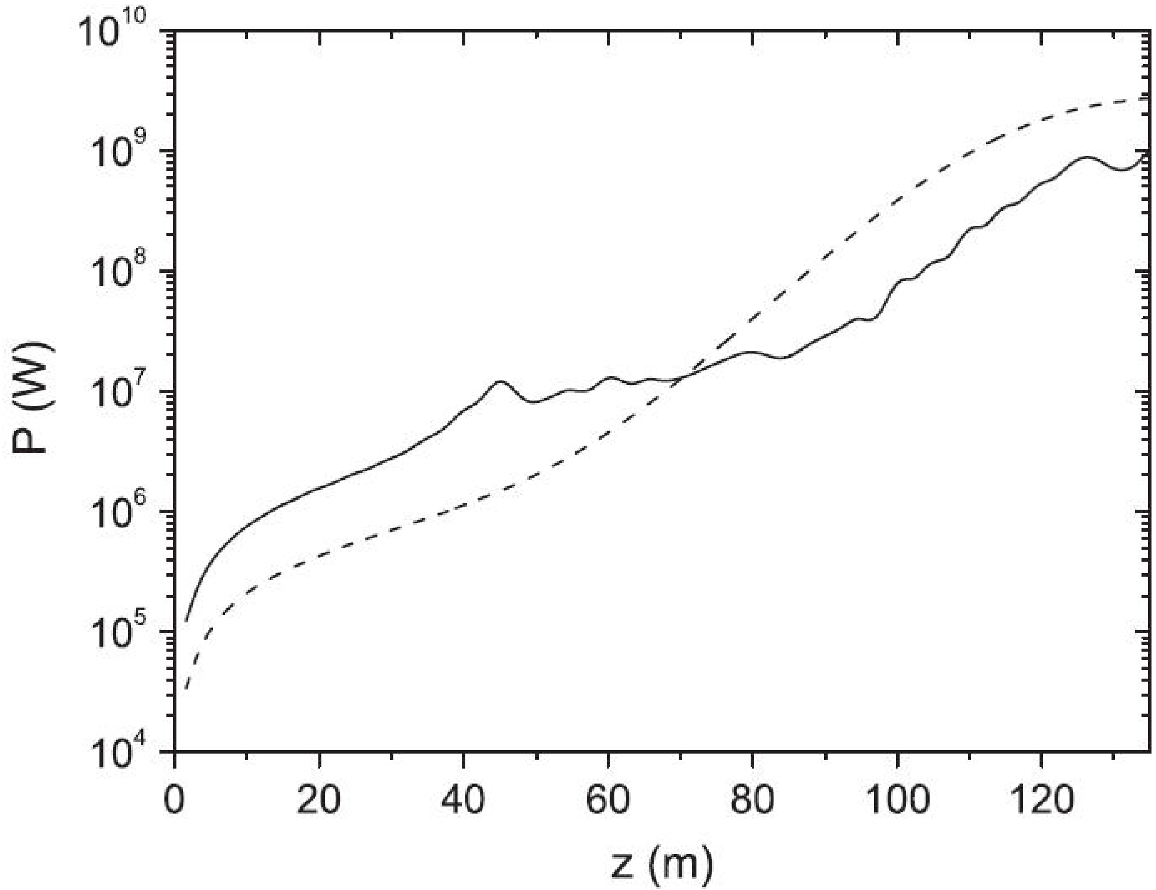

FIG. 8. An example for the European XFEL. Averaged peak power for the fundamental harmonic (solid) and the third harmonic (dash) versus magnetic length of SASE1 undulator. The wavelength of the third harmonic is 0.2 Å (photon energy 62 keV). The fundamental is disrupted with the help of phase shifters installed after 5 m long undulator segments. The phase shifts are $4\pi/3$ after segments 1–8 and 21–26, and $2\pi/3$ after segments 9–16. Simulations were performed with the code FAST.

Harmonic Lasing and pSASE

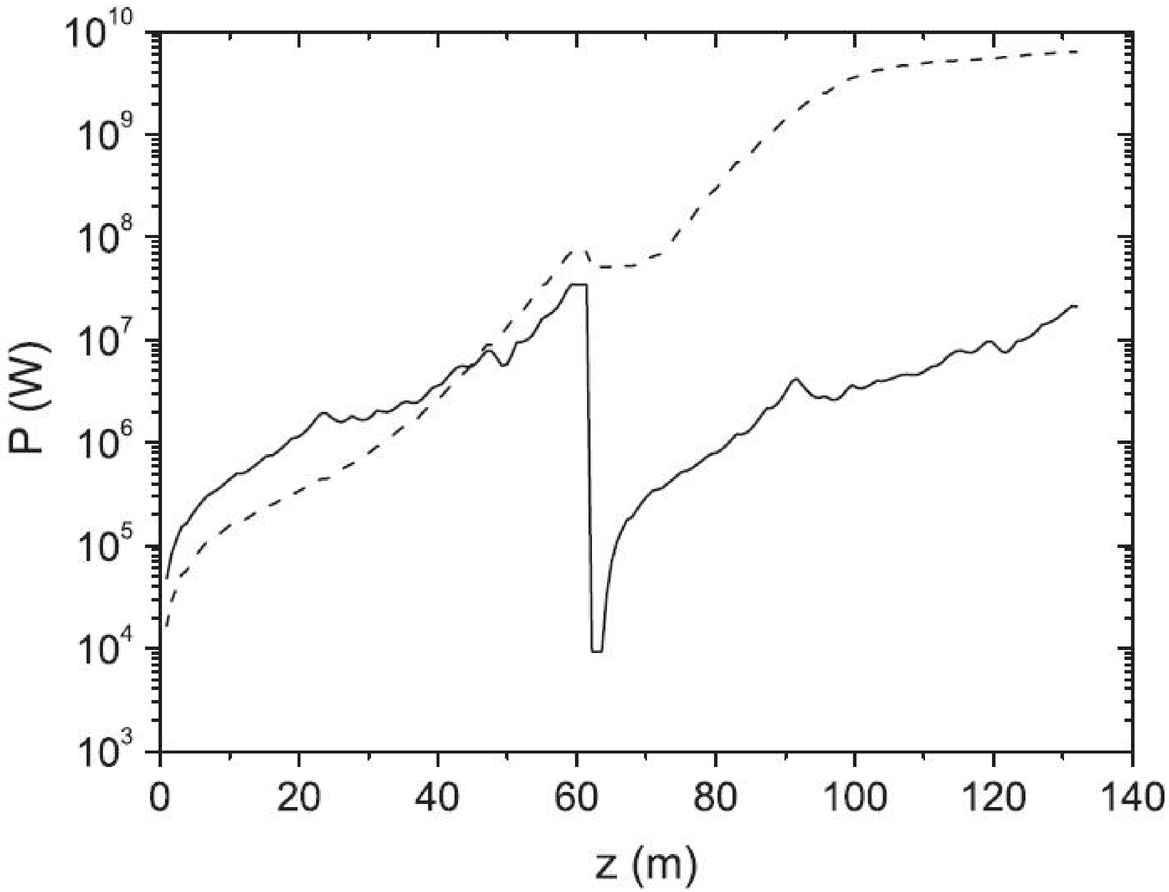

FIG. 7. Averaged peak power for the fundamental harmonic (solid) and the third harmonic (dash) versus geometrical length of the LCLS undulator (including breaks). The wavelength of the third harmonic is 0.5 Å (photon energy 25 keV). Beam and undulator parameters are in the text. The fundamental is disrupted with the help of the spectral filter (see the text) and of the phase shifters. The phase shifts are $4\pi/3$ after segments 1–5 and 17–22, and $2\pi/3$ after segments 6–10 and 23–28. Simulations were performed with the code FAST.

Harmonic Lasing and pSASE

E. A. Schneidmiller and M. V. Yurkov, Phys. Rev. ST Accel. Beams 15, 080702 (2012).

D. Xiang, Y. Ding, Z. Huang and H. Deng., Phys. Rev. ST AB 16, 010703 (2013).

DESY 13-135

July 2013

Svitozar Serkez[a], Vitali Kocharyan[a], Evgeni Saldin[a], Igor Zagorodnov[a], Gianluca Geloni[b]

Purified SASE undulator configuration to enhance the performance of the soft x-ray beamline at the European XFEL

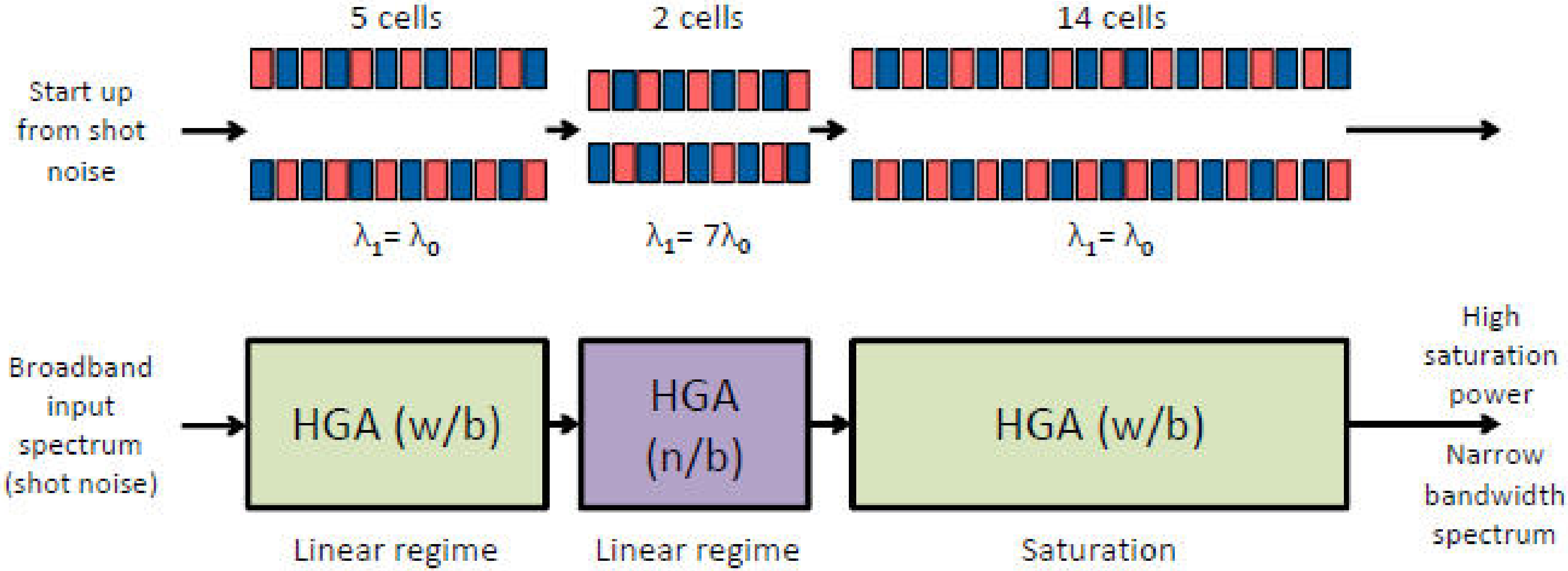

Fig. 2. The actual pSASE undulator configuration proposed for the SASE3 beamline, which is expected to operate in the photon energy range between 1.3 keV and 3 keV.

Harmonic Lasing and pSASE

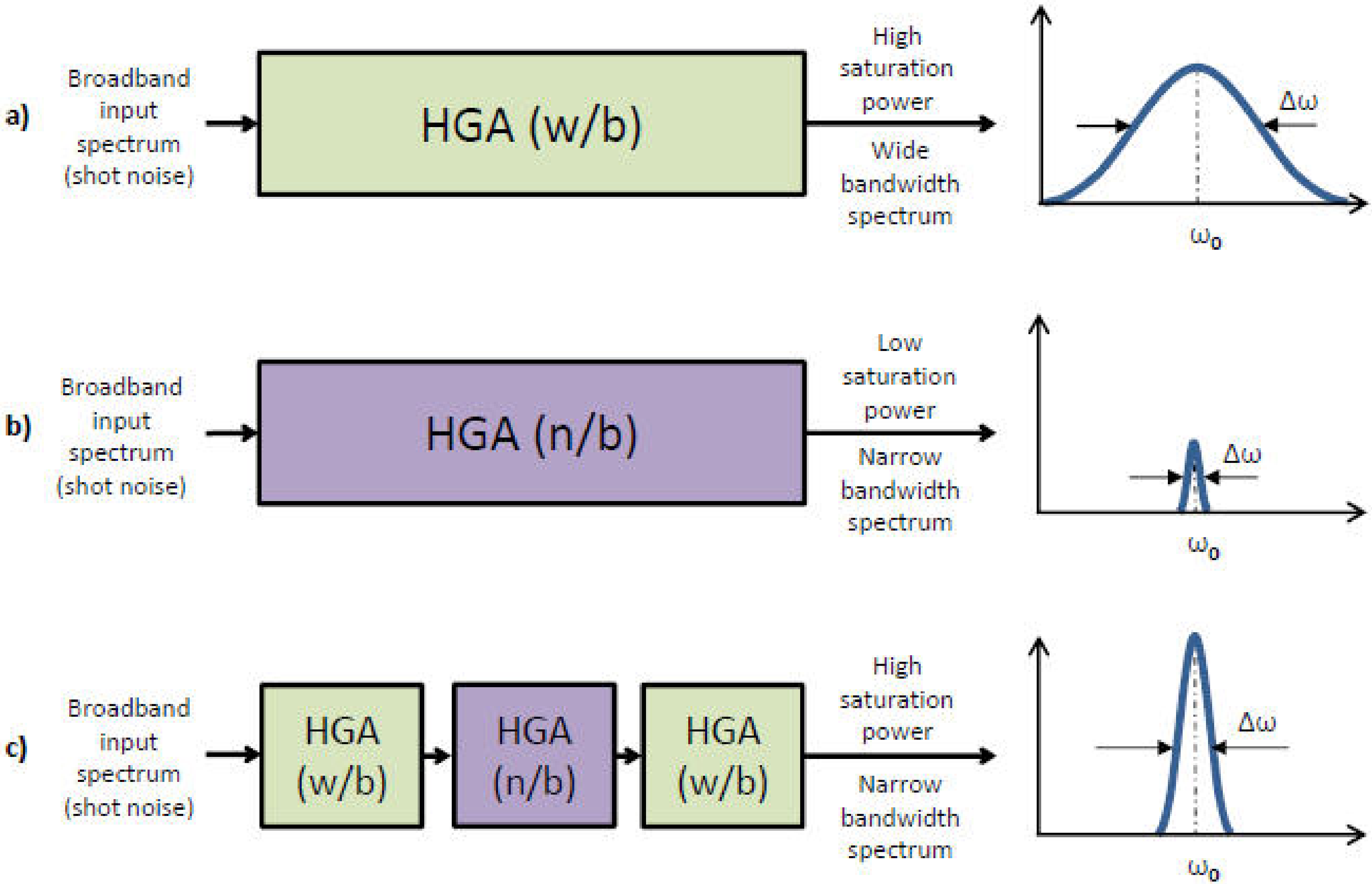

Harmonic Lasing and pSASE

SASE, Q=100 pC

Courtesy
V.Kocharyan

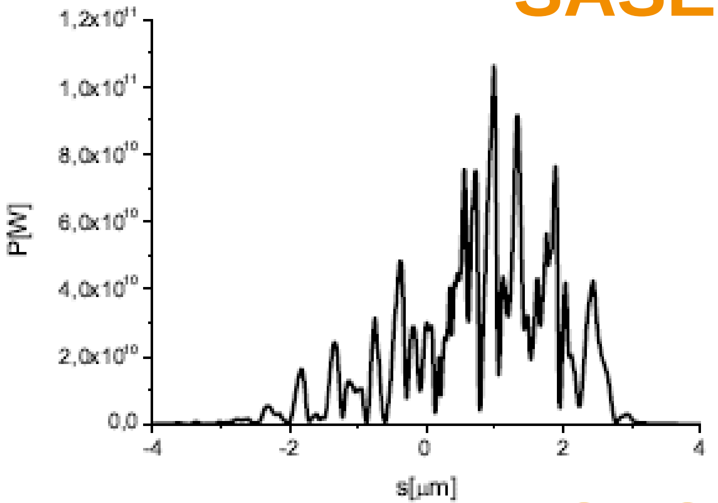

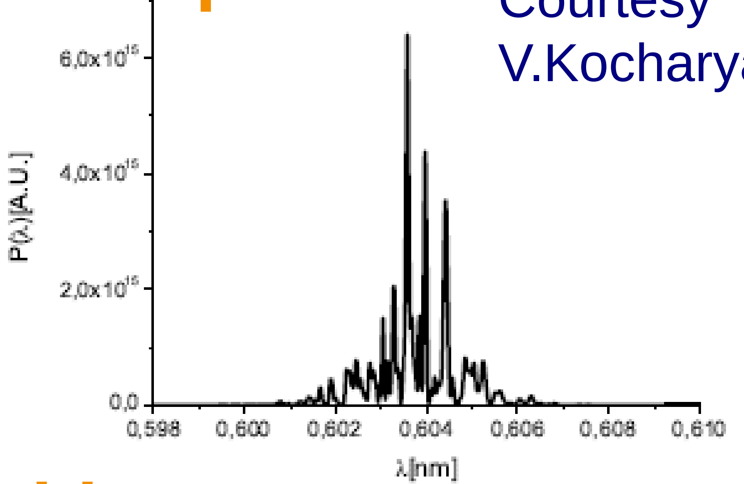

pSASE with taper